PROCESSING OF DUAL-ORTHOGONAL CW POLARIMETRIC RADAR SIGNALS

The picture on the cover represents the time-frequency distribution of the de-ramped signals in the FM-CW polarimetric radar (see Chapter 7 of this thesis).

PROCESSING OF DUAL-ORTHOGONAL CW POLARIMETRIC RADAR SIGNALS

Proefschrift

ter verkrijging van de graad van doctor
aan de Technische Universitet Delft,
op gezag van de Rector Magnificus prof.dr.ir. J.T.Fokkema
voorzitter van het College voor Promoties,
in het openbaar te verdedigen op maandag 11 mei 2009 om 12.30 uur

door

Galina BABUR
Engineer (Master of Science) in
Tomsk State University of Control Systems and Radioelectronics, Russia

Geboren te Sobolivka, Oekraïne

Dit proefschrift is goedgekeurd door de promotor:

Prof. dr. ir. L.P. Ligthart

Samenstelling promotiecommissie:

Rector Magnificus, voorzitter	
Prof. dr. ir. L.P. Ligthart	Technische Universiteit Delft, promotor
Prof.ir. P. van Genderen	Technische Universiteit Delft
Prof.dr.ir. F.B.J Leferink	University of Twente
Prof.dr.rer.nat. Madhukar Chandra	Technische Universitaet Chemnitz
Prof.dr. A.G. Tijhuis	Technische Universiteit Eindhoven
Dr. V.I. Karnychev	Tomsk State University of Control Systems and Radioelectronics
F. Le Chevalier, M.Sc.	Thales, France

ISBN/EAN: 978-90-76928-16-6

Keywords: dual-orthogonal signals, polarimetric radar, FM-CW radar

Printed in The Netherlands

To my family

Contents

1 Introduction

1.1 Background of the Research

Radar is a system that transmits a wave of known shape and receives echoes returned by observed objects. The transmitted wave can be a pure frequency (tone) or its amplitude, phase, or frequency can be modulated. On reception the wave must be amplified and analyzed in one way or another [1]. For conventional (single-channel) radar any observed object (or any resolution cell) is described with a time-variable complex coefficient, namely the reflection coefficient. However it does not take into account the vector structure of electromagnetic waves and so information about observed radar objects can be lost.

Polarimetric radar allows the utilization of **complete** electromagnetic vector information about observed objects [2]. It is based on the fact that in general any radar object (or any resolution cell) can be described by an 2x2 scattering matrix (SM) with four time-variable complex elements describing amplitude, phase and polarization transformation of a wave scattering radar object. Two signals with orthogonal (e.g. horizontal and vertical) polarizations are used for SM-elements estimations. Each sounding signal is applied for two co- and cross-polarization reflection coefficients in two SM columns. Cross-polarization reflection coefficients define the polarization change of the incident wave. So in addition to polarization orthogonality extra (dual) orthogonality of sounding signals is needed for estimating the scattering matrix elements in polarimetric radar.

Orthogonality of the signals in terms of their inner product is the choice of the radar designer. It may be realized in time or frequency domain, or as orthogonality of waveforms using sophisticated signals. In case of sophisticated signals the elements of the object scattering matrix are retrieved by correlating the received signal on each orthogonally polarized channel with both transmitted waveforms [3]. The concept of dual-orthogonal polarimetric radar signals and some signal types are considered in **Chapter 2**.

We note here that scattering matrix elements in polarimetric radar can be measured simultaneously or consecutively. Consecutive measurements (orthogonality in time domain) mean that a signal with first polarization is transmitted and the corresponding co- and cross-reflection coefficients are estimated; after that a signal with second polarization is transmitted and a second set of co- and cross-polarization reflection coefficients are estimated. As a result four elements are estimated in two stages during two radar duty cycles. As for simultaneous measurements they allow for estimating all four SM-elements at the same time during one radar duty cycle. Simultaneous measurement of SM-elements is preferable because [1]:

1. The evolution over time of the observed object aspect angle changes the relative phase shift between scatterers in a given resolution cell and thus changes the phase difference between the two polarized components of the wave, and hence its polarization.
2. This change in aspect angle also modifies the basic backscattering matrices of the various reflectors (since these matrices depend on aspect angle), and hence also the global backscattering matrix of the object.

By these reasons the simultaneous measurements are of interest for modern polarimetric agile radar. Simultaneous measurements can be executed when orthogonality of waveforms (appropriate for sophisticated signals) is used. In this case the sounding signal consists of two sophisticated signals and is called vector sounding signal. Such type of sounding signal provides the unique possibility to split all elements of the scattering matrix and to measure all of them simultaneously during one pulse or single sweep time. Typical sophisticated signals are signals with linear frequency modulation (LFM) and phase code modulation (PCM). The use of sophisticated signals for simultaneous measurement of SM-elements in polarimetric radar is also desirable since they may have the following advantages:

- high resolution: sophisticated signals provide the resolution of a short pulse while the signal length can be long;
- high energy: signals' energy increases with their length, without changing the transmitter peak power.

Both high resolution and high energy are available when signal compression is used in a radar receiver. Signal compression can be utilized from correlation processing applicable to all sophisticated signals or from stretch (de-ramping) processing applicable to linear frequency modulated signals. **Chapter 3** of the thesis presents an overview of possible techniques for the compression of dual-orthogonal sophisticated signals and gives the comparison of correlation processing and de-ramping processing.

Sophisticated signals allow also an additional way to increase the energy of the received signals when transmission and reception of the signals in polarimetric radar is utilized continuously. Continuous wave transmissions in comparison with the pulsed transmissions have low continuous power for the same detection performance because an 100% duty cycle radar is employed [4]. For this reason polarimetric radar with continuous waveforms is of interest. However, we should distinguish narrow-band continuous wave (CW) radars and wide-band radars with continuous waveforms (wideband CW radar [5], modulating CW radar [6]). Sophisticated signals can be successfully used in radars with continuous waveforms.

Since the length of the sounding sophisticated signals (duty cycle of radar with continuous waveforms) can be comparatively large, different bandwidth-specific effects appear in the received signals; e.g. object motion is considered to result in a Doppler frequency shift for a conventional narrow-band model of the signals. However, the narrowband model is an approximation of the wideband model where object motion results in a scaling of the received signal. **Chapter 4** presents the investigation of both compression techniques, namely correlation processing and de-ramping processing when signal bandwidth effects take place and differences between the models appear. In case of correlation processing the bandwidth effects for the wide-band signal and the narrow-band model can be analyzed via the matrix ambiguity functions. The de-ramping processing is also considered for both existing signal models. With chapter 4 the first part of the thesis is closed.

The second part of the thesis is devoted to advanced processing in polarimetric radar with continuous waveforms, namely to de-ramping processing in polarimetric radar with simultaneous measurement of scattering matrix elements. De-ramping processing, also called “active correlation” [4] or “deramp FFT” [7], is a kind of “stretch processing” [8]. Radar using LFM sounding signals and utilizing the de-ramping procedure is named *FM-CW radar* [9] where FM-CW means “frequency-modulated continuous waves”. Polarimetric FM-CW radar with dual-orthogonal sophisticated (namely dual LFM) signals is considered to be a new generation of radar.

De-ramping processing has been chosen for detailed investigation in the second part of this thesis because it has much less computational complexity in comparison with correlation processing. It is more accessible and for this reason more attractive for utilization in modern polarimetric radars. However FM-CW polarimetric radar can have some problems. **Chapter 5** to **Chapter 7** proposed their solutions.

Chapter 5 presents a novel solution for high-level isolation between branches in FM-CW radar channels. The radar hardware is splitting the received signals with orthogonal polarizations and provides the isolation between polarimetric radar channels. The isolation between the branches in channels is determined within the time interval in which useful scattered signals occupy the same bandwidth. A pair of LFM-signals having the same form and a time shift relatively from each other is proposed for use in FM-CW polarimetric radar. The proposed solution utilizes the quasi-simultaneous measurements of SM-elements, but the advantages of sophisticated signals and continuous waveforms remain.

Chapter 6 presents a novel flexible de-ramping processing applicable for FM-CW radars. The proposed technique allows for solving three tasks which can affect FM-CW-radar performance, namely a change in signal bandwidth, shift of beat frequency bands and selection of the range interval among the observed ranges for high-range resolution. The first task provides the varying of radar range resolution without considerable receiver upgrade and offers therefore flexibility of the here-proposed technique. Shifting the beat signals’ bandwidth (the second task) provides flexibility in filters because the filtering of beat signals can then take place at preferred frequencies. The third task allows for an observation of a part of the full radar range, namely the selection of a range interval by using flexibility in localization of the beat signals' bandwidth, while in addition there is no need to change the amplitude-frequency responses of the used filters.

Chapter 7 proposes a technique for the suppression of cross-correlation interfering signals appearing in the beat-signal channels of FM-CW polarimetric radar. This technique uses information about the time interval, when the interfering signal influences the polarimetric receiver channels. The blanking/suppression of the beat signals in that time interval gives the possibility to improve the SM-elements estimation quality and completely remove cross-correlation interferences for the price of a small degradation in radar resolution and useful signal levels (around 1.6 dB).

Chapter 8 summarizes the main results of the thesis and lists the recommendations for further research.

1.2 Polarimetric Radar Sounding Basics

Fig. 1.1 shows the sounding of polarimetric radar with continuous waveforms when two different antennas are used for transmission and reception. $\dot{\mathbf{S}}(t)$ is a scattering matrix of the observed radar object, with four time-variable complex elements, which are co-polarized and cross-polarized reflection coefficients of the vector sounding signal components having orthogonal (e.g. "1" – horizontal, "2" – vertical) polarizations.

Radar object scattering of the sounding signal is part of the radar channel connected to the polarization transform. The polarization of the signal can be changed not only during the scattering processes, but also due to radiation, propagation and reception of electromagnetic waves. All parts of the radar channel, which include a transmitting antenna, propagation medium, and receiving antenna are of interest. Generally the scattering matrix estimated in the radar receiver can be presented as a sequential multiplication of scattering matrices of all radar channel components [10]:

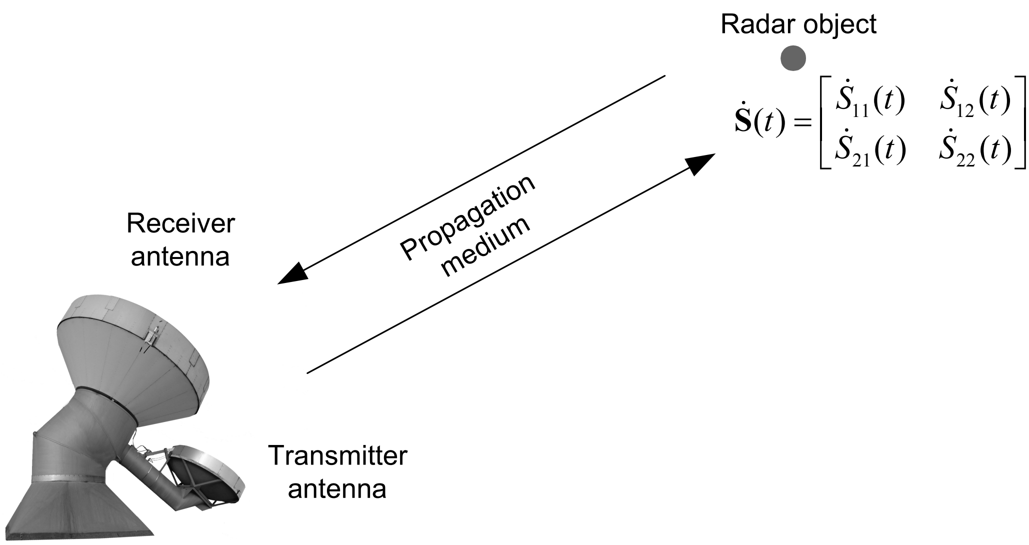

Fig. 1.1 – Polarimetric radar sounding.

$$\dot{\mathbf{S}}^{/}(t,\tau) = \dot{\mathbf{R}} \cdot \dot{\mathbf{P}}_{-}(t,\tau) \cdot \dot{\mathbf{S}}(t) \cdot \dot{\mathbf{P}}_{+}(t,\tau) \cdot \dot{\mathbf{T}}\,, \tag{1.1}$$

where $\dot{\mathbf{T}}$ is the polarization diagram of the transmitter antenna, $\dot{\mathbf{R}}$ is the polarization diagram of the receiver antenna, $\dot{\mathbf{S}}(t)$ is the true polarization scattering matrix of the observed object, $\dot{\mathbf{P}}_{-}(t,\tau)$ and $\dot{\mathbf{P}}_{+}(t,\tau)$ are the forward and backward propagation matrices, which describe the amplitudes, phases and polarization changes of the electromagnetic waves during propagation.

Compensation of different radar channel parts for true scattering matrix estimation lies outside the scope of this thesis. So in this thesis the scattering matrix of the observed object means a general scattering matrix described with Eq. 1.1.

This thesis is devoted to the processing of dual orthogonal polarimetric radar signals with continuous waveforms used for the simultaneous estimation of all SM elements in the high-resolution Doppler polarimetric radar system PARSAX (TU Delft, the Netherlands).

References

1. F. Le Chevalier, “Principles of radar and sonar signals processing”, Artech House, Inc., 2002.
2. W.M. Boerner et. Al. “Direct and Inverse Methods in Radar Polarimetry”, Part 1, Kluwer Academic Publishers, 1992.
3. D. Guili, M. Fossi, L. Facheris, “Radar Object Scattering Matrix Measurement through Orthogonal Signals”, IEEE Procidings-F, Vol. 140, № 4, August 1993.
4. M. Jankiraman, “Design of Multi-Frequency CW Radars”, Scitech Publishing, Inc., 2007.
5. D.R. Wehner, “High-Resolution Radar”, second edition, Artech House, Inc., 1995.
6. E.F. Knott, J.F. Shaeffer, M.T. Tuley, “Radar Cross Section”, 2nd edn., SciTech Publishing Inc., 2004.
7. D. C. Munson, Jr. and R. L. Visentin, “A signal processing view of stripmapping synthetic aperture radar,” IEEE Trans. Acoust., Speech, Signal Processing, vol. 37, no. 12, Dec. 1989, pp. 2131-2147.
8. W.J. Caputi, "Stretch: A Time-Transformation Technique". IEEE Transactions on Aerospace and Electronic Systems, Volume AES-7, Issue 2, March 1971, pp. 269-278.
9. Luck, David G. C. “Frequency Modulated Radar”, published by McGraw-Hill, New York, 1949, 466 pages.
10. O.A. Krasnov, L.P. Ligthart, Z. Li, P. Lys, F. van der Zwan, “The PARSAX - Full Polarimetric FMCW Radar with Dual-Orthogonal Signals”, Radar Conference, 2008, EuRAD 2008, Oct. 2008, pp. 84-87.

PART 1

THEORY

2 Polarimetric Radar Signals with Dual Orthogonality

This chapter describes the concept of orthogonal sophisticated signals (Section 2.1), which are applicable in polarimetric radar with simultaneous measurement of scattering matrix elements, namely dual-orthogonal sophisticated signals. Also this chapter provides a short overview of such signals and their properties (Section 2.2).

2.1 Concept of the Dual-Orthogonal Polarimetric Radar Signals

Polarization is the property of a single-frequency electromagnetic wave describing the shape and orientation of the locus of the electric and magnetic field vectors as function of time [1]. In common practice, when only plane waves or locally plane waves are considered, it is sufficient to specify the polarization of the electrical field vector $\dot{\mathbf{E}}$. The electric field of the vector sounding signal can be written as

$$\dot{\mathbf{E}}_T(t) = \begin{bmatrix} \dot{E}_{1T}(t) \\ \dot{E}_{2T}(t) \end{bmatrix}, \tag{2.1}$$

where $\dot{E}_{1T}(t)$ and $\dot{E}_{2T}(t)$ mean two components of the transmitted (subscript "*T*") electrical field with orthogonal (e.g. horizontal and vertical) polarizations. The dot above the variable means that it has complex values.

In general any radar object (or any resolution cell) can be described by a 2x2 scattering matrix (SM) $\dot{\mathbf{S}}(t)$ with four time-variable complex elements, which are co-polarized and cross-polarized reflection coefficients of the signals with orthogonal polarizations

$$\dot{\mathbf{S}}(t) = \begin{bmatrix} \dot{S}_{11}(t) & \dot{S}_{12}(t) \\ \dot{S}_{21}(t) & \dot{S}_{22}(t) \end{bmatrix}, \tag{2.2}$$

where

$\dot{S}_{11}(t)$ is the complex reflection coefficient of an incident horizontally polarized wave which determines the scattered wave in the same plane;

$\dot{S}_{22}(t)$ is the complex reflection coefficient of an incident vertically polarized wave which determines the scattered wave in the same plane;

$\dot{S}_{12}(t)$, $\dot{S}_{21}(t)$ are complex reflection coefficients defining the 90 degree change of wave polarization in the scattered waves.

In case of monostatic radar, when both transmit and receive antennas are located at the same location, the polarization transformation is described by the 2x2 backscattering matrix (BSM). BSM is a special case of the scattering matrix as defined in Eq. 2.2 [2].

Each element of the scattering matrix (Eq. 2.2) has a complex value depending on the properties of the scattering object and on its orientation relative to the radar antennas. For the measurement of the scattering matrix elements a vector sounding signal consisting of two signals with orthogonal (e.g. horizontal and vertical) polarization is required. The values of the scattering matrix elements may be dependent on the sounding signal frequency, because the scattering properties can be different per radar frequency.

It is necessary to note that the matrix $\dot{\mathbf{S}}$ describes the amplitude, phase and polarization transformation of a monochromatic wave radiating from the radar towards the object. If the transmitted signal can not be considered as monochromatic and contains a set of frequencies, the radar object should be described by a set of scattering matrices, one matrix per spectral component of the sounding signal [2]. In this case amplitudes, phases and polarization of the scattered signal are defined by the superposition of the scattering matrices.

During the process of polarimetric radar observation the transmitted field is transformed into

$$\begin{bmatrix} \dot{E}_{1R}(t,\tau) \\ \dot{E}_{2R}(t,\tau) \end{bmatrix} = \begin{bmatrix} \dot{S}_{11}(t,\tau) & \dot{S}_{12}(t,\tau) \\ \dot{S}_{21}(t,\tau) & \dot{S}_{22}(t,\tau) \end{bmatrix} \cdot \begin{bmatrix} \dot{E}_{1T}(t) \\ \dot{E}_{2T}(t) \end{bmatrix}, \tag{2.3}$$

where subscript "*R*" means reception and τ means the roundtrip time delay. The scattering matrix in Eq. 2.3 includes all parts of the radar channel (see Section 1.2): the transmitting antenna, the propagation medium, the observed radar object and the receiving antenna.

In radar polarimetry the term "orthogonality" plays an important role. Therefore orthogonality should be defined carefully. Orthogonality of signals means that their scalar product in the appropriate basis is equal to zero. E.g. in the time domain the scalar product is determined like a correlation integral. So time orthogonality means that the correlation integral is equal to zero.

The orthogonality of the signals can be utilized in five different bases: polarization, time, frequency, space and waveform.

Polarization	The signals are transmitted with orthogonal polarizations.
Time	The signals are separated in time domain.
Frequency	The signals are separated in frequency domain.
Space	The signals are transmitted in different directions.
Waveforms	The signals have orthogonal waveforms.

Next we consider existing types of orthogonality with respect to their application in polarimetric radar with simultaneous measurement of scattering matrix elements.

In polarimetric radar two signals with **orthogonal polarizations** are transmitted. The observed radar object may change the polarization of the incident wave. If the same signals are transmitted with orthogonal polarizations $\left(\dot{E}_{1T}(t)=\dot{E}_{2T}(t)=\dot{E}_{T}(t)\right)$, equation (2.3) becomes:

$$\begin{bmatrix} \dot{E}_{1R}(t,\tau) \\ \dot{E}_{2R}(t,\tau) \end{bmatrix} = \begin{bmatrix} \left(\dot{S}_{11}(t,\tau)+\dot{S}_{12}(t,\tau)\right)\cdot\dot{E}_{T}(t) \\ \left(\dot{S}_{21}(t,\tau)+\dot{S}_{22}(t,\tau)\right)\cdot\dot{E}_{T}(t) \end{bmatrix}. \tag{2.4}$$

In this case we are unable to separate co- and cross-polarized SM elements.

Therefore in polarimetric radar with simultaneous measurement of scattering matrix elements the sounding signals need to have an extra orthogonality in addition to polarization orthogonality. Signals having two such orthogonalities are called *dual orthogonal* signals.

So the other four orthogonality types are of interest for application in polarimetric radar, especially, as will be demonstrated also, in the high-resolution Doppler polarimetric radar system PARSAX developed at TU Delft, the Netherlands [3].

Time orthogonality means that the sounding signals are transmitted in different time intervals. This approach uses the consequent transmission of sounding signals with orthogonal polarizations combined with pulse-to-pulse polarization switching. The transmitted signals are alternatively switched to two orthogonally-polarized channels. The electric field of the vector sounding signal can be presented as

$$\dot{\mathbf{E}}_{T}(t) = \begin{bmatrix} \dot{E}_{1T}(t_1) \\ \dot{E}_{2T}(t_2) \end{bmatrix}. \tag{2.5}$$

In polarimetric radar with extra time orthogonality the sounding can be realized in the following way [3]. During the first switch setting, only the horizontal-polarized component is transmitted and, as result, the received signal equals to

$$\begin{bmatrix} \dot{E}_{1R}(t_1,\tau) \\ \dot{E}_{2R}(t_1,\tau) \end{bmatrix} = \begin{bmatrix} \dot{S}_{11}(t_1,\tau) \\ \dot{S}_{12}(t_1,\tau) \end{bmatrix}\cdot\dot{E}_{1T}(t_1). \tag{2.6}$$

During the second switch setting, the transmitted signal has only the vertical-polarized component and the received signal becomes

$$\begin{bmatrix} \dot{E}_{1R}(t_2,\tau) \\ \dot{E}_{2R}(t_2,\tau) \end{bmatrix} = \begin{bmatrix} \dot{S}_{21}(t_2,\tau) \\ \dot{S}_{22}(t_2,\tau) \end{bmatrix}\cdot\dot{E}_{2T}(t_2). \tag{2.7}$$

The polarization of the signals scattered by the observed objects can vary over time because scatterers (scattering elements of the observed object) can change their relative phase shifts as a result of motion (rotation) of the object or the radar. If the observed object (or/and the radar) is not stable, the extra time orthogonality in sounding signals can result in a disparity of estimations between the scattering matrix columns.

So time orthogonality is suitable as extra orthogonality when a polarimetric radar observes objects that can be considered as stable during the SM measurement time.

Frequency orthogonality of the sounding signals means that they occupy non-overlapping frequency bands. Separation of the scattered signals via frequency filtration allows for extracting simultaneous polarimetric information. The electric field vector of the transmitted signal in this case can be presented as

$$\dot{\mathbf{E}}_T(t) = \begin{bmatrix} \dot{E}_{1T}(t, f_1) \\ \dot{E}_{2T}(t, f_2) \end{bmatrix} \tag{2.8}$$

and equation (2.3) becomes:

$$\begin{bmatrix} \dot{E}_{1R}(t,\tau,f_1,f_2) \\ \dot{E}_{2R}(t,\tau,f_1,f_2) \end{bmatrix} = \begin{bmatrix} \dot{S}_{11}(t,\tau,f_1)\cdot\dot{E}_{1T}(t,f_1) + \dot{S}_{12}(t,\tau,f_1)\cdot\dot{E}_{2T}(t,f_2) \\ \dot{S}_{21}(t,\tau,f_1)\cdot\dot{E}_{1T}(t,f_1) + \dot{S}_{22}(t,\tau,f_1)\cdot\dot{E}_{2T}(t,f_2) \end{bmatrix}. \tag{2.9}$$

However, the scattering properties (reflection coefficients) of the same radar object may be often a function of the sounding frequencies. At the same time the sounding signal bandwidths determine the radar resolution. In low-resolution polarimetric radar the frequency orthogonal signals may have a narrow frequency bandwidth. In high-resolution polarimetric radar (e.g. the PARSAX radar), the frequency orthogonality demands a pair of orthogonal signals with a relatively large frequency band between each other. Such frequency interval may result in a non-negligible disparity between the measured matrix columns.

So extra frequency orthogonality of the vector sounding signal components may result into disparity of estimations between scattering matrix columns if the scattering properties of the observed radar object are dependent on sounding frequencies.

Space orthogonality of the vector sounding signal components makes no sense for monostatic radar object observations. All radar signals should be transmitted towards the direction of the object under observation. However space orthogonality can be usefully employed as extra orthogonality for sophisticated signals for observation of objects located in different coverage sectors.

Orthogonality of the waveforms (connected with the components of vector sounding signal) means that their cross-correlation integral (as particular case of the scalar product) equals to zero even if they occupy the same time interval and the same frequency bandwidth. Again, the auto-correlation integrals compress signals with orthogonal waveforms. We get shorter signals with increased amplitudes. Orthogonality of waveforms can be provided when sophisticated signals are used.

So vector sounding signal in polarimetric radar with simultaneous measurement of scattering matrix elements can be performed with two signals having orthogonal waveforms. Simultaneous independent transmission of such signals over two orthogonally polarized channels can then be realized. The scattering matrix elements are retrieved by correlating the received signal on each orthogonally polarized channel with both transmitted waveforms [4]. Simultaneous measurement of all four elements of the scattering matrix allows to obtain maximum volume of information about the observed radar objects.

The additional benefit of using signals with orthogonal waveforms is the possibility to increase the energy of the sounding signals, which comes from the increase of their duration, without changing the transmit peak power.

Hence sophisticated dual-orthogonal polarimetric radar signals are of interest.

2.2 Sophisticated Signals with Orthogonal Waveforms

Orthogonal sophisticated signals can be used most optimally in radars with continuous waveforms. In this case the considered signal duration corresponds to the signal repetition period (the radar duty cycle).

Sophisticated signals are characterized by their high energy of long signals, combined with the resolution of short pulses due to signal compression. Sophisticated signals, which are also called "*high pulse compression waveforms*", have large time-bandwidth product $T \cdot \Delta F >> 1$, where T is the signal duration (or the repetition period if signals are periodical) and ΔF is the signal bandwidth. The time-bandwidth product is also called *"BT-product"* or *"compression ratio"* [5].

The costs of signal compression include:

– extra transmitter and receiver complexity;
– interfering effects of side-lobes after compression.

The advantages generally outweigh the disadvantages; this explains why pulse compression is used widely [4, 6, 7].

Real sounding signals are functions of time. So the vector sounding signal consisting of two sophisticated signals with orthogonal waveforms can be written as two time-dependent functions:

$$\dot{\mathbf{u}}(t) = \begin{bmatrix} \dot{u}_1(t) \\ \dot{u}_2(t) \end{bmatrix}, \tag{2.10}$$

where subscripts "*1*, *2*" mean first and second sophisticated signal, respectively.

When digital signal processing is used in radar systems, a signal representation as a time-ordered sequence of samples is more preferable. In this case the vector sounding signal $\dot{\mathbf{u}}(t)$ may be written as

$$\dot{\mathbf{u}} = \begin{bmatrix} \dot{\mathbf{u}}_1 \\ \dot{\mathbf{u}}_2 \end{bmatrix}, \tag{2.11}$$

where $\dot{\mathbf{u}}_1 = [\dot{u}_1(1)\ \dot{u}_1(2)\ \ldots\ \dot{u}_1(K)]$ and $\dot{\mathbf{u}}_2 = [\dot{u}_2(1)\ \dot{u}_2(2)\ \ldots\ \dot{u}_2(K)]$ are two sequences of K samples of sophisticated signals with orthogonal waveforms. The sampling interval is chosen according to the Nyquist theorem.

Signal compression in radar can be utilized using two well-known processing techniques:

1. correlation processing;
2. de-ramping processing.

Correlation processing is applicable to all types of sophisticated signals. De-ramping processing, called also stretch processing [3, 7, 8], is applicable to frequency-modulated signals. A further consideration of both processing techniques is given in Chapter 3.

The main characteristic of a sophisticated signal is its correlation function. The correlation function depends only on the signal and does not depend on the observed radar object or the type of signal processing. The correlation function consists of an informative part (main lobe around the maximum correlation) and an interfering part (side-lobes). The width of the main-lobe determines the range resolution of the sounding signal. The side-lobes (side-lobe maxima) restrict the dynamic range of received signals amplitudes. There are different techniques for side-lobe compression, which are suitable for various types of sophisticated signals [9, 10].

By definition the correlation function of a signal $\dot{u}_1(t)$ (its auto-correlation function) can be written as the correlation integral:

$$\dot{R}_{11}(\tau) = \int_{-\infty}^{\infty} \dot{u}_1(t) \cdot \dot{u}_1^*(t-\tau)dt\,, \tag{2.12}$$

where superscript (*) means complex conjugation.

If the signal $\dot{u}_1(t)$ has a continuous waveforms (periodic signal) it has a continuous energy. Its auto-correlation function is determined by averaging over the signal repetition period T, i.e.

$$\dot{R}_{11}(\tau) = \frac{1}{T}\int_{-T/2}^{T/2} \dot{u}_1(t) \cdot \dot{u}_1^*(t-\tau)dt\,. \tag{2.13}$$

The correlation function of the vector signals $\dot{\mathbf{u}}(t)$, consisting of two components $\dot{u}_1(t)$ and $\dot{u}_2(t)$, can be written as

$$\begin{bmatrix} \dot{R}_{11}(\tau) & \dot{R}_{12}(\tau) \\ \dot{R}_{21}(\tau) & \dot{R}_{22}(\tau) \end{bmatrix} = \begin{bmatrix} \int_{-\infty}^{\infty} \dot{u}_1(t)\cdot\dot{u}_1^*(t-\tau)dt & \int_{-\infty}^{\infty} \dot{u}_1(t)\cdot\dot{u}_2^*(t-\tau)dt \\ \int_{-\infty}^{\infty} \dot{u}_2(t)\cdot\dot{u}_1^*(t-\tau)dt & \int_{-\infty}^{\infty} \dot{u}_2(t)\cdot\dot{u}_2^*(t-\tau)dt \end{bmatrix}, \tag{2.14}$$

where $\dot{R}_{11}(\tau)$ and $\dot{R}_{22}(\tau)$ are the auto-correlation functions of $\dot{u}_1(t)$ and $\dot{u}_2(t)$; $\dot{R}_{12}(\tau)$ and $\dot{R}_{21}(\tau)$ are their cross-correlation functions. The cross-correlation functions are their complex conjugates with mirror symmetry, meaning that $\dot{R}_{12}(\tau) = \dot{R}_{21}^{*}(-\tau)$. Also it is necessary to note that in polarimetric radar the cross-correlation level (maximum level of cross-correlation functions) can be higher than the level of the side-lobes of the auto-correlation functions (see the following Paragraphs) and their effect will be taken into account, when pairs of sophisticated signals are chosen for polarimetric radar.

If the vector sounding signal $\dot{\mathbf{u}}(t)$ is periodical, its correlation function has the following form:

$$\begin{bmatrix} \dot{R}_{11}(\tau) & \dot{R}_{12}(\tau) \\ \dot{R}_{21}(\tau) & \dot{R}_{22}(\tau) \end{bmatrix} = \frac{1}{T} \cdot \begin{bmatrix} \int\limits_{-T/2}^{T/2} \dot{u}_1(t) \cdot \dot{u}_1^{*}(t-\tau)dt & \int\limits_{-T/2}^{T/2} \dot{u}_1(t) \cdot \dot{u}_2^{*}(t-\tau)dt \\ \int\limits_{-T/2}^{T/2} \dot{u}_2(t) \cdot \dot{u}_1^{*}(t-\tau)dt & \int\limits_{-T/2}^{T/2} \dot{u}_2(t) \cdot \dot{u}_2^{*}(t-\tau)dt \end{bmatrix}, \tag{2.15}$$

where T is the repetition period of the vector sounding signal and is equal to the duty cycle of the polarimetric radar with continuous waveforms.

In case of digital processing when signal $\dot{\mathbf{u}}_1$ is represented as a sequence of K samples, the samples of its correlation function can be calculated via multiplication of two vectors:

$$\dot{R}_{11}(k) = \dot{\mathbf{u}}_1 \dot{\mathbf{u}}_{1k}^{H}, \; -K+1 \le k \le K-1, \tag{2.16}$$

where k is the sample time along the time (range) axis, $\dot{\mathbf{u}}_{1k}$ contains the elements of $\dot{\mathbf{u}}_1$ shifted by k samples and the remainder is filled with zeros, and superscript "*H*" shows the Hermitian transpose; for example

$\dot{\mathbf{u}}_{1_2} = [0 \; 0 \; \dot{u}_1(1) \; ... \; \dot{u}_1(K-2)]$ for *k = 2* and $\dot{\mathbf{u}}_{1_{-2}} = [\dot{u}_1(3) \; ... \; \dot{u}_1(K) \; 0 \; 0]$ for *k = −2*.

Properties of two digital sophisticated signals, $\dot{\mathbf{u}}_1$ and $\dot{\mathbf{u}}_2$, are described by

$$\begin{bmatrix} \dot{R}_{11}(k) & \dot{R}_{12}(k) \\ \dot{R}_{21}(k) & \dot{R}_{22}(k) \end{bmatrix} = \begin{bmatrix} \dot{\mathbf{u}}_1 \dot{\mathbf{u}}_{1k}^{H} & \dot{\mathbf{u}}_1 \dot{\mathbf{u}}_{2k}^{H} \\ \dot{\mathbf{u}}_2 \dot{\mathbf{u}}_{1k}^{H} & \dot{\mathbf{u}}_2 \dot{\mathbf{u}}_{2k}^{H} \end{bmatrix}, \; -K+1 \le k \le K-1, \tag{2.17}$$

where $\dot{R}_{11}(k)$ and $\dot{R}_{22}(k)$ are samples of the auto-correlation functions, $\dot{R}_{12}(k)$ and $\dot{R}_{21}(k)$ are samples of the cross-correlation functions, respectively. The sizes of auto- and cross-correlation functions of digital signals are equal to ($2K-1$) samples.

When periodic digital signals are used the remainder is not filled with zeros, for example

$$\dot{\mathbf{u}}_{1_2} = [\dot{u}_1(K-1) \; \dot{u}_1(K) \; \dot{u}_1(1) \; ... \; \dot{u}_1(K-2)] \text{ for } k = 2$$

and

$$\dot{\mathbf{u}}_{1_{-2}} = [\dot{u}_1(3) \; ... \; \dot{u}_1(K) \; \dot{u}_1(1) \; \dot{u}_1(2)] \text{ for } k = -2,$$

meaning that the shifts are circular.

The correlation function of the periodic vector digital signal equals to

$$\begin{bmatrix} \dot{R}_{11}(k) & \dot{R}_{12}(k) \\ \dot{R}_{21}(k) & \dot{R}_{22}(k) \end{bmatrix} = \frac{1}{K} \cdot \begin{bmatrix} \dot{\mathbf{u}}_1 \dot{\mathbf{u}}_{1k}^H & \dot{\mathbf{u}}_1 \dot{\mathbf{u}}_{2k}^H \\ \dot{\mathbf{u}}_2 \dot{\mathbf{u}}_{1k}^H & \dot{\mathbf{u}}_2 \dot{\mathbf{u}}_{2k}^H \end{bmatrix}, \quad round\left(-\frac{K}{2}\right) \le k \le round\left(\frac{K}{2}\right), \tag{2.18}$$

where "*round*" means the rounding-off operation to the nearest integer.

The sizes of auto- and cross-correlation functions of periodic digital signals are equal to (K) samples.

The choice of sophisticated signals and their parameters allows to achieve the desired range resolution after signal compression utilized in the radar receiver.

Range resolution of a pair of sophisticated signals used in polarimetric radar is determined by the main-lobe widths of their correlation functions.

Range resolution is the ability of a radar system to distinguish between two or more objects on the same bearing but at different ranges. Range resolution estimation is based on an equivalent rectangle of the main lobe pattern [11]. The forms of the correlation function main-lobes vary for a selected signal type, while the main-lobe width can be determined at varying levels for selected signals. For example, the width is defined at the −3 dB level for the normalized auto-correlation functions when LFM-signals are used [12], but some sources propose an −4 dB level for LFM-signals [5, 13, 14]. The main-lobe width of the normalized auto-correlation functions for PCM-signals is determined at its 0.5 (50%) level.

For active radars the maximum range resolution of a sophisticated signal is determined by the following expression:

$$\Delta R = \frac{\Delta\tau \cdot c}{2}, \tag{2.19}$$

where $\Delta\tau$ is the main-lobe width at the appropriate level, c is velocity of light.

The range resolution for different types of sophisticated signal is considered hereafter.

The most widely known examples of sophisticated signals with orthogonal waveforms are [2, 3, 6, 7]

- a pair of LFM-signals with up-going and down-going frequency slope;
- a pair of PCM signals.

Let us consider in next paragraphs these types of signals and some additional ones.

2.2.1 LFM Signals

LFM-signals, also called "chirp signals", are widely used in radar [8]. Such signals have constant amplitude for the sweep duration and their frequency varies linearly with time.

A pair of orthogonal sophisticated signals for simultaneous measurement of scattering matrix elements can be presented by a pair of LFM-signals with opposite (up-going and down-going) slopes. The vector transmitted signal (Eq. 2.10) can be written as

$$\begin{bmatrix} \dot{u}_1(t) \\ \dot{u}_2(t) \end{bmatrix} = \begin{bmatrix} env(t)\cdot \exp\left[j2\pi\left(\frac{k_0}{2}\cdot t^2 + f_{01}\cdot t \right) + \varphi_{01} \right] \\ env(t)\cdot \exp\left[j2\pi\left(-\frac{k_0}{2}\cdot t^2 + f_{02}\cdot t \right) + \varphi_{02} \right] \end{bmatrix}, \tag{2.20}$$

where $\mathrm{env}(t)$ is a rectangular window with length T, where T is the signal duration or duty cycle for the radar with continuous waveforms, and k_0 is a positive constant (called sweep rate, with dimension [$1/sec^2$]) which determines the frequency deviation of $\dot{u}_1(t)$ and $\dot{u}_2(t)$; φ_1 and φ_2 are initial phases. Frequencies $f_{01} \equiv F_{\min}$ and $f_{02} \equiv F_{\max}$ are the initial frequencies of LFM-signals with up-going and down-going slopes, respectively. The frequency variations as functions of time $f(t)$, are shown in Fig. 2.1; $\Delta F = F_{\max} - F_{\min}$ determines the frequency sweep of the vector transmitted signal, T in this case is the sweep (saw-tooth) duration. Such linear frequency modulation with opposite slope provides both equal spectrum widths and equal durations of the signals.

The BT-product of LFM-signals is equal to $\Delta F \cdot T = k_0 \cdot T^2$. It is known that the range resolution of a sophisticated signal is determined by its correlation function, namely the main lobe width. Fig. 2.2 shows the real part of the LFM-signal with *time-bandwidth product* 15 and the absolute value of its correlation function. Amplitude-time characteristics of the LFM-signal and its correlation function are presented in Fig. 2.2 and 2.3, respectively.

The correlation function of an LFM-signal has one narrow peak (main lobe) and several side-lobes. The main lobe width equals to $1/\Delta F$. The peak side-lobe level is determined by the first

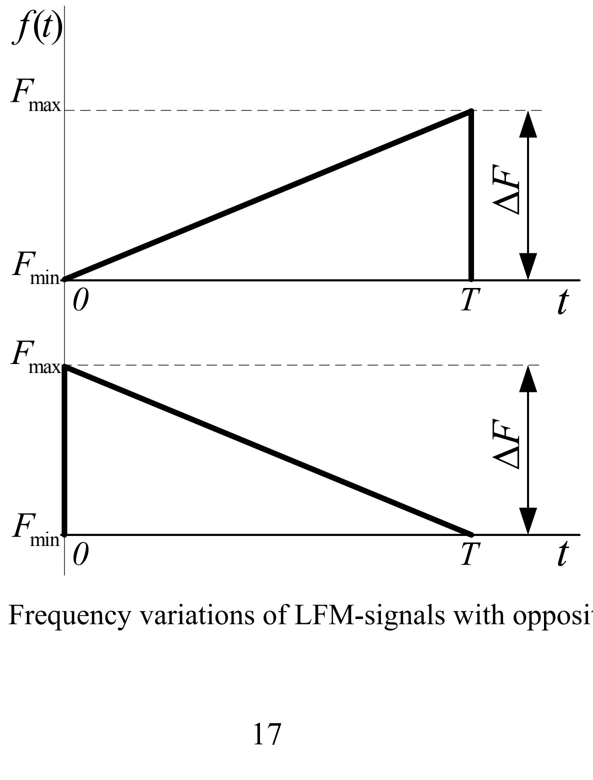

Fig. 2.1. - Frequency variations of LFM-signals with opposite slopes.

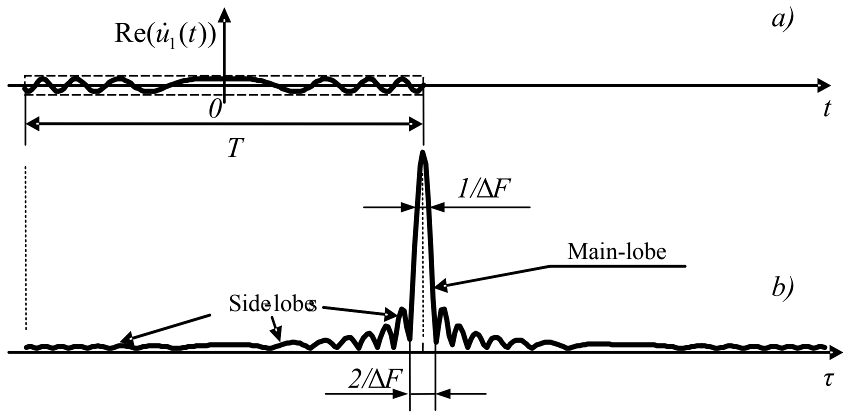

Fig. 2.2. - a) Real part of a LFM-signal with its envelope, b) absolute value of its correlation function.

side-lobe, which has an −13 dB level with respect to the main-lobe independently on the BT-product. The peak side-lobe level can be controlled by introducing a weighting function (window), however it has side effects. Side-lobe reduction leads to widening of the main lobe and to reduction of the signal-to-noise ratio. The advantages of side-lobe reduction often outweigh the disadvantages, so weighting functions are used widely.

When a pair of LFM-signals with opposite slope is used, they are described by two auto-correlation functions and two cross-correlation functions correspondently. Fig. 2.3 shows the absolute values of the auto-correlation functions ($\dot{R}_{11}(\tau)$, $\dot{R}_{22}(\tau)$) and the cross-correlation functions ($\dot{R}_{12}(\tau)$, $\dot{R}_{21}(\tau)$) of LFM-signals with BT-products equals to *15*. Such small value of the BT-product was chosen for a better visibility.

In polarimetric radar with simultaneous measurement of scattering matrix elements the received signals in both channels contain replicas of both orthogonal sounding signals. Such cross-correlation makes the same negative impact as been made by side-lobes of the auto-correlation function. But cross-correlation functions may have a relatively high level over the wide time interval (Fig. 2.3) meaning that the unfavorable effect can be larger.

The range resolution of LFM-signals is determined by the main-lobe width and equals to $1/\Delta F$ [9, 11, 12]. So Eq. 2.19 can be written as

$$\Delta R = \frac{c}{2 \cdot \Delta F} . \qquad (2.21)$$

It should be marked that Eq. 2.21 shows the maximum range resolution. Window weighting, commonly used for side-lobe suppression, results in a widening of the main lobe of the compressed LFM signal (not the main lobe of the correlation function). In addition the main lobe of the compressed signal can be sharpen using different complicated algorithms; however, their use can result in additional problems.

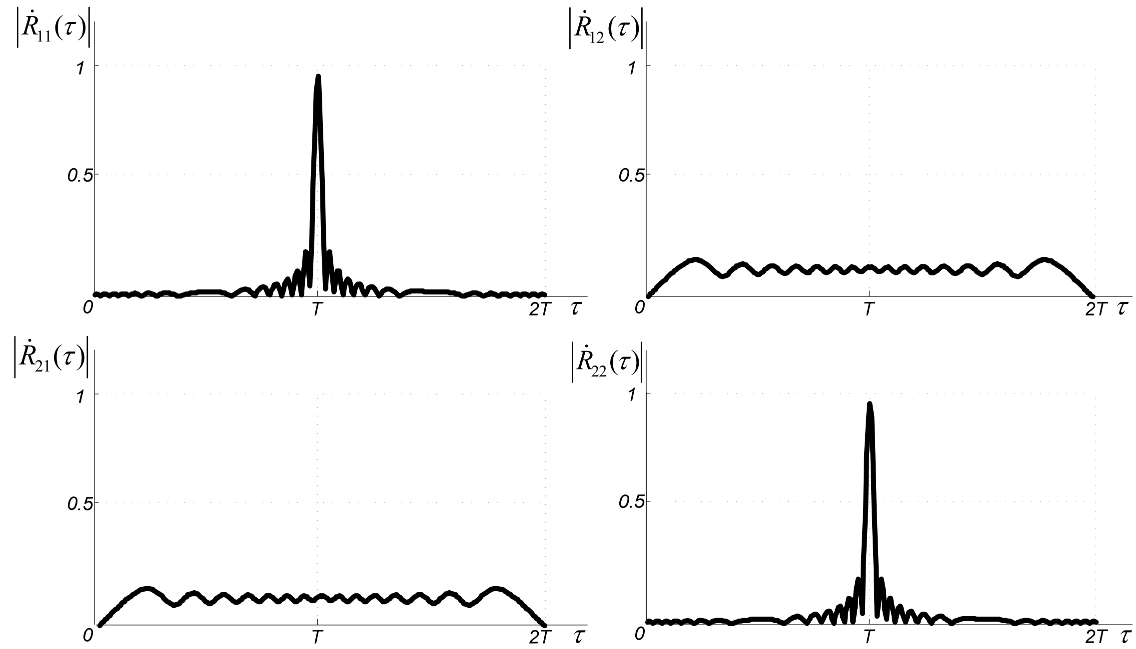

Fig. 2.3 − Auto- and cross- correlation functions of a pair of LFM-signals with opposite slope.

2.2.2 PCM Signals

Signals with phase code modulation (PCM) have a constant amplitude for the transmit duration T and the phase of the carrier changes in the subpulses according a defined code sequence. The phase changes discretely subpulse-to-subpulse with a time interval $\Delta t_{sp} = T/N$, where T is the PCM-signal duration (or signal repetition period), and N is the number of subpulses.

The bandwidth of a PCM-signal is determined by one subpulse bandwidth, which can be expressed as $1/\Delta t_{sp}$ or N/T. As result, the BT-product of a PCM-signal is equal to the number of subpulses N.

The number of phase variations determines the binary and multi-level phase code modulation. Binary codes are most popular in radar applications. The binary code consequences consist of *1* and *0* or *+1* and *–1*. So the phase changes either *0* or π depending on the code sequence elements. An example of such PCM-signal (*m*-sequence length 15: {*1, 1, 1, 1, -1, -1, -1, 1, -1, -1, 1, 1, -1, 1, -1*}) and its envelope is shown in Fig. 2.4.a.

PCM-signal processing is realized at low frequencies (base band)without regarding the carrier frequency. So the correlation function of a PCM-signal corresponds to its compressed envelope. For an *m*-sequence length 15, the compression ratio (BT-product) is equal to 15. The amplitude versus time function of the PCM-signal leads to correlation function as given in Fig. 2.4.b. The relatively small value for the BT-product was chosen for better visibility of the function features. For comparison, this low value is equal to the BT-product of the LFM-signals presented in the previous paragraph (Fig. 2.2 - 2.3).

The main-lobe width of the compressed PCM-signal is derived from the normalized correlation function at an 0.5 level [9, 10, 15]. The main-lobe width for PCM-signals equals to one subpulse duration Δt_{sp}. The range resolution is determined by Eq. 2.19, where $\Delta\tau \equiv \Delta t_{sp}$. It should be noted that additional processing techniques (e.g. weighting) can not change the main-lobe width and so the range resolution, correspondently.

By employing sequences with orthogonal waveforms as orthogonally-polarized components of the vector sounding signal, simultaneous measurement of scattering matrix elements in polarimetric radar can be utilized. This means that this pair of sophisticated PCM signals with orthogonal waveforms can therefore be representative for a pair of orthogonal signals.

When a pair of PCM-signals is used, they can be described by two auto-correlation functions and two cross-correlation functions. Fig. 2.5 shows the absolute values of the auto-correlation functions ($\dot{R}_{11}(\tau)$, $\dot{R}_{22}(\tau)$) and the cross-correlation functions ($\dot{R}_{12}(\tau)$, $\dot{R}_{21}(\tau)$) of two *m*-sequences with BT-product equal to *15* (first code: {*1, 1, 1, 1, -1, -1, -1, 1, -1, -1, 1, 1, -1, 1, -1*}; second code: {*1, 1, 1, 1, -1, 1, -1, 1, 1, -1, -1, 1, -1, -1, -1*}).

The cross-correlation level for PCM-signals (Fig. 2.5) is higher than for LFM-signal (Fig. 2.3) even though the BT-products are equal. The side-lobe level for PCM-signals is nearly uniform while the side-lobes of LFM-signals are high (−13 dB for any BT-product) close to the main lobe and decreasing quickly away from the main-lobe (Fig. 2.3).

PCM-signals are applicable to correlation techniques (using matched filters of correlation receivers) and can not be applied to the de-ramping technique, which is the frequency method in

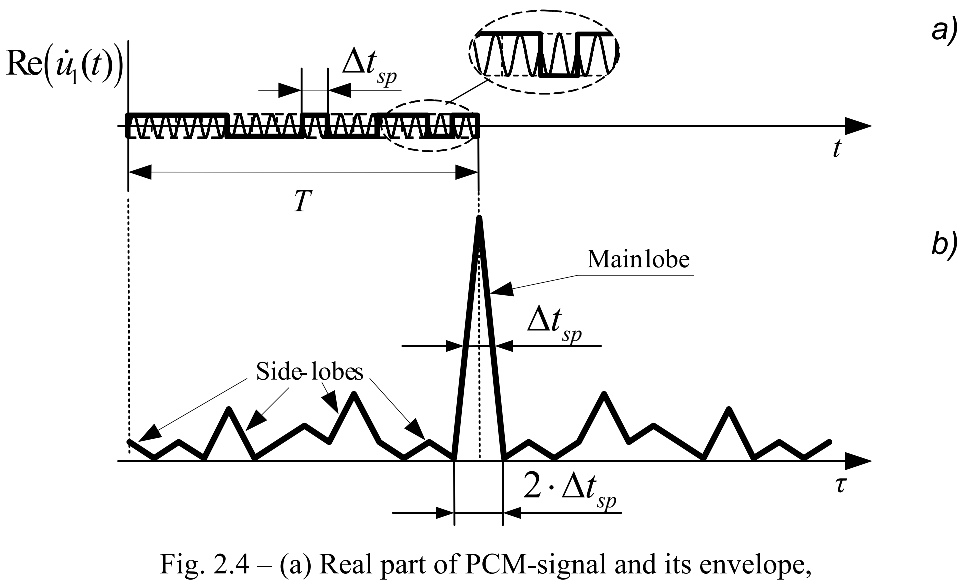

Fig. 2.4 – (a) Real part of PCM-signal and its envelope,
(b) absolute value of its correlation function.

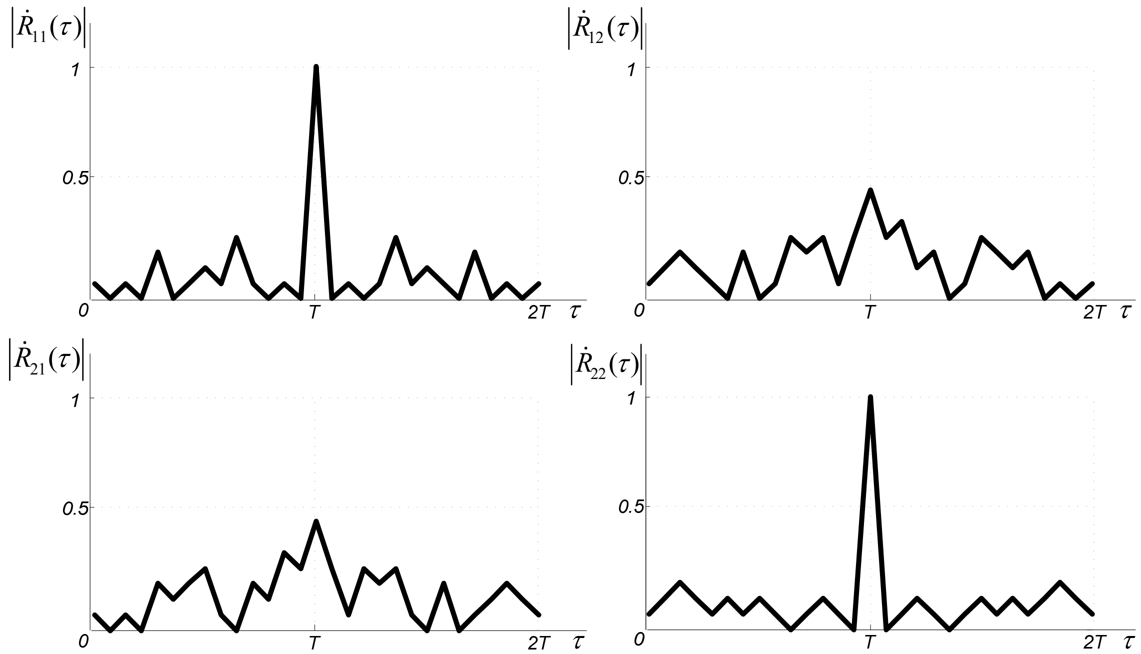

Fig. 2.5 − Auto- and cross- correlation functions of a pair of orthogonal PCM-signals.

LFM range measurements, because the PCM-signal frequency does not depend on the observed object range.

2.2.3 Three Other Types of Sophisticated Signals

Here we consider three other types of frequency and code modulated signals with orthogonal waveforms applicable in the PARSAX radar. All considered signals have equal energy (equal amplitudes and equal durations).

a) Linear superposition of LFM-signals

Waveforms composed of a number of subpulses with constant frequency were proposed in [16] like randomized signals with stepped frequency continuous waveforms. So the randomized LFM-signal (namely the superposition of its parts) is of interest here.

The frequency-time functions, which are considered here as signals, are given in Fig 2.6. The first sophisticated signal is a usual LFM-signal with an up-going chirp. The second sophisticated signal is a linear superposition of parts of an LFM-signal with down-going chirp.

Fig. 2.7 shows the high level of cross-correlation and the comparatively high level of side-lobes for the second sophisticated signal which is the superposition of the down-going LFM-signal (the BT-product of the signals equals to 15 in order to make the comparison with the signals described in previous sections). So, *correlation processing* of these signals is not very interesting.

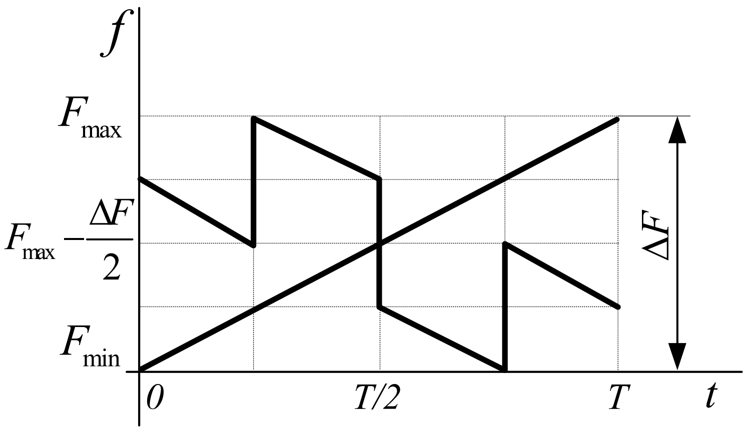

Fig. 2.6 – Frequency variations of two different types of LFM-signals.

In case of *de-ramping processing* (considered in Chapter 3) there is a specific advantage and disadvantage of the here-considered signals compared with the LFM-signals having an opposite slope.

Advantage. The signals at every instant of time are localized at different frequency ranges. That can result in an increased isolation between branches in both channels of the polarimetric radar receiver.

Disadvantage. In case of the de-ramping processing (see Section 3.3.2) a loss of energy will occur, and it will depend on the number of frequency hops.

b) LFM-pulses in different frequency domains

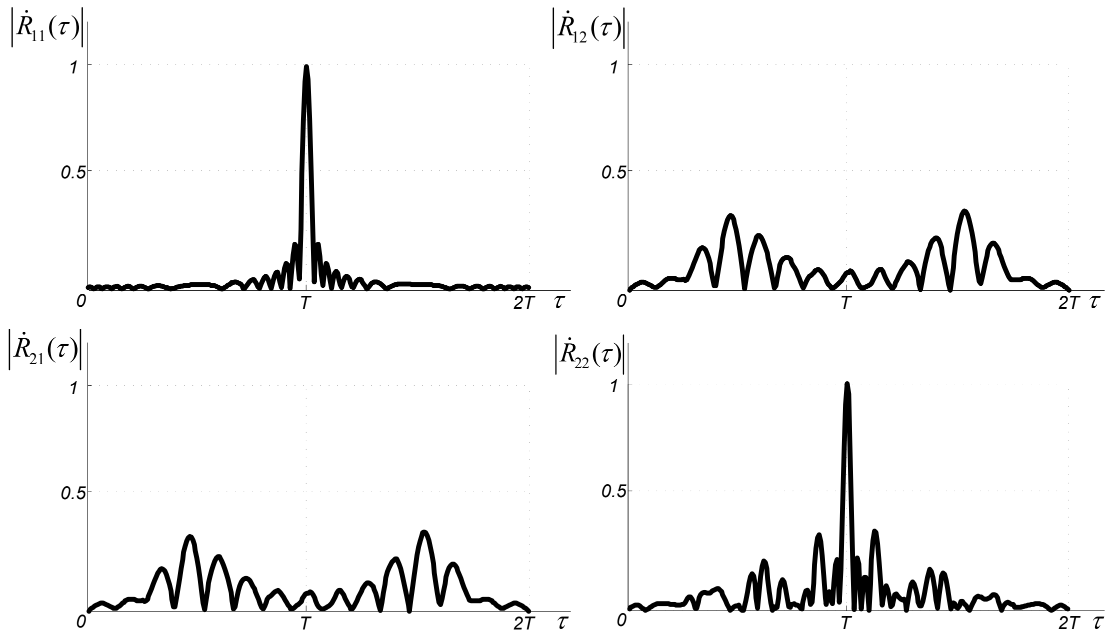

Fig. 2.7 − Auto- and cross- correlation functions of the linear superposition of LFM-signals.

The frequency range of sounding signals in the PARSAX radar is limited to the allowable transmitted signal bandwidth ΔF . One variant of LFM-signals with frequency orthogonality is presented in Fig. 2.8. The advantage and disadvantages of the considered signals compared to the pairs of LFM-signals and PCM-signals are the following.

Advantage. Frequency orthogonality of the vector sounding signal components results in a low cross-correlation level.

Disadvantages. According to Fig. 2.8 the signals have half-bandwidths $\Delta F/2$, of the

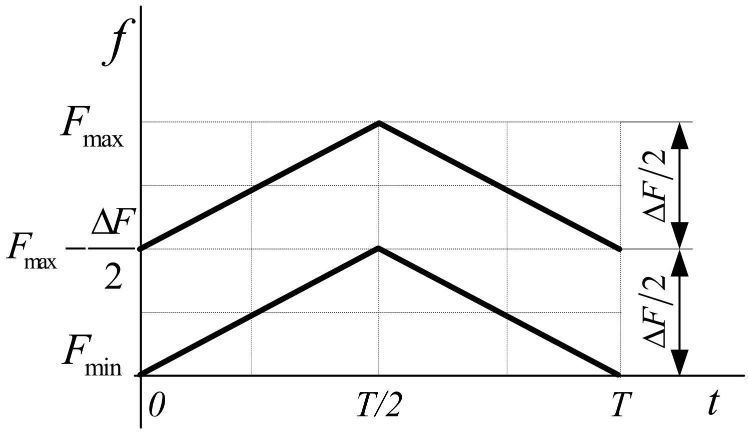

Fig. 2.8 – Shifted frequency-time functions of LFM-signals (one period).

maximum allowable frequency band ΔF . It means a reduction to half of the radar range resolution. Moreover the sounding signals do not occupy overlapping frequency bands; in polarimetric radar it can result in a disparity between the estimations of scattering matrix columns (see Section 2.1).

c) Two LFM-signals with a time shift relative to each other

Two LFM-signals having the same form but a time shift relatively to each other can be utilized in polarimetric radar with continuous waveforms. The frequency-time variations of both signals with time are shown in Fig. 2.9.

Correlation processing of such signals can be utilized in spite of the fact they have the same form and are both localized in the same time and frequency domains. However, the unambiguous range provided by time-shifted LFM-signals will be twice as little than by a pair of LFM-signals with opposite slopes.

De-ramping processing of two LFM-signals with such time shift can still be utilized. The time shift between the LFM-signals is equivalent to a frequency shift. So at every time moment the signals occupy different frequencies what can be interpreted for the de-ramping procedure like extra frequency orthogonality (de-ramping processing is described in Chapter 3). The advantage and disadvantage of the considered signals with regard to LFM-signals with opposite slopes are the following.

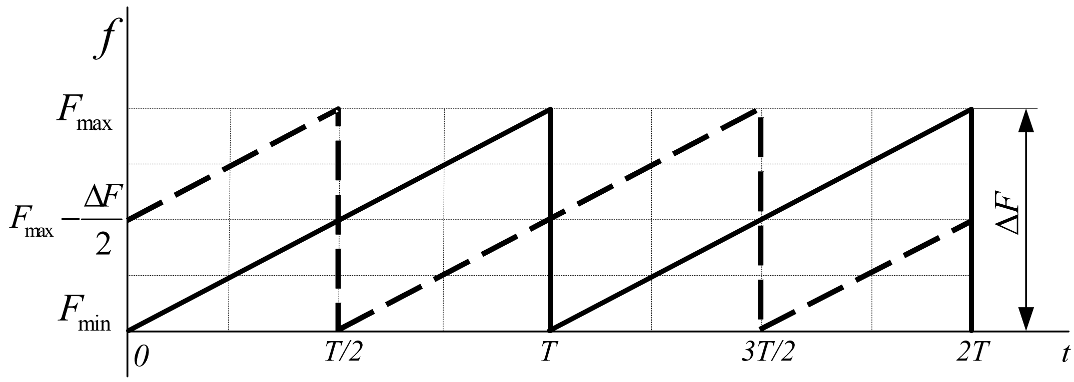

Fig. 2.9 − Frequency-time variations of two continuous LFM-signals with a time shift.

Advantage. Low cross-correlation level can be provided (see Chapter 5).

Disadvantage. Estimation of the scattering matrix columns is realized with a time shift, which can be equal, for example, to half of the sweep-time period $T/2$. So the radar utilizes not simultaneous but quasi-simultaneous measurement of the scattering matrix elements.

The time shift doesn't change the range resolution of the LFM-signals, which corresponds to the signals bandwidth $\Delta F = F_{\max} - F_{\min}$. So, the range resolution remains according to Eq. 2.21.

A detailed analysis of LFM-signals with such a time shift and their application to PARSAX is presented in Chapter 5 of this thesis.

d) FCM-signals

Signals with frequency code modulation (FCM) have a constant amplitude and a carrier frequency, which changes in subpulses according to the code sequence. The use of a sequence of multi-level frequency code modulation determines the number of frequency variations in the carrier for the FCM-signals. In the binary case the code sequences consist of *1* and *0* or *+1* and *–1* and determine two carrier frequencies. Fig. 2.10 shows the FCM-signal with a Barker code of length 7 ({*1, 1, 1, -1, -1, 1, -1*}), T is the transmitted signal length, τ is the subpulse length, *N=7* is the number of subpulses.

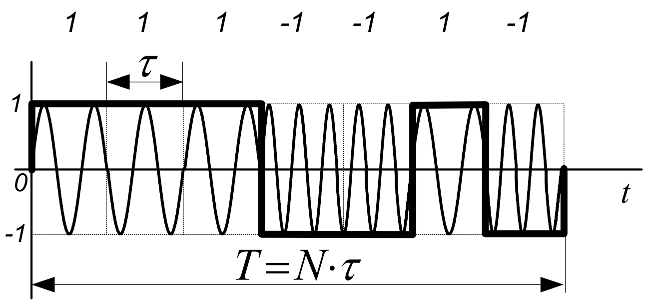

Fig. 2.10 – FCM-signal.

FCM-signal processing is realized at low frequencies (base band) without regarding the high carrier frequencies. The BT-product for FCM-signals (as well as for PCM-signals) equals to the number of subpulses (N). The correlation functions of FCM-signals are identical to the correlation functions of PCM-signals. So FCM-signals have the same advantages as PCM signals.

The disadvantage of FCM-signals in comparison to PCM-signals is that the scattering properties of the radar object may be different for different sounding frequencies. High-frequency radar demands a wide bandwidth for sounding signals. However, the frequency difference in the carrier oscillations can, therefore, not be small. So, the values of the scattering matrix elements for different sounding frequencies (which correspond to the different parts of the signal, see Fig. 2.10) can result in additional errors in the estimation of the scattering matrix elements.

This disadvantage essentially limits the FCM-signals application in high-resolution polarimetric radar.

2.3 Conclusion

The chapter has described the concept of sophisticated dual-orthogonal polarimetric radar signals. All types of signal orthogonality have been analyzed concerning to their applicability in polarimetric radar with simultaneous measurement of scattering matrix elements. Sophisticated signals with orthogonal waveforms and their applications have been considered.

References

1. IEEE Standard Numer 149-1979: Standard Test Procedures 1973, Revision of IEEE Stds. 145-1969, Definitions of Terms for Antennas, Published by the Institute of Electrical and Electronics, Inc., New York, 1979.
2. D.B. Kanareykin, N.F. Pavlov, V.A. Potekhin, “Polarization of Radar Signals” [in Russian] edited by V.Y. Dulevich, Moscow: Sovetskoe Radio, 1966.
3. O.A. Krasnov, L.P. Ligthart, Z. Li, P. Lys, F. van der Zwan, “The PARSAX – Full Polarimetric FMCW Radar with Dual-Orthogonal Signals”, Radar Conference, 2008, EuRAD 2008, Oct. 2008, pp. 84-87.
4. D. Guili, M. Fossi, L. Facheris, “Radar Object Scattering Matrix Measurement through Orthogonal Signals”, IEEE Proceedings-F, Vol. 140, № 4, August 1993.
5. D.R. Wehner, “High-Resolution Radar”, second edition, Artech House, Inc., 1995.
6. D. Giuli, M. Fossi, L. Facheris, "Radar Target Scattering Matrix Measurement through Orthogonal Signals," IEEE Proceedings, Part F. Radar and Signal Processing, vol. 140, Aug. 1993, pp. 233-242.

7. C. Titin-Schnaider and S. Attia, “Calibration of the MERIC Full-Polarimetric Radar: Theory and Implementation”, Aerospace Science and Technology, Vol. 7, Dec. 2003, pp. 633-640.
8. M. Jankiraman, “Design of Multi-Frequency CW Radars”, Scitech Publishing, Inc., 2007.
9. G. Galati, “Advanced Radar Techniques and Systems”, Peter Peregrinus Ltd., 1993.
10. S.D. Blunt, K. Gerlach, “Adaptive pulse compression repair processing”, Radar Conference, 2005 IEEE International 9-12 May 2005, pp. 519-523.
11. C. E. Cook, M. Bernfeld, Radar signals. New York, Academic Press, 1967.
12. N. Levanon, E. Mozeson, “Radar Signals”, John Wiley & Sons, Inc., 2004.
13. G. Sosulin, “Theoretical Foundations of Radar and Navigation”, Radio i Svyaz', Moscow, 1992 (in Russian).
14. V. Dulevich et al., Theoretical Foundations of Radar, Soviet Radio, Moscow, 1978 (in Russian).
15. I.N. Amiantov, “Selected Problems of Statistical Theory of Communication”, Moscow: Sovetskoe Radio, 1971 (in Russian).
16. A. Meta, “Signal Processing of FMCW Synthetic Aperture Radar Data”, Dissertation at Delft University of Technology, 2006.

3 Processing of the Dual-Orthogonal Sophisticated Radar Signals

This chapter presents an overview of possible techniques for the compression of dual-orthogonal sophisticated signals. A comparison of the described correlation processing and de-ramping processing is made.

3.1 Introduction to Optimum Filtering in Polarimetric Radar

There are a few different criteria in optimum filtering techniques:

- signal-to-noise criterion,
- likelihood ratio criterion (in statistical decision theory or parameter estimation theory),
- Bayesian probability criterion,

which are created in order to extract the desired information from the received radar signal most efficiently [1]. The last two criteria are related to the decision-making theory, which is not considered in this thesis. So here optimum filtering means maximization of the signal-to-noise ratio (SNR).

If noise is considered to be additive, stationary and uncorrelated with the signal scattered by the observed object then the optimum filter for SNR maximization is the matched filter and correlator.

In case of radar signal processing the matched filter and correlator are optimal for additive white Gaussian noise only when the radar object can be represented as a point scatterer. If the radar object includes a set of scatterers then the filters are not optimal. However there are re-iterative algorithms using the filter output signal for estimation of the complex radar object and for reprocessing the input signal [2-4]. The matched filter and correlator are also not optimum for object detection in strong clutter [5]. In these circumstances different algorithms for clutter suppression can be applied [6, 7]. However, for a prior uncertainty concerning a radar object affected by additive white Gaussian noise, the matched filter and correlator are used as optimum filters.

An optimum filter uses the known form of the transmitted signal. In polarimetric radar with simultaneous measurement of scattering matrix elements the transmitted signal is formed with two sophisticated signals having orthogonal waveforms (see Section 2.2). Let $\dot{u}_1(t)$ and $\dot{u}_2(t)$ be complex signals simultaneously transmitted via two orthogonal polarizations (1 – horizontal, 2 – vertical). When neglecting noise, the received vector signal $\dot{\mathbf{x}}(t) = \begin{bmatrix} \dot{x}_1(t) & \dot{x}_2(t) \end{bmatrix}^T$ can be written as multiplication of the radar object scattering matrix and vector sounding signal:

$$\dot{\mathbf{x}}(t) = \dot{\mathbf{S}}(t - \tau/2) \cdot \dot{\mathbf{u}}(t - \tau), \tag{3.1}$$

where τ is the time delay of the received signal. Eq. 3.1 can be written as

$$\begin{bmatrix} \dot{x}_1(t) \\ \dot{x}_2(t) \end{bmatrix} = \begin{bmatrix} \dot{S}_{11}(t-\tau/2)\cdot\dot{u}_1(t-\tau) + \dot{S}_{12}(t-\tau/2)\cdot\dot{u}_2(t-\tau) \\ \dot{S}_{21}(t-\tau/2)\cdot\dot{u}_1(t-\tau) + \dot{S}_{22}(t-\tau/2)\cdot\dot{u}_2(t-\tau) \end{bmatrix}, \tag{3.2}$$

where $\dot{x}_1(t)$ and $\dot{x}_2(t)$ are the received signal components having orthogonal polarizations.

When optimal processing is performed the *a-priori* knowledge about the forms of the transmitted waveforms is used for maximizing the signal-to-noise ratio. The impulse response is equal to the time-reversed conjugate of the signal waveform. It means that for processing of the vector sounding signal the impulse response function of the optimal filter $\dot{\mathbf{h}}(t)$ has to be equal to

$$\dot{\mathbf{h}}(t) = \dot{\mathbf{u}}^*(-t), \tag{3.3}$$

or

$$\begin{bmatrix} \dot{h}_1(t) \\ \dot{h}_2(t) \end{bmatrix} = \begin{bmatrix} \dot{u}_1^*(-t) \\ \dot{u}_2^*(-t) \end{bmatrix}, \tag{3.4}$$

where the superscript (*) represents the complex conjugate. The frequency response function $\dot{\mathbf{H}}(f)$ of the filter is therefore the complex conjugate of the signal spectrum $\dot{\mathbf{U}}(f)$:

$$\dot{\mathbf{H}}(f) = \dot{\mathbf{U}}^*(f), \tag{3.5}$$

or

$$\begin{bmatrix} \dot{H}_1(f) \\ \dot{H}_2(f) \end{bmatrix} = \begin{bmatrix} \dot{U}_1^*(f) \\ \dot{U}_2^*(f) \end{bmatrix}. \tag{3.6}$$

When sophisticated sounding signals are used, the compression of the received signals has to be done in the radar receiver. This compression and consequent SM estimation can be implemented in time domain or in frequency domain. For example, the scattering matrix estimation can be defined using the correlation integral (signal compression in time domain):

$$\hat{\dot{\mathbf{S}}}(\tau) = \int_{-\infty}^{\infty} \dot{\mathbf{x}}(t) \cdot \dot{\mathbf{h}}^*(\tau - t)dt \tag{3.7}$$

The limits of the integral (3.7) are equal to infinity assuming non-periodic signals for the following reasons. The received signal should be considered as non-periodic, although the transmitted signal is periodic. This behavior can be explained since the received signal varies over time (see Chapter 1) because the relative phase shifts between object scatterers change in time. For this reason simultaneous measurement of scattering matrix elements are needed. Also the polarimetric radar with continuous waveforms utilizes estimations over each period. So, in general, the received signal can not be considered as fully periodic. For de-ramping processing (see Paragraph 3.3.2) periodicity is not required because the signal, which is processed each period, corresponds to one definite period of the sounding signal.

For correlation processing (Paragraphs 3.2.1, 3.2.2 and 3.3.1) the non-periodicity of the received signal does matter. The analyzed time interval of the received signal may contain a part of a scattered signal, which corresponds to previous period(s) of the sounding signal. But this part is less than the repetition period. So, side-lobes located far from the main-lobe of the compressed signal can be slightly different for a non-periodic signal and the identical periodic signal. This error takes place but the use of the non-periodic signal model is more valid than the use of the periodic signal model for the received radar signals.

In terms of an input echo signal $\dot{\mathbf{x}}(t)$ and impulse response of the optimal filter $\dot{\mathbf{h}}(t)$ the convolution integral in Eq. (3.7) can also be written as

$$FT\left[\int_{-\infty}^{\infty} \dot{\mathbf{x}}(t) \cdot \dot{\mathbf{h}}^{*}(\tau - t) dt\right] = \dot{\mathbf{X}}(f) \cdot \dot{\mathbf{H}}^{*}(f), \tag{3.8}$$

where FT means Fourier transform.

Optimum filtering can be realized in time domain like a convolution or in frequency domain like spectra multiplication because convolution in time domain corresponds to multiplication in frequency domain and vice versa.

When the radar observes moving objects, the set of filters should take into account the objects' motion and overlap in possible velocities via the Doppler effect in case of the narrow-band model or via the scaling effect in case of the wide-band model. The influence of object motion on the signal processing when sophisticated sounding signals are used, is considered in Chapter 4.

In this chapter four methods and the corresponding filters' schemes are described. All methods utilize compression of sophisticated signals. The first three methods (Paragraphs 3.2.1, 3.2.2, 3.3.1) are considered to be optimal; they can be named "correlation processing". The fourth method (de-ramping processing, Paragraph 3.3.2) using the stretch technique [8] is not optimal, because it does not maximize SNR. However the de-ramping processing has an undisputed advantage of simplicity, so it is used widely [9, 10].

3.2 Algorithms and Performance of Polarimetric Signal Processing in Time-Domain

3.2.1 Multi-Channel Correlator

In order to obtain the estimations of all scattering matrix elements the orthogonally-polarized components of the received signal are simultaneously correlated in separate branches with the delayed replicas of $\dot{u}_1(t)$ and $\dot{u}_2(t)$ or, equivalently saying, the components are processed by filters matched to $\dot{u}_1(t)$ and $\dot{u}_2(t)$ (see Fig. 3.1) [11, 12]. The processing of the received signals with orthogonal polarizations ($\dot{x}_1(t)$ and $\dot{x}_2(t)$) takes place in Channel 1 and Channel 2, respectively.

The use of the correlator assumes *a-priori* knowledge of the time delay and initial phase of the received signal. The unknown initial phase requires handling of in-phase and quadratures-phase components of the received signal.

The receiver calculates the correlation integral between the vector input signal, $\dot{\mathbf{x}}(t) = \begin{bmatrix} \dot{x}_1(t) & \dot{x}_2(t) \end{bmatrix}$, and the copy of the sounding signal, $\dot{\mathbf{u}}(t-\tau_0) = \begin{bmatrix} \dot{u}_1(t-\tau_0) & \dot{u}_2(t-\tau_0) \end{bmatrix}^T$, with the expected time shift, τ_0. We derive:

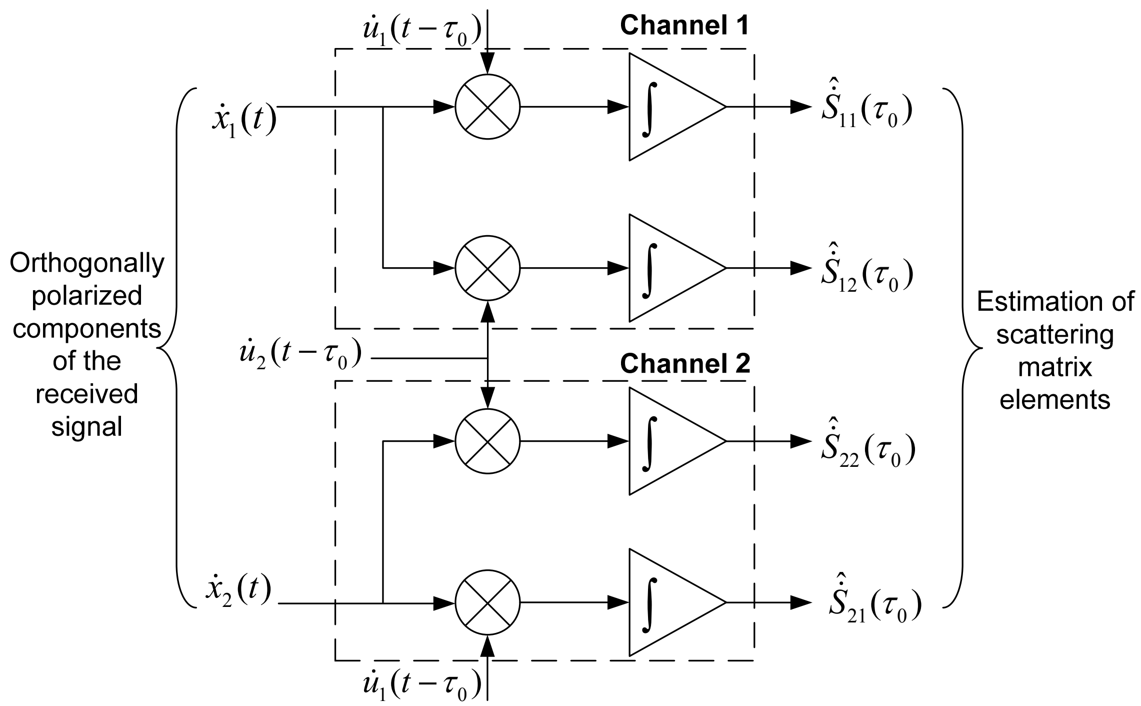

Fig. 3.1 – Simplified scheme of the correlator.

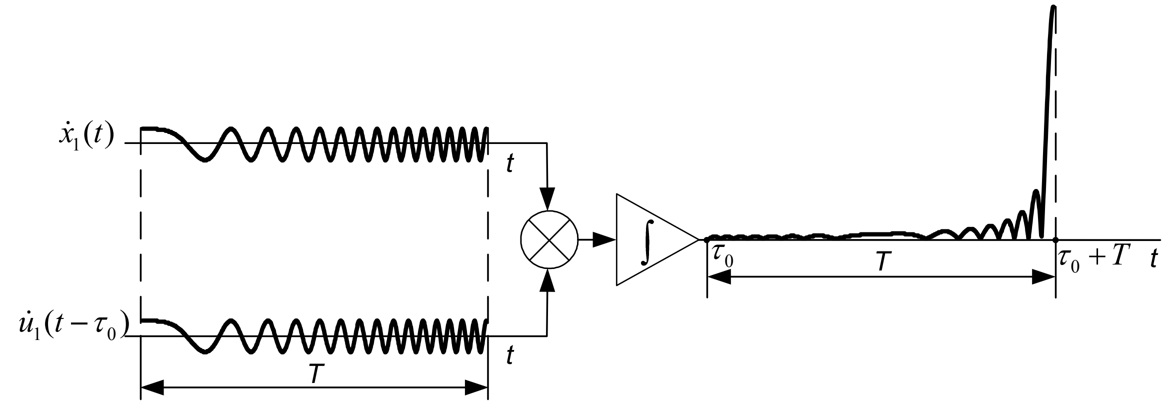

Fig. 3.2 – Compression of the known signal in the correlator.

$$\begin{bmatrix} \hat{\hat{S}}_{11}(\tau_0) & \hat{\hat{S}}_{12}(\tau_0) \\ \hat{\hat{S}}_{21}(\tau_0) & \hat{\hat{S}}_{22}(\tau_0) \end{bmatrix} = \begin{bmatrix} \int\limits_{\tau_0}^{\tau_0+T} \dot{x}_1(t)\cdot\dot{u}_1^*(t-\tau_0)dt & \int\limits_{\tau_0}^{\tau_0+T} \dot{x}_1(t)\cdot\dot{u}_2^*(t-\tau_0)dt \\ \int\limits_{\tau_0}^{\tau_0+T} \dot{x}_2(t)\cdot\dot{u}_1^*(t-\tau_0)dt & \int\limits_{\tau_0}^{\tau_0+T} \dot{x}_2(t)\cdot\dot{u}_2^*(t-\tau_0)dt \end{bmatrix}, \quad (3.9)$$

where τ_0 is constant, $\hat{\hat{S}}_{ij}(\tau_0)$, *i, j = 1,2*, are four values, namely the estimations of the scattering matrix elements for a predetermined (expected) time delay τ_0, which is a constant for one measurement, T is the sounding signal duration (FM-CW radar duty cycle). The expected time delay τ_0 can not be more than T for FM-CW radar. When τ_0 is more than T, the ambiguity in range estimation appears. The integrals are calculated within the time interval $\left[\tau_0 ... \tau_0+T\right]$. The boundaries for integration are fixed because the signals are assumed to be synchronized with each other and all having *T*-duration.

Fig. 3.2 shows the signal processing when the replica, $\dot{x}_1(t)$, is a delayed LFM sounding signal, $\dot{u}_1(t-\tau_0)$, having the same initial phase. The correlator output gives half of the correlation function of the signal.

The scheme presented in Fig. 3.2 can be used if both time delay and initial phase of the received signal are known. The initial phase of a signal received by a radar system is unknown, so each branch of the correlation receiver has to be splitted so that two quadratures exist.

Eq. 3.9 gives the estimations of SM elements for one time delay (τ_0) only and is therefore a result for one range. For observation of all ranges simultaneously many correlators (branches, channels) adopted for all possible time delays (all observed ranges) have to be used. For this reason the correlator is usually named *multi-channel correlator*. For high-resolution radar a large number of range-dependent channels is demanded. It complicates the scheme significantly. In addition, if the observed object motion has to be taken into account as well, extra sets of channels are needed to overlap the possible velocities of moving objects. Furthermore in case of polarimetric radar with simultaneous measurement of scattering matrix elements the number of branches is multiplied by four. So the final scheme is complicated significantly. The correlator will not be considered in the following chapters.

3.2.2 Matched Filter

By definition the matched filter is a filter which, for a specified signal waveform, will result in the maximum attainable signal-to-noise ratio at the filter output when both signal and additive white Gaussian noise have passed the filter [13, 14].

The idea behind the matched filter is correlation using convolution. The estimations of the scattering matrix elements in case of matched filtering for polarimetric radar with continuous waveforms are calculated from:

$$\begin{bmatrix} \hat{\dot{S}}_{11}(\tau) & \hat{\dot{S}}_{12}(\tau) \\ \hat{\dot{S}}_{21}(\tau) & \hat{\dot{S}}_{22}(\tau) \end{bmatrix} = \begin{bmatrix} \int\limits_0^{2T} \dot{x}_1(t)\cdot\dot{u}_1^*(\tau-t)dt & \int\limits_0^{2T} \dot{x}_1(t)\cdot\dot{u}_2^*(\tau-t)dt \\ \int\limits_0^{2T} \dot{x}_2(t)\cdot\dot{u}_1^*(\tau-t)dt & \int\limits_0^{2T} \dot{x}_2(t)\cdot\dot{u}_2^*(\tau-t)dt \end{bmatrix}. \tag{3.10}$$

where $\hat{\dot{S}}_{ij}(\tau)$, *i, j = 1,2*, are the estimation of the scattering matrix elements as function of time delay (range). For radars with continuous waveforms and duty cycle T the integrals are calculated within the time interval $\left[0...2T\right]$. The roundtrip time delay, τ, can not exceed the FM-CW radar duty cycle, T, because of possible ambiguity in range estimation.

The principle of matched filtering is shown in Fig. 3.3. The matched filter (MF) for a discrete case is presented by a multi-tapped delay line which impulse response corresponds to $\dot{h}_1(\tau)=\dot{u}_1^*(\tau-t)$ and an adder (integrator equivalent). The marks "1" and "2" correspond to the beginnings and ends of the input signal and delay line, respectively.

For polarimetric radar with simultaneous measurement of scattering matrix elements the

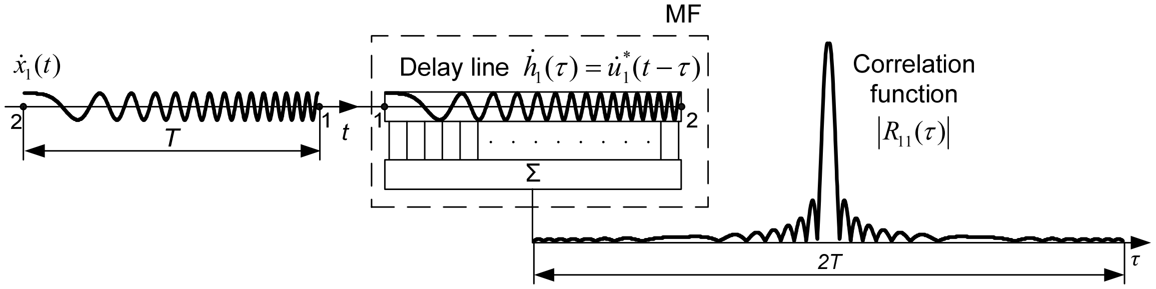

Fig. 3.3 – Signal compression in the matched filter.

receiver includes four matched filters (Fig. 3.4), whose impulse responses ($\dot{h}_1(\tau)$ and $\dot{h}_2(\tau)$) are the time-reverse conjugate of the vector sounding signal components ($\dot{u}_1(t)$ and $\dot{u}_2(t)$).

3.3 Algorithms and Performance of the Polarimetric Signal Processing in Frequency-Domain

3.3.1 Matched Filtering in Frequency Domain (via direct FFT Multiplication)

Matched filtering in frequency domain is based on the fact that convolution in time domain is equivalent to multiplication in frequency domain. So the convolution can employ a Fourier transform (FT) process equivalent for convolution. In the dissertation we assume that in practice the frequency spectrum is calculated via the Fast Fourier Transform (FFT); we therefore use FFT hereinafter. The process is sometimes called *fast convolution* [15].

The algorithm of matched filtering in frequency domain requires the following steps [15, 16]:
– convert the received signal to frequency domain (by using the Fast Fourier Transform − FFT);
– multiply the output with the frequency domain version of the reference function;
– convert the product back to time domain (by using the Inverse Fast Fourier Transform − IFFT).

In case of polarimetric radar with simultaneous measurement of scattering matrix elements both components of the received signal, $\dot{x}_1(t)$ and $\dot{x}_2(t)$, are converted to the frequency domain and multiplied with the spectra of complex conjugated replicas of the transmitted waveforms ($\dot{u}_1(t)$, $\dot{u}_2(t)$). The conversion of the products back to time domain using FFT results into compressed range data, namely into estimations of the scattering matrix elements. The complex

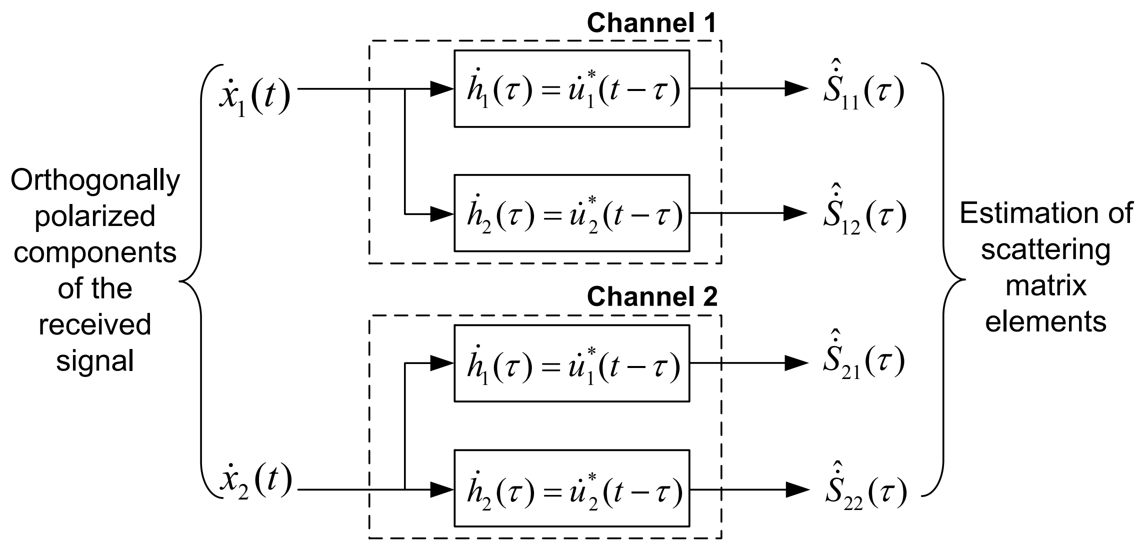

Fig. 3.4 − Matrix matched filter (processing in time domain).

conjugation of the spectra is realized by the blocks with the ( )*-superscript (Fig. 3.5). It should be noted that although the processing is realized in frequency domain the estimations of scattering matrix elements are functions of time (namely of the roundtrip time delay, τ):

$$\begin{bmatrix} \hat{\dot{S}}_{11}(\tau) & \hat{\dot{S}}_{12}(\tau) \\ \hat{\dot{S}}_{21}(\tau) & \hat{\dot{S}}_{22}(\tau) \end{bmatrix} = IFFT \begin{bmatrix} \dot{X}_1(f)\cdot\dot{U}_1^*(f) & \dot{X}_1(f)\cdot\dot{U}_2^*(f) \\ \dot{X}_1(f)\cdot\dot{U}_1^*(f) & \dot{X}_2(f)\cdot\dot{U}_2^*(f) \end{bmatrix}. \tag{3.11}$$

where $\hat{\dot{S}}_{ij}(\tau)$, *i, j = 1,2*, are estimations of the scattering matrix elements and the superscript (*) means complex conjugation. $\dot{X}_1(f)$ and $\dot{X}_2(f)$ are the signals spectra received with orthogonal (horizontal and vertical) polarizations, $\dot{U}_1(f)$ and $\dot{U}_2(f)$ are the spectra of the vector sounding signal components with orthogonal polarizations.

We remark here that a polarimetric radar with continuous waveforms gives estimations of SM elements every duty cycle, knowing that the received signal can not be considered as periodic. So the spectra (Eq. 3.11) do not have a discrete form as spectra of periodic signals.

The matched filtering in frequency domain corresponds to matched filtering in time domain, because convolution in time domain corresponds to multiplication in frequency domain. The choice for matched processing (performed in time domain or in frequency domain) depends on technological possibilities. Digital signal processing with filter kernels shorter than about 60 points

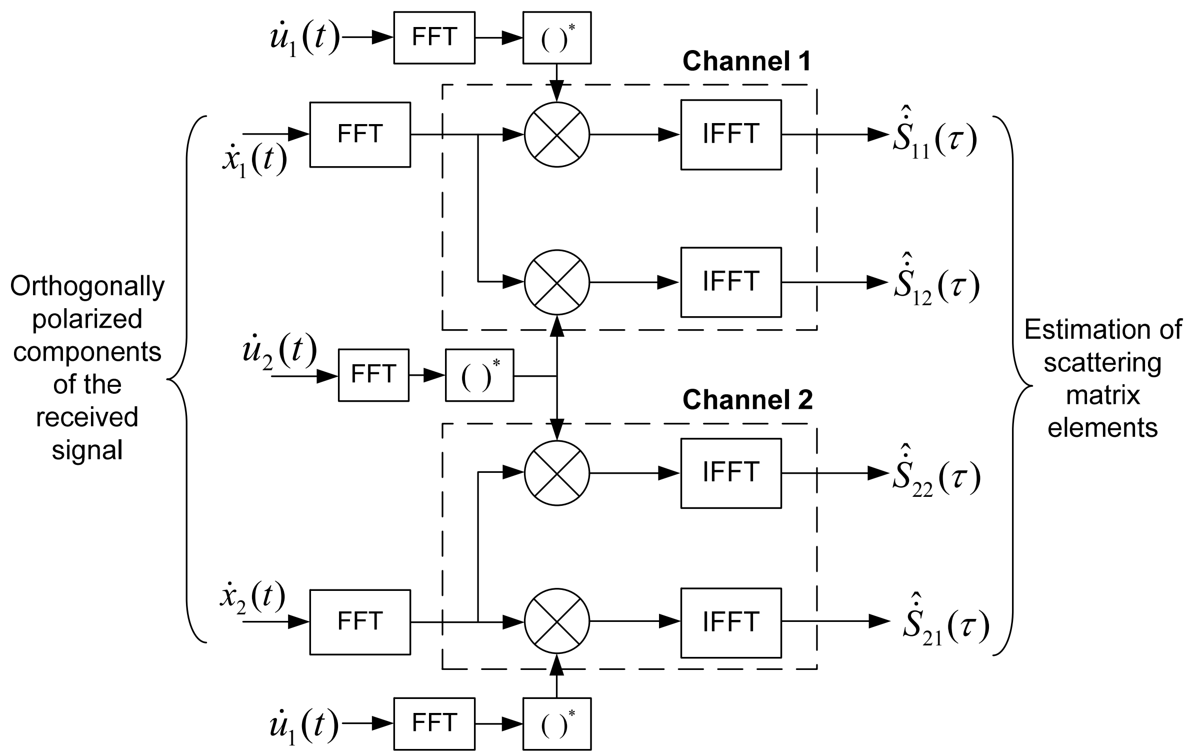

Fig. 3.5 − Matched filter (processing in the frequency domain).

matched filtering can be implemented faster with standard convolution (in time domain, Paragraph 3.2.2), where the execution time is proportional to the kernel length; longer filter kernels can be implemented faster with FFT-convolution (in frequency domain, as presented in the current paragraph) [17].

3.3.2 De-ramping Processing of LFM-signals

An alternative for correlation processing is the signal compression approach using the de-ramping processing which is applicable to frequency modulated signals, and LFM-signals in particular. Radars using sounding signals with continuous waveforms and utilizing the de-ramping procedure are named *FM-CW radars* [18] where FM-CW means "frequency-modulated continuous waves". Sounding LFM-signals are used taking into consideration that the receiver starts receiving the backscattered signals while the transmitter is still transmitting.

The de-ramping technique is a frequency method of range measurement which is used in radar with continuous waveforms [9, 10], specifically in radar with large BT-product signals having linear frequency modulation, also called frequency modulated (FM) ramps [15]. The estimations of the observed range profiles are calculated in frequency domain.

De-ramping processing is also called "active correlation" [13] or "de-ramp FFT" [20] and is a kind of "stretch processing" [21].

Fig. 3.6 shows a simplified scheme of a de-ramping filter for polarimetric radar with simultaneous measurement of scattering matrix elements. In order to obtain the estimations of all

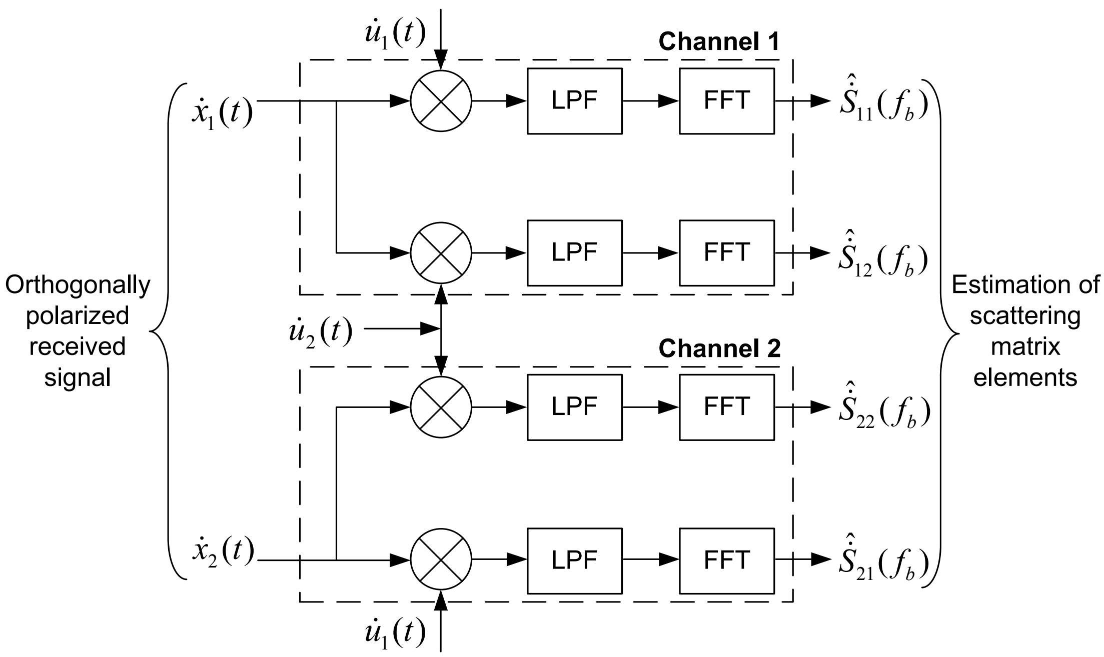

Fig. 3.6 – Simplified scheme for the de-ramping filter approach.

scattering matrix elements each of the received signals ($\dot{x}_1(t)$, $\dot{x}_2(t)$) is mixed with replicas of the transmitted waveforms ($\dot{u}_1(t)$, $\dot{u}_2(t)$) and is reduced in slope, i.e. the signals are de-ramped. The signals after demodulation and low-pass filtering are called the beat signals. By applying a Fourier transform (that is the Fast Fourier Transform - FFT) onto the beat signals, the resulting spectrum as a function of beat frequencies (f_b) for each ramp corresponds to range profiles for all four elements of the scattering matrix. The processing is summarized by

$$\begin{bmatrix} \hat{\dot{S}}_{11}(f_b) & \hat{\dot{S}}_{12}(f_b) \\ \hat{\dot{S}}_{21}(f_b) & \hat{\dot{S}}_{22}(f_b) \end{bmatrix} = FFT\left[LPF\begin{bmatrix} \dot{x}_1(t)\cdot\dot{u}_1^*(t) & \dot{x}_1(t)\cdot\dot{u}_2^*(t) \\ \dot{x}_2(t)\cdot\dot{u}_1^*(t) & \dot{x}_2(t)\cdot\dot{u}_2^*(t) \end{bmatrix}\right], \text{ for } t\in\left[\tau_{\max}...T\right] \tag{3.12}$$

where FFT means Fast Fourier transform, LPF means low-pass filtration, $\tau_{\max}$ is maximum time delay of the received signal and T is the LFM-signals' sweep time which equals the duty cycle of the radar with continuous waveforms. Beat frequencies are analyzed in the frequency band $(0...f_{b\max}]$. The maximum beat frequency ($f_{b\max}$) is defined in the low-pass filters (LPFs) and determines the maximum time delay ($\tau_{\max}$) and therefore the maximum observed range ($R_{\max}$).

Fig. 3.7 explains the principle of the de-ramping procedure. The beat frequency (f_b) is a measure for the object range [22, 23]. The received signal has a time shift relative to the transmitted one. The time shift of an LFM-signal corresponds to its beat frequency shift, which is proportional to the roundtrip time delay τ (Fig. 3.7.a):

$$f_b = \frac{\Delta F}{T}\tau, \tag{3.13}$$

where ΔF is the frequency sweep, T is the sweep repetition interval. The roundtrip time delay τ is connected with the observed object range R via

$$f_b = \frac{\Delta F}{T}\cdot\frac{2R}{c}, \tag{3.14}$$

where c is the light velocity. The de-ramping filter (Fig. 3.6) includes LPFs whose boundary frequencies determine $\tau_{\max}$ and so $R_{\max}$ of the radar objects under observation.

When more than one point object is observed by the radar the mixers' outputs will contain more than one beat frequency. Since the system is assumed to be linear, there will be a frequency component corresponding to each point object (or each resolution cell). In principle, the range to each object may be determined by measuring the individual frequency components.

De-ramping processing is a kind of signal compression. A Fourier transform applied to the sinusoidal beat signals with $(T-\tau_{\max})$-duration transforms (compresses) into one corresponding beat frequency spectrum. The signal-to-noise ratio is increased depending on the BT-product of the sounding LFM-signal [13].

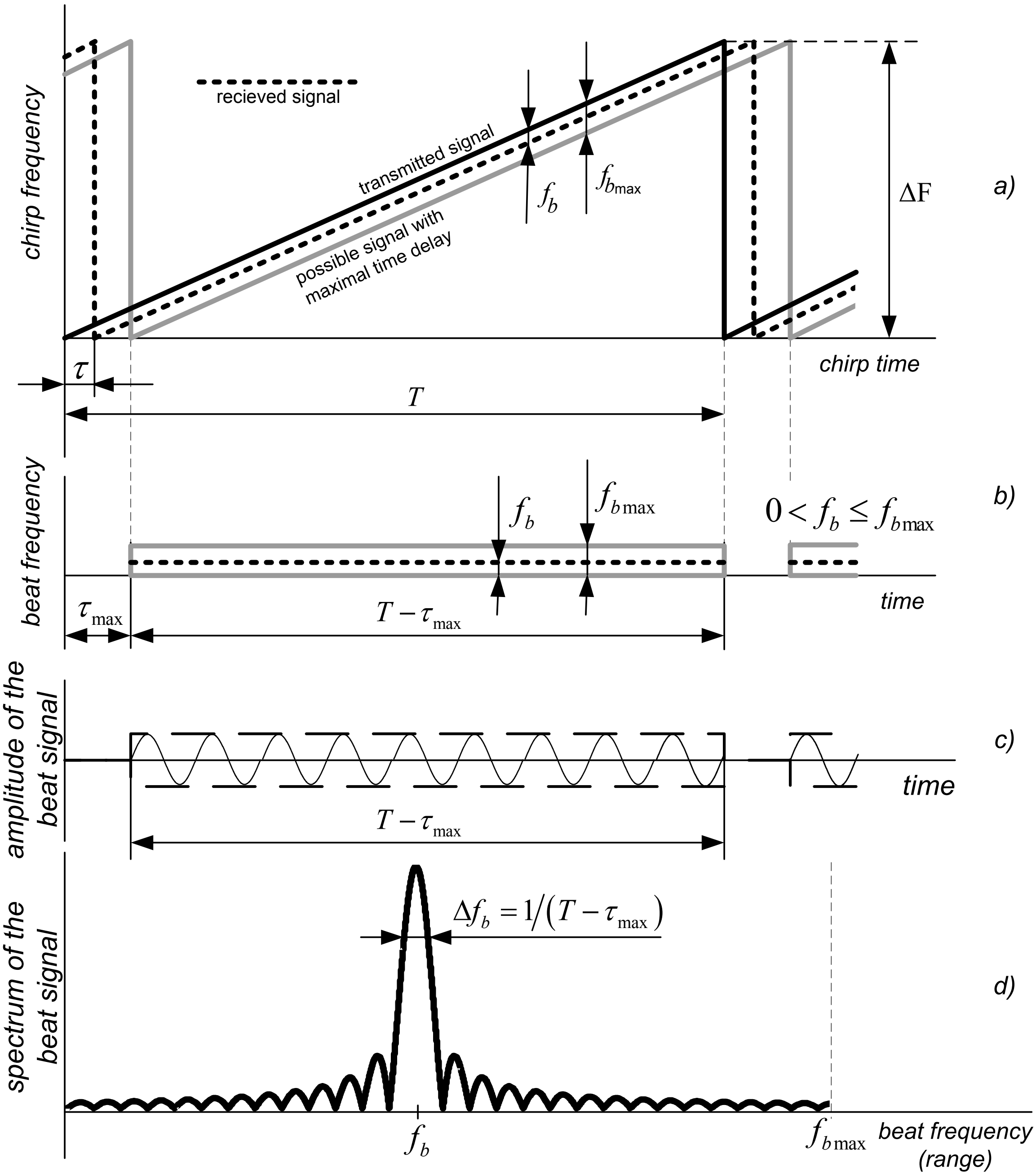

Fig. 3.7 – Overview of the FM-CW principle.

a) Frequency plot of the chirp signal.

b) Beat frequency of the signal proportional to object range.

c) Amplitude of the beat signal

d) Spectrum of the beat signal (compressed signal).

The range resolution in the de-ramping procedure should be considered separately. It is not determined from the correlation function main-lobe width like for the correlation methods (see previous paragraphs). The range resolution for the de-ramping processing is determined from the spectra width of the compressed de-ramped signals which are pulsed sine-signals. So the range is determined in frequency domain from the sine-signal of limited duration. If the sine-waves were continuous, their spectra would have been delta-functions. For a pulsed sinusoid (beat signal) the spectrum bandwidth is inversely proportional to its duration, $\Delta f_b = 1/(T - \tau_{\max})$, (Fig. 3.7.c).

The maximum object range is determined from the maximum time delay of the echo signal ($\tau_{\max}$) and is given by (Fig. 3.7.a):

$$\tau_{\max} = \frac{T}{\Delta F} f_{b\max}, \tag{3.15}$$

where $f_{b\max}$ is the maximum beat frequency. From Eq. 3.13 we derive for the maximum range

$$R_{\max} = \frac{T \cdot f_{b\max}}{\Delta F} \cdot \frac{c}{2}. \tag{3.16}$$

Eq. 3.16 means that the maximum beat frequency ($f_{b\max}$) is proportional to the maximum object range ($R_{\max}$). The beat signal bandwidth (Δf_b) is proportional to the range resolution (ΔR). This can be written as

$$\begin{cases} f_{b\max} \sim R_{\max}; \\ \Delta f_b \sim \Delta R. \end{cases} \tag{3.17}$$

The range resolution can be expressed as

$$\Delta R = \frac{\Delta f_b \cdot R_{\max}}{f_{b\max}} = \frac{R_{\max}}{f_{b\max} \cdot (T - \tau_{\max})}. \tag{3.18}$$

From equations (3.16) and (3.18) we compute the range resolution after de-ramping processing

$$\Delta R = \frac{T}{\left(T - \tau_{\max}\right)} \cdot \frac{c}{2 \cdot \Delta F}. \tag{3.19}$$

So the range resolution after de-ramping processing is worse in comparison with correlation methods by the factor $\frac{T}{\left(T - \tau_{\max}\right)}$. This factor shows the degradation in range resolution due to processing over the limited time interval $\left(T - \tau_{\max}\right)$. Fig. 3.8 shows the degradation in range resolution depending on the maximum measured time delay, proportional to the maximum object range. For instance for a ratio of maximum time delay to sweep time equal to 1:10, we find a range resolution degradation, which is equal to 11.1% relative to the maximum potential range resolution of the sounding LFM-signal. So some loss in range resolution is the cost for using de-ramping processing.

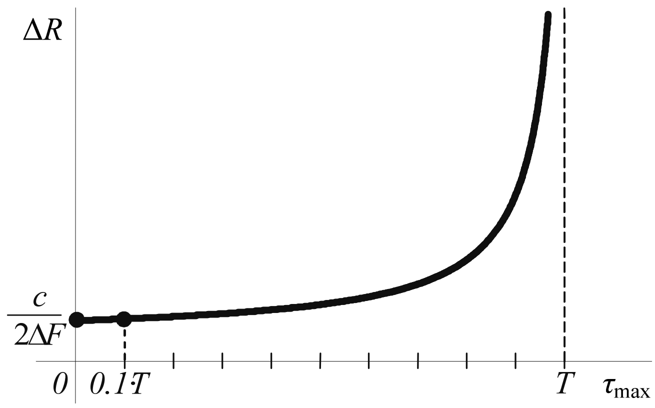

Fig. 3.8 – Range resolution for de-ramping procedure depending on the maximum measured time delay of the received signal.

An undisputed advantage of the de-ramping processing is the considerable simplification of signal processing in comparison with correlation methods. The frequencies of the analyzed signal are reduced from the sounding signal frequencies to a bandwidth limited by the maximum beat frequency. It allows considerable reduction in analyzed signal samples applied for digital signal processing.

The non-zero side-lobe levels of the compressed-signal (Fig. 3.7.d) are side-lobes in frequency domain after de-ramping processing and have the same negative influence as side-lobes in the time domain have when applying correlation methods. They limit the dynamic range of amplitudes for analyzing useful received beat frequency signals.

The side-lobe level can be reduced by applying a windowing function to the beat signal prior to the Fourier transform [22]. However, windowing has side effects. Side-lobes reduction leads to widening of the main lobe and therefore to reduction in range resolution. This should be taken into consideration when a windowing function is chosen.

3.4 Performance Comparison of the Various Processing Techniques (Channels Isolation, Cross-Correlation)

In this chapter four methods have been described. They can be grouped into types of processing or the domain (time or frequency) in which the processing takes place (see Fig. 3.9). The three methods referring to correlation processing calculate the correlation between the received signal and the replica of the sounding signal. These methods have different realizations but their mathematical expressions do not conflict with each other. So their performances can be described jointly. The performance of the de-ramping method, which refers to stretch processing, is applicable on frequency-modulated signals only and is considered separately.

Comparison is done according the following criteria:

1. Range resolution.
2. Peak side-lobe level (PSL) as a measure for protection from a maximum residual
3. Isolation. In case of dual-orthogonal signals the isolation is a measure for protection from a maximum residual "cross-channel" return, coming from the same object or from an interfering object.
4. Signal's energy.

Range resolution has been considered throughout the thesis. For the correlation processing (Sections 3.2.1, 3.2.2 and 3.3.1) the range resolution is determined by the auto-correlation functions of the orthogonal sophisticated signals, namely their main lobe widths (see Section 2.2). It's necessary to note here that if weighting is used it can change the compressed signal main-lobe and therefore range resolution. So weighting-range resolution effects should be taken into account when frequency-modulated signals are used, because it widens the compressed signal peak. Weighting does not change the peaks (main lobes) for compressed code-modulated signals. The range resolution for the de-ramping processing (see Section 3.3.2) is less than for the correlation methods. It decays when the relation of the useful signals duration to the radar duty cycle is decreased (Fig. 3.8).

Next we compare the PSL, isolation, and signals' energy for the correlation processing and de-ramping processing.

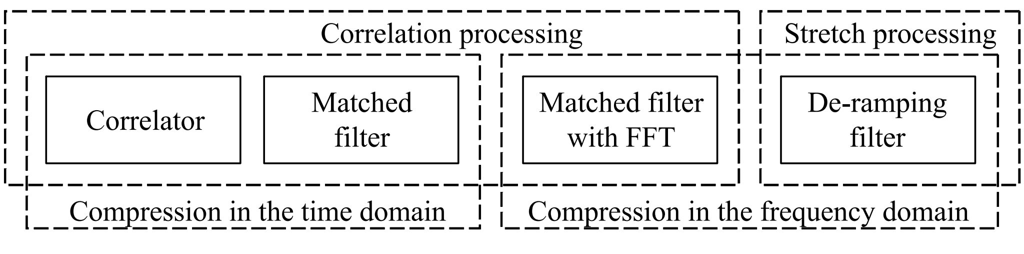

Fig. 3.9 – Processing techniques to be used for sophisticated signal compression.

3.4.1 Correlation Processing

The PSL and isolation are defined by the autocorrelation ($R_{ii}(\tau)$) and cross-correlation ($R_{ij}(\tau)$) functions of the sophisticated signals [9, 11]:

$$PSL_i = \min_{\tau \notin \Omega_i} \left[20 \cdot \log \frac{|R_{ii}(0)|}{|R_{ii}(\tau)|} \right], \tag{3.20}$$

$$I_i = \min_{\forall \tau} \left[20 \cdot \log \frac{|R_{ii}(0)|}{|R_{ij}(\tau)|} \right], \; i, j = 1, 2, \tag{3.21}$$

where index i denotes the waveform simultaneously transmitted, and Ω_i is the interval of τ values corresponding to the main-lobe of $R_{ii}(\tau)$.

The PSL is different for various types of sophisticated signals. The peak side-lobe level for PCM-signals with *m*-sequences is shown in Fig. 3.10 for the case of non-periodic signals. The PSL is inversely proportional to the square root of the BT-product of this sounding PCM-signal. In case of periodic signals the PSL is inversely proportional to the BT-product of the sounding signal what means a high PSL-level. However, the received signal can not be considered as periodic in general and periodic signals' processing is not considered in this thesis.

The isolation for m-sequences is shown in Fig. 3.11 depending on the BT-product. The isolation is less than PSL; so in polarimetric radar using dual-orthogonal sophisticated signals the cross-correlation signals are more harmful for estimating the SM elements, than the side-lobes of the compressed signal.

The PSL for an LFM-signal is shown in Fig. 3.12 for different BT-products and for two cases: when the signals are compressed without weighting and with weighting, namely with the use of the Hamming window. Fig. 3.12 shows that the side-lobes existing due to the auto-correlation of the vector sounding signal components can be suppressed significantly if a weighting window function is used.

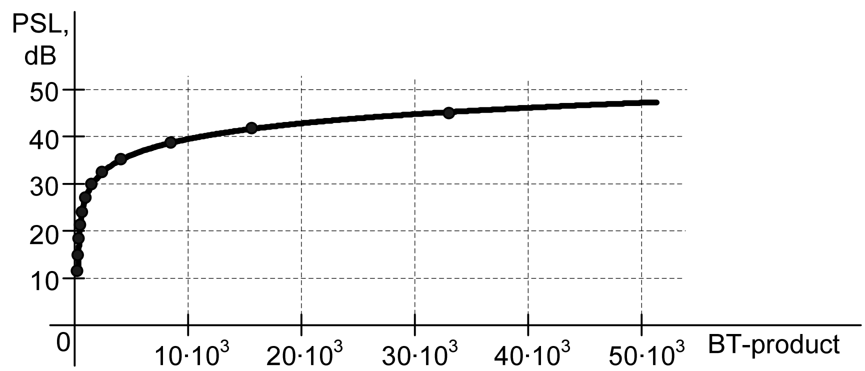

Fig. 3.10 – PSL for *m*-sequences depending on the BT-product.

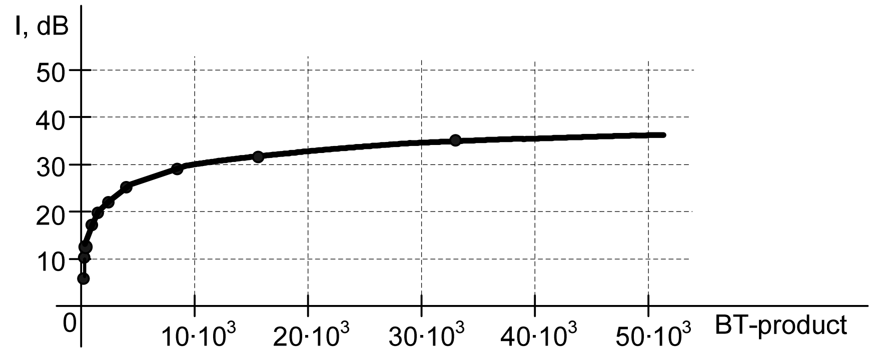

Fig. 3.11 – Isolation (I) for *m*-sequences depending on the BT-product.

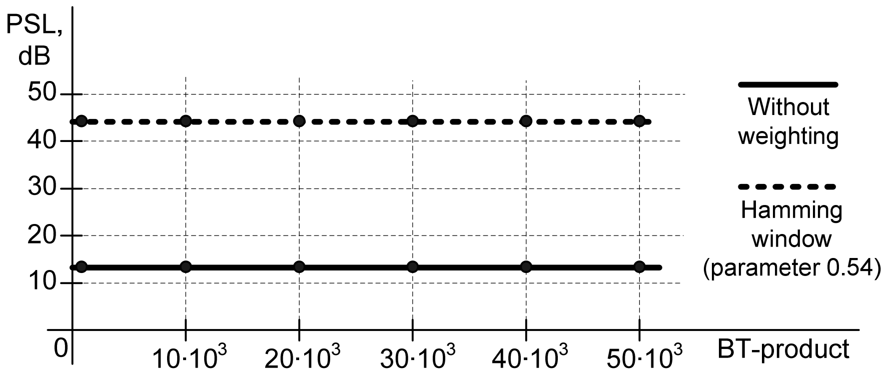

Fig. 3.12 – PSL for LFM-signals depending on the BT-product; without weighting and with weighting (Hamming window).

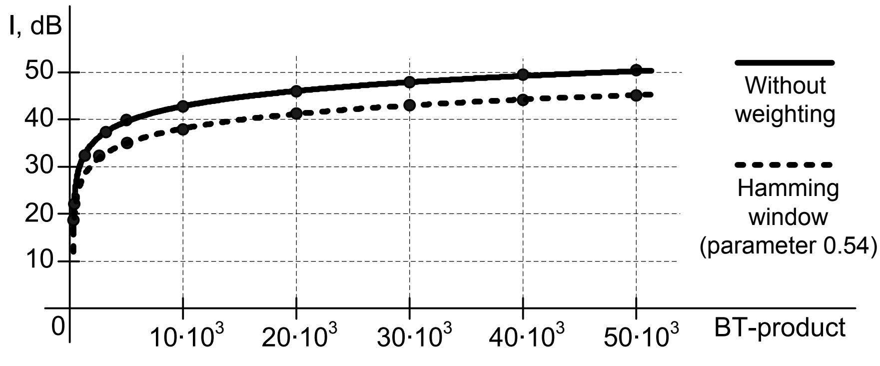

Fig. 3.13 – Isolation (I) for LFM-signals depending on the BT-product; without weighting and with weighting (Hamming window).

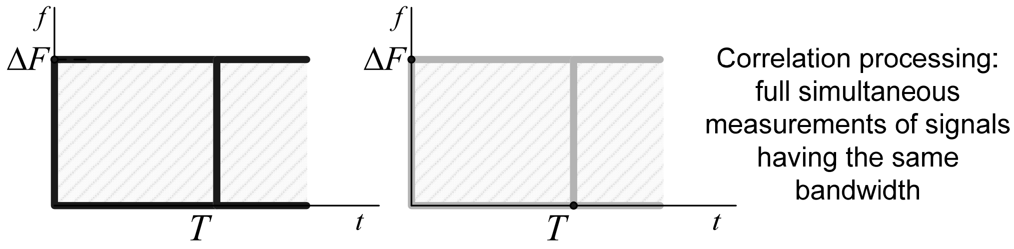

Fig. 3.14 – Time-frequency representation of two dual-orthogonal signals of the radar with continuous waveforms.

The isolation of LFM-signals (Fig. 3.13) as for PCM-signals increases with the BT-product. It should be marked that weighting degrades the isolation because the amplitude of the LFM-signal is decreased at the edges (see also Section 5.1).

A last criterion is energy. Energy of the useful signals having the same amplitudes is defined by the ratio of the useful signal duration and the radar duty cycle. Fig. 3.14 shows the time-frequency representation of two dual-orthogonal signals of the radar with continuous waveforms when correlation processing is used. The useful signals occupy the whole duty cycle (T) and the whole bandwidth (ΔF). Correlation processing results therefore into the maximum energy of the processed signal. Fig. 3.14 is presented here for comparison with the time-frequency representation of the signals for de-ramping processing, when the duty cycle and/or bandwidth are used partially (see Fig. 3.18).

3.4.2 De-ramping Processing

The term peak side-lobe level (PSL) can be connected to output signals resulting from the de-ramping procedure, as expressed in the frequency domain. By analogy the PSL for the de-ramping procedure (waveforms are LFM-signals) is determined by,

$$PSL \triangleq \min_{f \notin F_i} \left[20 \cdot \log \frac{|Func(0)|}{|Func(f)|} \right], \tag{3.22}$$

where F_i is the interval of f values corresponding to the main-lobe of $Func(f)$, the index i denotes the waveforms, simultaneously transmitted. If weighting is not used the function $Func(f)$ corresponds to the $\mathrm{sinc}(f)$ function and the PSL is constant (about -13 dB, see Fig. 3.12). When weighting is applied, the PSL can be decreased.

The isolation should get specific attention for different de-ramping types; some types are investigated here.

We consider the following three types of de-ramping processing:

a) LFM-signals with opposite slope

The first de-ramping type uses dual-orthogonal sounding signals, namely LFM-signals with opposite slope. Fig. 3.15.a shows the frequency plot of the signals (black and gray lines correspondently) and their beat frequencies. The scattered signals are marked as dashed lines. T is the duty cycle of the radar, ΔF means the sweep frequency (the vector sounding signal bandwidth), f_b are the beat frequencies in polarimetric radar channels, τ is the time delay of the received signal.

A strong correlation region is marked for the case when the signals in the polarimetric radar channels occupy the same frequencies over the same time interval. The maximum beat frequency of the mixed signals and the slope in the frequency curve of the low-pass filters (the de-ramping filter scheme is shown in Fig. 3.6) determine the area of strong correlation. The frequency curve slope is a choice of the radar designer.

The thick solid lines in Fig. 3.15.a correspond to the sounding signals, the thick dashed lines represent the scattered signals having maximum roundtrip time delay ($\tau_{\max}$). The thin solid lines show a few arbitrary scattered signals as an example of the arbitrary radar scene. Fig. 3.15 shows that received scattered signals can have roundtrip travel time (τ) more than $\tau_{\max}$. We know that in the de-ramping signal processing this roundtrip travel time τ has a unique relationship with beat frequency f_b (see Paragraph 3.3.2). LPF in every receiver channel limits the beat frequency band and, as result, determines maximum roundtrip time delay $\tau_{\max}$. It is true for tone (useful) signals. As for cross (LFM) signals, the LPFs limit their frequency band and, therefore, limit the duration of their presence in the radar receiver branches, but do not determine their roundtrip time delays.

The cross beat signals decrease the isolation between receiver's branches of the FM-CW polarimetric radar with simultaneous measurement of SM elements. As far as roundtrip travel time τ is not limited for the cross (LFM) signals, such signals from the whole analyzed time interval can influence the receiver and decrease the SM-estimation accuracy. So, the estimation and improvement of the isolation between branches of the polarimetric radar receiver is one of the main problems, which are under consideration in this thesis. The novel techniques, which are based on the de-ramping signal processing method and provide high-level isolation between branches in FM-CW radar receiver, are presented in Chapter 5 and Chapter 7.

Fig. 3.15(b) represents resulting beat signals on the idealized time-frequency plane, with negative frequencies. Such frequencies are a mathematical abstraction and do not exist in reality. The real representation of the signals has to be done on the plane "absolute value of frequency"-time, which are presented in Fig. 3.16. Numerical simulation of such representation of beat signals on the time-frequency plane, which has been done using a Short-Time FFT and which shows V-shaped cross beat signals and horizontal tone signals, is presented in Chapter 7 of this thesis.

When ideal low-pass filters are used in the de-ramping scheme the isolation I is a measure for protection of the maximum residual "cross-channel" return coming from the same object or from an interfering object and can be calculated via the cross-beat frequency (Fig. 3.15.b). The analyzed interval is equal to $(T-\tau_{\max})$. The cross-beat frequencies are linear modulated signals (Fig. 3.15.b) which, as known, have a spectrum close to a uniform one inside the analyzed bandwidth ($0...f_{b\max}$). Cross-beat frequencies correspond to LFM signals with $\tau_{\max}/2$-durations and $f_{b\max}$-bandwidths.

We note also that τ for cross-correlation components is not limited to $\tau_{\max}$. The received signals (Fig. 3.15.a) are not limited to this $\tau_{\max}$ value. The limitation of the maximum roundtrip time delay for beat signals is realized by the LPFs (see Fig. 3.6) whose boundary frequency ($f_{b\max}$) uniquely determines $\tau_{\max}$ only for sinusoidal (useful) signals but not for cross (interfering) LFM-signals. Low-pass filtering limits only the duration of those LFM-signals by the $\tau_{\max}/2$ value (see Fig. 3.15.b). The localization of cross LFM-signals in the first branch utilizing estimations $\hat{\dot{S}}_{11}(f_b)$

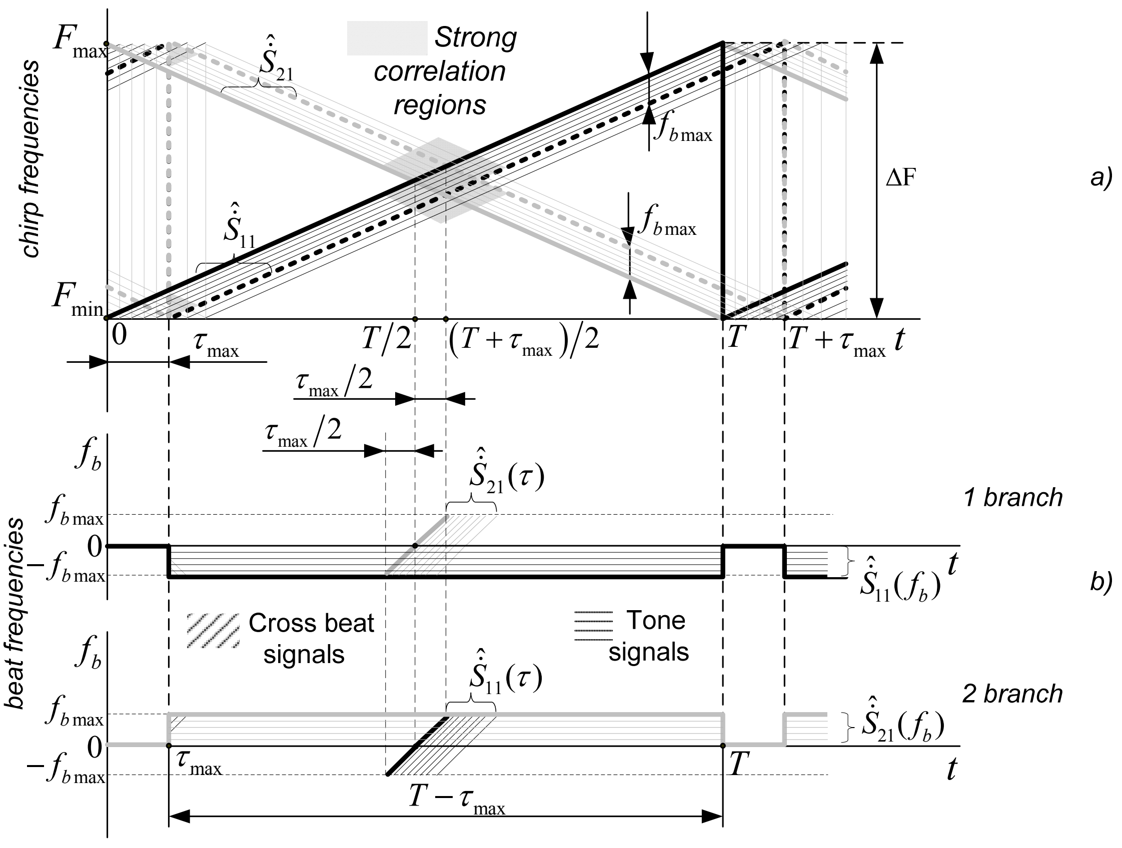

Fig. 3.15 – Frequency plot of continuous LFM-signals with opposite slopes in the first radar channel (a) and time-frequency representation of their beat signals (b).

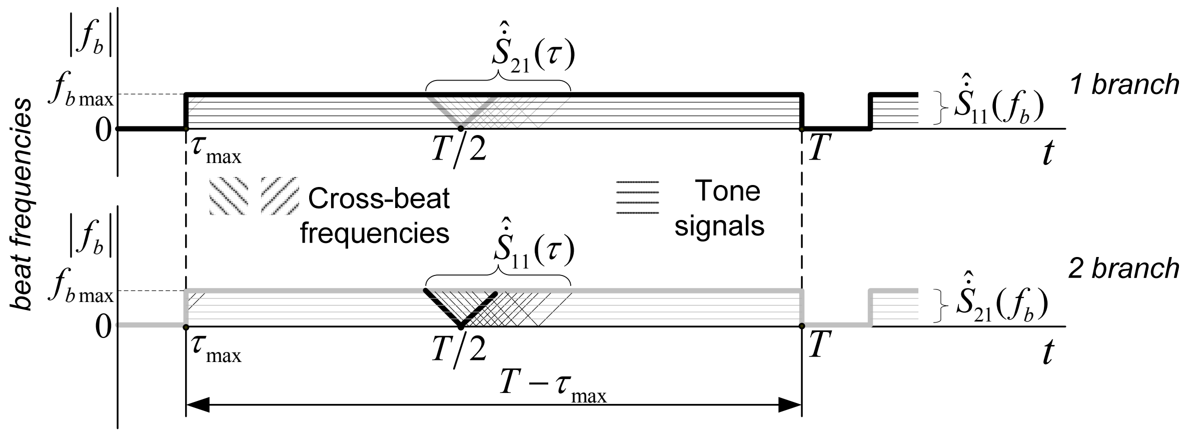

Fig. 3.16 – Time-frequency representation of beat signals for absolute values of beat frequencies.

and their complex amplitudes depends on $\dot{\hat{S}}_{21}(\tau)$. As for the second branch utilizing estimations $\dot{\hat{S}}_{21}(f_b)$, the complex amplitudes and localization of cross-LFM-signals are determined from $\dot{\hat{S}}_{11}(\tau)$. The zero range ($\tau = 0$) for cross-signals corresponds to the time point $T/2$ on the time axis (Fig. 3.15.b). We here again have to remember that a roundtrip time delay τ is not limited to $\tau_{\max}$ for cross LFM-signals. Cross LFM-signals define the isolation between branches in both channels of polarimetric radar.

We note that time-frequency representation of the beat signals shown in Fig. 3.15.b is a mathematical idealization, because frequencies can not be divided into negative and positive ones in reality. Beat signals will have a time-frequency distribution as shown in Fig. 3.16.

The isolation is a function not only of the sounding signals but also of the de-ramping parameter $\tau_{\max}$. The sounding signals' parameters for determining the isolation are the signals' repetition period (the radar duty cycle, T) and BT-product which identifies the beat frequency for the defined time delay. Also when real LPFs are used, a strong correlation region is identified in the overlap region (Fig. 3.15-b), and LPFs' frequency responses should be taken into account when the isolation is estimated. A detailed study of isolation for FM-CW polarimetric radar may be a topic for future research.

The technique for the cross-correlation components' suppression is presented in Chapter 7.

Two additional de-ramping types with continuous LFM-signals and using a time shift are described here.

b) Simultaneous measurements of coinciding signals over a limited time interval (Variant 1);

c) Quasi-simultaneous measurements of non-fully coinciding signals (Variant 2).

These two de-ramping types use signals, which can not be named as signals with dual orthogonality; the signals may still have the same form but with a shift in time and frequency domain.

A time shift for the de-ramping procedure is equivalent to a frequency shift. So a time shift more than the corresponding maximum beat frequency means frequency orthogonality in every

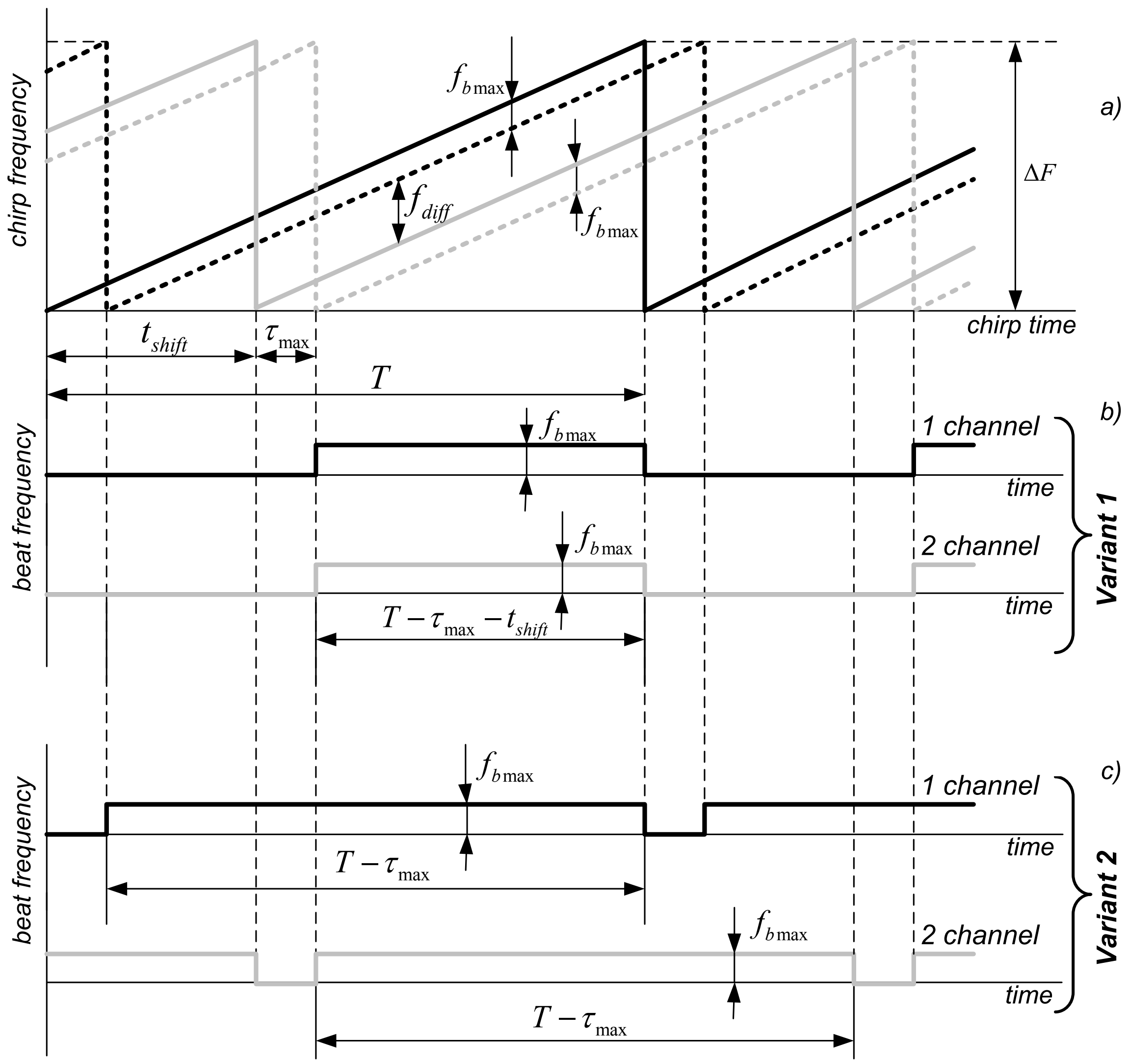

Fig. 3.17 – Frequency plot of continuous LFM-signals with a time shift relatively to each other and their beat frequencies for Variants 1 and 2.

time point (cross-beat frequency is equal to zero). Such frequency difference allows suppressing cross-correlation very effectively and provides a high isolation level limited only by amplitude-frequency responses of LPFs used in the de-ramping filter.

Fig. 3.17.a shows the frequency plot of the chirp signals (black and gray lines correspondently) and their beat frequencies (Fig. 3.17.b-c). There are no thin lines for arbitrary scattered signals like in Fig. 3.15 because of a prior uncertainty concerning the observed radar object and there is no information about it. The sounding signals corresponding to the signals with zero roundtrip travel time ($\tau = 0$) are marked as solid lines (Fig. 3.17.a). The possible scattered signals having maximum roundtrip time delay ($\tau = \tau_{\max}$) are marked as dashed lines. T is the duty cycle of the radar, ΔF means the sweep frequency, $f_{b\max}$ is the maximum beat frequency in FM-CW polarimetric radar, f_{diff} is the minimum frequency difference in the radar channels in every time point, t_{shift} is the time shift between sounding signals having different (vertical/horizontal) polarizations, $\tau_{\max}$ is the maximum possible time delay of the received signal.

When the proposed signals (Variant 1 and Variant 2) are used in polarimetric radar with simultaneous measurement of scattering matrix elements they can be named as *quasi-dual-*

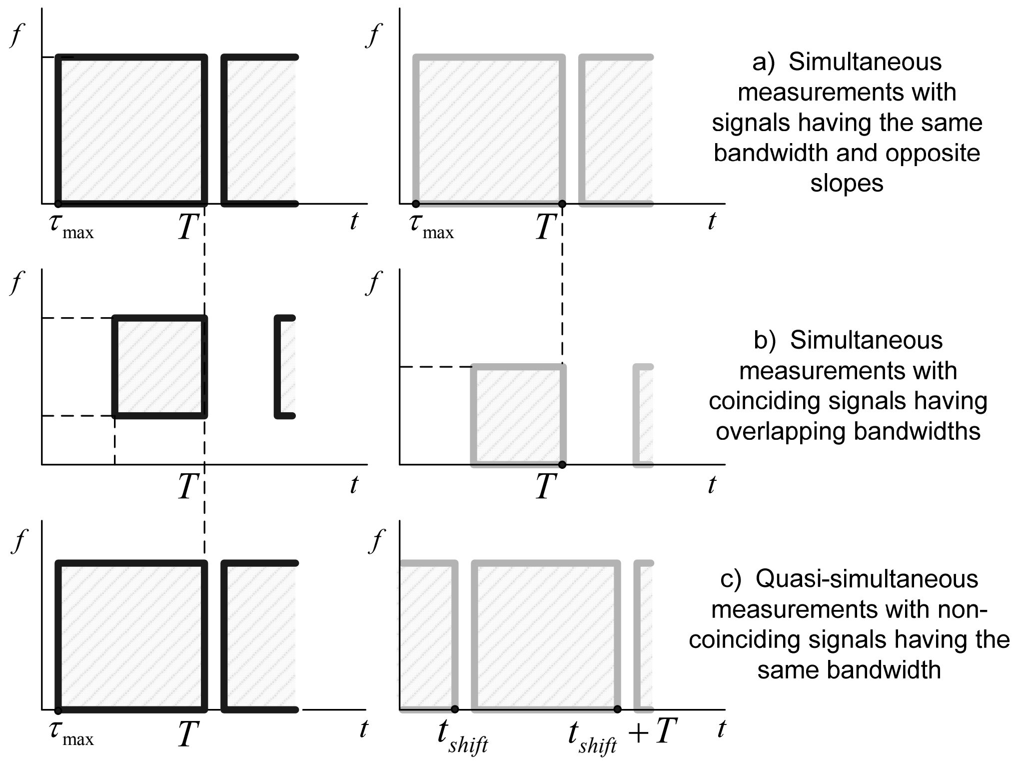

Fig. 3.18 – Time-frequency distribution of two sounding LFM-signals for FM-CW polarimetric radar having three different de-ramping types.

orthogonal signals. The sounding signals are radiated on orthogonal polarizations (orthogonality) and in every time point their frequencies are different (quasi-orthogonality), despite the sounding signals have the same waveforms and occupy the same frequency and time domain. The here proposed Variant 2 is analyzed in Chapter 5 of this thesis.

The maximum time shift between sounding LFM-signals is equal to half of the signal repetition period. It corresponds to a frequency difference in the radar channels, $f_{diff} = \frac{\Delta F - 2f_{b\max}}{2}$, where $f_{b\max}$ is the maximum beat frequency for both radar channels, and to a relative frequency difference, $\frac{f_{diff}}{\Delta F} = \frac{1}{2} - \frac{f_{b\max}}{\Delta F}$.

The time-frequency distribution of the useful signals for polarimetric radars with continuous waveforms is shown in Fig. 3.18 with different scales for frequency and time. T is the duty cycle of the FM-CW polarimetric radar, t_{shift} is the time shift of the sounding LFM-signals.

3.4.3 Main Characteristics of the Processing Techniques

The main characteristics of correlation and de-ramping processors of sophisticated radar sounding signals are shown in Table 3.1.

Simultaneity of the measurements is provided for all here described methods except for the proposed de-ramping method (when continuous non-coinciding LFM-signals with relative time shift are used, Var.2). It should be noted that the duty cycles for radars with continuous waveforms have the same length for all methods.

Bandwidth. The sounding signals occupy the whole bandwidth, allowed for polarimetric radar. The exception is the second proposed de-ramping method (when continuous coinciding LFM-signals with a relative time shift are used, Var.1).

Energy. The energy of the signals is the highest for correlation methods because the whole received signal period is taken for processing (see Fig. 3.14). The energy is less for de-ramping processing because only a part of every duty cycle is used (see Fig. 3.18).

Isolation. The isolation in polarimetric radars with continuous waveforms and simultaneous measurement of scattering matrix elements is defined by the cross-correlation components. For correlation processing the isolation is determined from the cross-correlation function of the sounding signals. For de-ramping processing the isolation is dependent on the strong-correlation region, where the received signals can occupy the same time interval and frequency band.

Range resolution is the highest for correlation methods; it is defined by the width of the correlation function main lobe. The de-ramping procedure used for frequency-modulated signals gives less range resolution in comparison with the correlation processing by a factor given in Eq. 3.19. When weighting is used it can decrease the range resolution significantly in de-ramping processing.

Table 3.1 – The main characteristics of the processing techniques.

	Correlation techniques	De-ramping techniques		
	Sophisticated signals (including LFM with opposite slope and PCM)	LFM-signals with opposite slope	Continuous coinciding LFM-signals with time shift (Var. 1)	Continuous non-coinciding LFM-signals with time shift (Var. 2)
Sounding signals have the same time representation (simultaneity of the measurements)	Yes	Yes	Yes	Quasi
Sounding signals have the same bandwidth	Yes	Yes	The bandwidths are partially overlapped	Yes
Energy of the useful signals	Very high	High	The energy decreases with increasing shift time	High
Isolation	The isolation is defined by the cross-correlation between the signals	The isolation is defined by the strong correlation regions (see Fig. 3.15)	Very high (can be provided)	Very high (can be provided)
Range resolution	Very high	High	The range resolution decreases with increasing shift time	High
Computational complexity	Very high (when convolution is used) High (when FFT is used)	Low	Low	Low

Computational complexity. Correlation in time domain apply convolution which results in very high computational complexity when sophisticated signals with large BT-product are used. Computational complexity of correlation processing in frequency domain (when FFT is used) is briefly explained in section 3.3.1. When de-ramping is used a significant reduction in sounding signals' bandwidth occurs. So a low computational complexity is achieved.

3.5 Conclusion

This chapter has presented an overview of correlation and de-ramping methods for dual-orthogonal sophisticated signals' processing. Moreover two de-ramping types using continuous LFM-signal with a relative time shift and utilizing simultaneous or quasi-simultaneous measurements have been proposed in addition to the standard de-ramping. A comparison of the correlation and de-ramping techniques and their performances has been made. The novel time-frequency representation of beat signals in FM-CW polarimetric radar with simultaneous measurement of SM elements has been proposed.

References

1. C. E. Cook, M. Bernfeld, "Radar signals", New York, Academic Press, 1967.
2. S.D. Blunt, K.Gerlach, "Adaptive pulse compression repair processing", Radar Conference, 2005 IEEE International 9-12 May 2005, pp. 519-523.
3. G.P. Babur, "Adaptive Filter of Polarimetric Radar with Compound Signals", Transactions of Tomsk Polytechnic University, Vol. 309, №8, 2006, pp. 89-93 (in Russian).
4. G.P. Babur, "Dynamic Range Expansion of Polarimetric Radar by Methods of Secondary Signal Processing"// First Interregional Scientific Conference "Modern Problems of Electronic Engineering", March 30-31, 2006, Rostov-on-Don, Russia. Proceedings, Iss. 1. Rostov-on-Don: RGPU, 2006, pp. 93-96 (ISBN 5-8480-0523-0) (in Russian).
5. F.E. Nathanson, "Radar Design Principles", Second ed-n., McGraw-Hill, New York, 1991.
6. Yi Xu, Wei Feng Feng, Jun Yan Hao, H.K. Hwang, Adaptive radar clutter suppression; OCEANS, 2001. MTS/IEEE Conference and Exhibition Volume 2, 5-8 Nov. 2001, pp. 762-768.
7. A. Lee, Shen Chunying, Zhou Hui, H.K. Hwang, Radar clutter suppression using adaptive algorithms; Aerospace Conference, 2004. Proceedings. 2004 IEEE Volume 3, 6-13 March 2004.
8. W.J. Caputi, "Stretch: A Time-Transformation Technique", Aerospace and Electronic Systems, IEEE Transactions on Volume AES-7, Issue 2, March 1971, pp. 269-278.
9. O.A. Krasnov, L.P. Ligthart, Zhijian Li, P. Lys, F. van der Zwan, "The PARSAX – Full Polarimetric FMCW Radar with Dual-Orthogonal Signals", Radar Conference, 2008, EuRAD 2008, Oct. 2008, pp. 84-87.
10. C. Titin-Schnaider, S. Attia, "Calibration of the MERIC full-polarimetric radar: theory and implementation", Aerospace Science and Technology, 7 (8), Dec 2003, pp. 633-640.

11. D. Guili, M. Fossi, L. Facheris, “Radar Object Scattering Matrix Measurement through Orthogonal Signals”, IEEE Proceedings-F, Vol. 140, № 4, August 1993.
12. W.M. Boerner et al. (eds.), Direct and Inverse Method in Radar Polarimetry, Part 2, pp. 1367-1388.
13. M. Jankiraman, “Design of Multi-Frequency CW Radars”, Scitech Publishing, Inc., 2007.
14. N. Levanon, E. Mozeson, “Radar Signals”, John Wiley & Sons, Inc., 2004.
15. D.R. Wehner, “High-Resolution Radar”, second edition, Artech House, Inc., 1995.
16. S.G. Qadir; J.K. Kayani; S. Malik, “Digital Implementation of Pulse Compression Technique for X-band Radar”, Applied Sciences & Technology, 2007. IBCAST 2007, pp. 35-39.
17. “The Scientist and Engineer’s Guide to Digital Signal Processing”, copyright ©1997-1998 by Steven W. Smith. Available http://www.DSPguide.com.
18. D.G.C. Luck, “Frequency Modulated Radar”, published by McGraw-Hill, New York, 1949, 466 p.
19. O.A. Krasnov, L.P. Ligthart, Z. Li, P. Lys, F. van der Zwan, “The PARSAX – Full Polarimetric FMCW Radar with Dual-Orthogonal Signals”, Radar Conference, 2008, EuRAD 2008, Oct. 2008, pp. 84-87.
20. D.C. Munson, R.L. Visentin, “A Signal Processing View of Strip-Mapping Synthetic Aperture Radar”, IEEE Transactions on Acoustics, Speech, and Signal Processing, Volume 37, Issue 12, Dec. 1989, pp. 2131-2147.
21. W.J. Caputi, “Stretch: A Time-Transformation Technique”, IEEE Transactions on Aerospace and Electronic Systems, Volume AES-7, Issue 2, March 1971, pp. 269-278.
22. J.J.M. de Wit, “Development of an Airborne Ka-Band FM-CW Synthetic Aperture Radar”, Dissertation at Delft University of Technology, 2005.
23. A. Meta, “Signal Processing of FMCW Synthetic Aperture Radar Data”, Dissertation at Delft University of Technology, 2006.

4. Bandwidths Effects on Range Processing

This chapter presents the investigation of two techniques for sophisticated signal processing, namely correlation processing and de-ramping processing. The investigation starts from the differences between the wide-band signal model and its approximation, namely the narrow-band signal model. The conditions when sounding signals' bandwidth effects take place and differences between the models are described. Bandwidth effects are different for correlation and de-ramping processing. In case of correlation processing the bandwidths effects for the wide-band signal model and the narrow-band are analyzed via matrix ambiguity functions. A novel wide-band correlaton processing approach applicable to dual-orthogonal polarimetric radar signals is proposed here. The de-ramping processing gets also attention for both types of signal models, namely for wide-band and narrow-band ones. A novel representation of wide-band de-ramping processing in FM-CW radar signals is proposed and the quantitative comparison of the signals' models is presented.

4.1 Wide-band and Narrow-band Signal Models

Two principal models exist for radar signal processing [1]: wide-band and narrow-band (see Table 4.1). In the narrow-band model it is assumed that the transmitted radar signal $\dot{u}(t)$ reflects from a single object (a point scatterer) moving with constant radial velocity *V*, and that the received signal $\dot{g}(t)$ experiences a Doppler frequency shift

$$f_d = \frac{-2V}{c} f_c, \tag{4.1}$$

where f_c is the carrier frequency of the sounding signal, *c* is the light velocity. When the radar object moves to the radar (and/or the radar moves to the observed object) velocity *V* is negative and the Doppler shift is positive and vice versa.

In the wide-band model the transmitted signal reflects from an object that is moving with constant radial velocity *V*, and in the received signal a time-scaling occurs according

$$s \cong 1 - \frac{2V}{c}, \tag{4.2}$$

where s is the scale factor. When the radar object moves to the radar (and/or the radar moves to the observed object) the scale factor is more than unity. The scale factor (Eq. 4.2) is described by a series [1]; however, the first terms of the series are sufficient for real radar object observations.

The Doppler shift, f_d, is an approximation for the scale parameter, s. However, such approximation restricts the bandwidth-time (BT) product of the sounding signals. In case the restriction is violated it may be efficient to use wide-band correlation processing with wavelets [2, 3], which are affected by a scale parameter and a time shift parameter.

The principal differences between the narrow-band and wide-band model can be seen in Table 4.1 [4]. In both models the time-delay τ of the received signal defines the distance to the radar object. The received signal $\dot{g}(t)$ is presented as signal formed under ideal (noise free) conditions.

Table 4.1 – Two principal models for radar signal processing: wide-band and narrow-band.

	Wide-band signal model	Narrow-band signal model
Parameter of object movement	$(1-s) \cong \frac{2V}{c}$	$f_d = \frac{-2V}{c} f_c$
Received signal, $g(t)$	$\dot{g}(t) \approx \sqrt{\lvert s \rvert} \cdot \dot{u}(s \cdot (t-\tau))$	$\dot{g}(t) \approx \dot{u}(t-\tau) \cdot e^{j2\pi f_d t}$
Ambiguity function	$\dot{X}(s,\tau) = \sqrt{\lvert s \rvert} \int\limits_{-\infty}^{\infty} \dot{u}(t) \cdot \dot{\psi}^{*}\left(s \cdot \left(t-\tau\right)\right) dt$	$\dot{X}(f_d,\tau) = \int\limits_{-\infty}^{\infty} \dot{u}(t) \cdot \dot{u}^{*}\left(t-\tau\right) e^{-j2\pi f_d \cdot t} dt$

The function $\dot{\psi}(t)$ is called the mother wavelet of the transform and is assumed to be physically realizable. It is essential to specify the condition under which wide-band signals can still be processed correctly according the narrow-band model, i.e. the received signal should satisfy the condition

$$\frac{2 \cdot \lvert V \rvert}{c} \ll \frac{1}{\Delta F \cdot T}, \tag{4.3}$$

where $\Delta F \cdot T$ is the BT-product of the sounding signal. It means that in case of sophisticated radar signals the use of the narrow-band model still realizes correct results if the BT product and/or radar object velocities are limited. However, the use of the wide-band model allows to avoid those limitations.

The difference between the wide-band signal model and the narrow-band one may be large. So both techniques for sophisticated signals processing, namely correlation processing and de-ramping processing, are of interest for bandwidth effect considerations.

4.2 Correlation Processing

The influence of the observed object motion for correlation processing can be estimated using the ambiguity functions of the sounding signals.

Generally the ambiguity function is a 3-D function of two variables: time delay (range) and parameter of object motion (Doppler frequency or scale factor). This function describes the local ambiguity in range and velocity of the observed objects. The cut of the ambiguity function at zero velocity is the correlation function of the signal.

In radar practice different forms of ambiguity function appear. Each has its own advantage for the particular situation in which it is used. In the thesis the wide-band/narrow-band ambiguity function for Doppler polarimetric radar is of prime interest.

4.2.1 Wide-band and Narrow-band Ambiguity Functions

The **narrow-band ambiguity function** is characterized by a time–frequency correlation. Physically, the ambiguity function represents the energy in the received signal as function of time delay (range) and Doppler frequency (velocity) [5]. The narrow-band ambiguity function is an approximation of the wide-band ambiguity function because the Doppler frequency is an approximation for the scale factor.

The wide-band ambiguity function [1, 6] represents the energy in a received signal as function of time delay (range) and scale factor (velocity). Its application makes sense when sophisticated signals with long duration are used and/or fast-moving objects are observed.

In case of polarimetric radar with simultaneous measurement of scattering matrix elements the matrix ambiguity function for both wide-band and narrow-band processing should be considered here.

Polarimetric radar has a vector transmitted signal $\dot{\mathbf{u}}(t)$ consisting of a pair of signals with orthogonal waveforms (see Section 2.2):

$$\dot{\mathbf{u}}(t) = \left[\dot{u}_1(t) \quad \dot{u}_2(t)\right]^T, \tag{4.4}$$

where superscript T means the operation of transposition. For the narrow-band model the matrix ambiguity function of the vector sounding signal $\dot{\mathbf{u}}(t)$ becomes

$$\dot{\mathbf{X}}(f_d,\tau) = \int_{-\infty}^{\infty} \dot{\mathbf{u}}(t)\cdot\dot{\mathbf{u}}^*\left(t-\tau\right)\cdot e^{-j2\pi f_d\cdot t}dt = \begin{bmatrix} \dot{X}_{11}(f_d,\tau) & \dot{X}_{12}(f_d,\tau) \\ \dot{X}_{21}(f_d,\tau) & \dot{X}_{22}(f_d,\tau) \end{bmatrix}, \tag{4.5}$$

where $\dot{X}_{ij}(f_d,\tau) = \int_{-\infty}^{\infty} \dot{u}_i(t)\cdot\dot{u}_j^*\left(t-\tau\right)\cdot e^{-j2\pi f_d\cdot t}dt$, $i, j = 1, 2$.

For the wide-band model the matrix ambiguity function of the vector sounding signal $\dot{\mathbf{u}}(t)$ can be written as

$$\dot{\mathbf{X}}(s,\tau) = \sqrt{|s|}\int_{-\infty}^{\infty} \dot{\mathbf{u}}(t)\cdot\dot{\boldsymbol{\psi}}^{*}\left(s\cdot(t-\tau)\right)dt = \begin{bmatrix} \dot{X}_{11}(s,\tau) & \dot{X}_{12}(s,\tau) \\ \dot{X}_{21}(s,\tau) & \dot{X}_{22}(s,\tau) \end{bmatrix}, \tag{4.6}$$

where $\dot{X}_{ij}(s,\tau) = \sqrt{|s|}\int_{-\infty}^{\infty} \dot{u}_i(t)\cdot\dot{\psi}_j^{*}\left(s\cdot(t-\tau)\right)dt$, i,j = 1,2. The vector function $\dot{\boldsymbol{\psi}}(t) = \left[\dot{\psi}_1(t) \quad \dot{\psi}_2(t)\right]^T$ consists of two orthogonal mother wavelets, which are assumed to be physically realizable.

A major problem in polarimetric radar occurs when the radar designer is confronted with BT-product restrictions for sophisticated sounding signals. Wide-band correlation processing allows to remove the restrictions concerning large BT-products.

4.2.1.1 LFM

The wide-band ambiguity function can be calculated if the mother wavelet has been chosen. The choice of the mother wavelet can be a theme for various investigations. In case of sounding LFM-signals the choice can be determined by the following considerations. If the mother wavelet, $\dot{\psi}_i(t)$, coincides with the transmitted signal $\dot{u}_i(t)$, the wide-band correlation processing is optimum [1] and the output signal-to-noise ratio is maximized for a received signal corrupted by additive white Gaussian noise. Consequently, the pair of mother wavelets $\left[\dot{\psi}_1(t) \quad \dot{\psi}_2(t)\right]^T$ determined by a pair of signals with orthogonal waveforms $\dot{\mathbf{u}}(t) = \left[\dot{u}_1(t) \quad \dot{u}_2(t)\right]^T$ will provide optimum filtering in polarimetric radar with simultaneous measurement of scattering matrix elements.

The LFM vector sounding signal can be written as a pair of signals with identical rectangular pulse and opposite (up-going and down-going) slope of linear frequency modulation inside the pulse. We can write

$$\dot{\mathbf{u}}(t) = \begin{bmatrix} \dot{u}_1(t) \\ \dot{u}_2(t) \end{bmatrix} = \begin{bmatrix} env(t)\cdot e^{j\cdot 2\pi\left(\frac{k}{2}\cdot t^2 + F_{\min}\cdot t\right)+\varphi_1} \\ env(t)\cdot e^{j2\pi\left(-\frac{k}{2}\cdot t^2 + F_{\max}\cdot t\right)+\varphi_2} \end{bmatrix}, \tag{4.7}$$

where *env*(*t*) is a rectangular window with pulse length *T* and *k* is a positive constant (sweep rate) with dimension 1/sec^2, which determines the frequency deviation of $\dot{u}_1(t)$ and $\dot{u}_2(t)$ within $\Delta F = \left[F_{\min}...F_{\max}\right]$ (see Paragraph 2.2.1).

Rectangular windowed LFM-signals are not physically realizable as mother wavelets. However, such realisability exists for Gaussian-weighted LFM-signals [1, 7]. It means that the vector function $\dot{\boldsymbol{\psi}}(t) = \left[\dot{\psi}_1(t) \quad \dot{\psi}_2(t)\right]^T$ consisting of two orthogonal mother wavelets

$$\dot{\boldsymbol{\psi}}(t)=\begin{bmatrix}\dot{\psi}_1(t)\\ \dot{\psi}_2(t)\end{bmatrix}=\begin{bmatrix}env'(t)\cdot e^{j\cdot 2\pi\left(\frac{k}{2}\cdot t^2+F_{\min}\cdot t\right)+\varphi_1}\\ env'(t)\cdot e^{j\cdot 2\pi\left(-\frac{k}{2}\cdot t^2+F_{\max}\cdot t\right)+\varphi_2}\end{bmatrix} \tag{4.8}$$

is physically realizable when $env'(t)$ is a Gaussian weighting window. So the Gaussian-weighted LFM-signals are used as mother wavelets. In addition a window weighting is often utilized for side-lobes suppression.

Numerical simulation of the wide-band ambiguity matrix and narrow-band ambiguity matrix will be presented here. We use for the simulation a bandwidth time product ($\Delta F\cdot T$) of the LFM-signals equal to 15 and T = 1 ms and f_c = *3.315* GHz. We note here that f_c is not a parameter for the wide-band signal model (see Table 4.1). The signal duration, T, and the carrier frequency f_c correspond to the parameters of the polarimetric radar system PARSAX (see Appendix A, Table A.1); however, a small BT-product (15) was chosen for better visibility of the modeled ambiguity functions only.

Figure 4.1 shows the absolute value of the normalized wide-band ambiguity matrix $\dot{\mathbf{X}}(s,\tau)$ of the vector signal consisting of two LFM-signals with opposite slopes. The magnitude of the wide-band ambiguity matrix peaks at $(s, \tau) = (1, 0)$.

The use of wide-band correlation processing is reasonable for a moving object observation

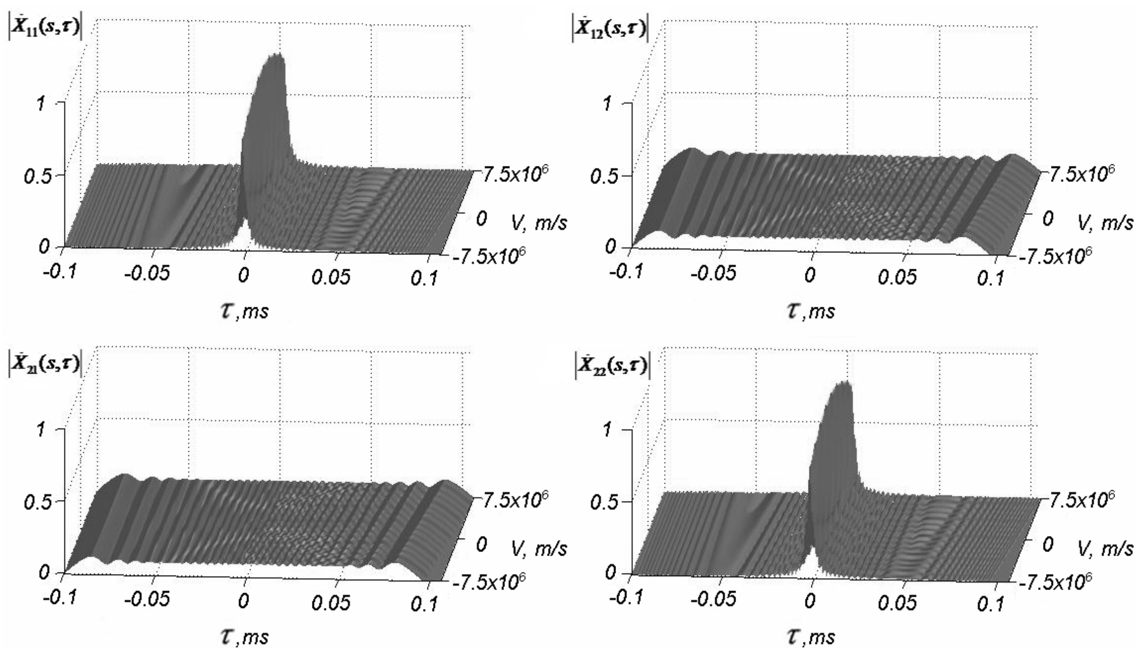

Fig. 4.1 - Absolute value of the normalized wide-band ambiguity matrix $\dot{\mathbf{X}}(s,\tau)$ of LFM-signals with up-going and down-going frequency modulation and a “wide” velocity range (BT=15, T=1 ms).

when its velocity and/or BT-product of sounding sophisticated signals are large and relativistic effects appear.

The Doppler shift f_d does not unambiguously correspond to the scale parameter s, because it depends on both the radial velocity of the radar object and the carrier frequency (light velocity is constant), whereas the scale parameter *s* depends only on the radial velocity of the radar object. For better visibility of the modeling results the scale parameter *s* has been chosen in the range (0.95, 1.05); this range corresponds to radial velocities of observed objects from $-7.5 \cdot 10^6$ to $7.5 \cdot 10^6$ m/s.

As can be seen in Fig. 4.1, non-zero levels in the cross-ambiguity functions $\dot{X}_{12}(s,\tau)$, $\dot{X}_{21}(s,\tau)$ and non-zero side-lobes in the ambiguity functions $\dot{X}_{11}(s,\tau)$, $\dot{X}_{22}(s,\tau)$ occur in the wide-band model due to the finite BT-product. However, we note that the wide-band model used in Fig. 4.1 clearly demonstrates no restriction on the BT-product of the sounding signal.

Figure 4.2 shows the absolute value of the normalized narrow-band ambiguity matrix $\dot{\mathbf{X}}(f_d,\tau)$ of the vector signal consisting of two LFM-signals with opposite slopes. The magnitude of the narrow-band ambiguity matrix peaks at (f_d, τ) = (*0*, *0*).

Also here non-zero level of cross-correlation functions $\dot{X}_{12}(f_d,\tau)$, $\dot{X}_{21}(f_d,\tau)$ and non-zero

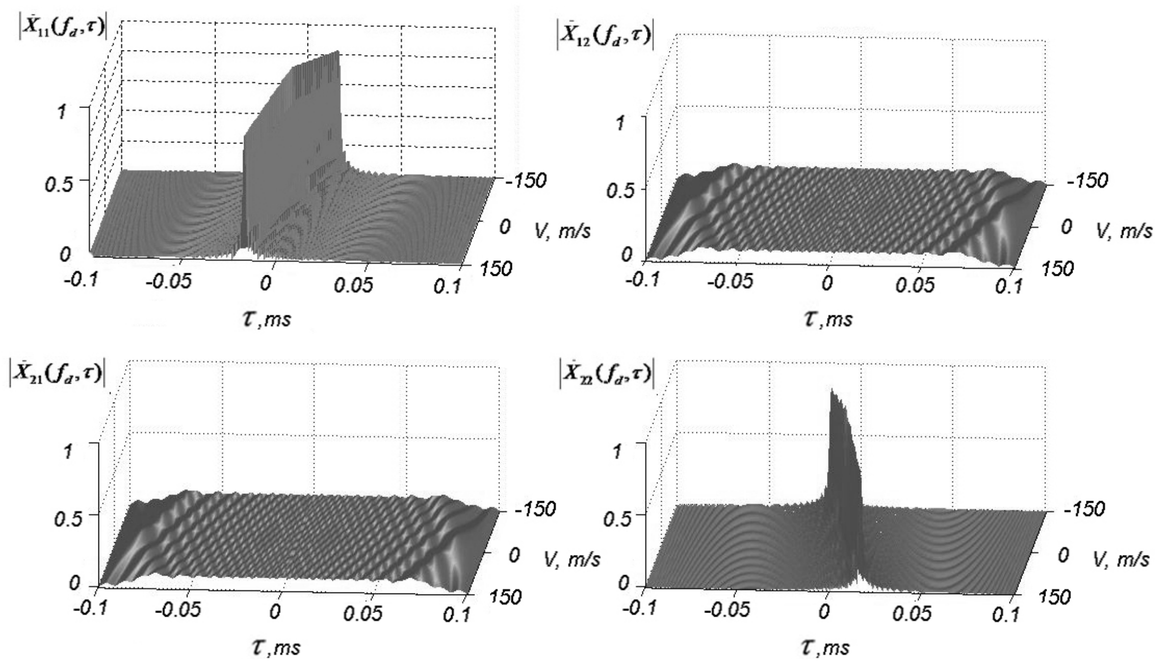

Fig. 4.2 – Absolute value of the normalized narrow-band ambiguity matrix $\dot{\mathbf{X}}(f_d,\tau)$ of LFM-signals with up-going and down-going frequency modulation and a “narrow” velocity range (BT=15, *T*=1 ms, f_c=3.315 GHz).

side-lobes of the ambiguity functions $\dot{X}_{11}(f_d,\tau)$, $\dot{X}_{22}(f_d,\tau)$ occur due to the finite BT-product. We observe, however, that in Fig. 4.2 the ambiguity functions of two LFM-signals ($\dot{X}_{11}(f_d,\tau)$ and $\dot{X}_{22}(f_d,\tau)$) have opposite knife-shaped ridges. This means that one fast-moving object can be interpreted like two non-existing objects having different ranges. It limits the capabilities in the accuracy of measuring the polarimetric matrix elements. A second observation is even more significant, i.e. if the narrow-band model is used and the BT-product increases, the radar object velocities affect the accuracies even more (Eq. 4.3). The use of the wide-band model allows to avoid those limitations.

The advantage of the wide-band correlation processing is that it does not have restrictions for both the BT-product of the sounding compound signals and the radial velocity of the observed radar objects. Further analysis of differences in the wide-band ambiguity matrix and the narrow-band is recommended as theme for future research.

4.2.1.2 PCM

A wavelet function should be chosen for calculating the wide-band ambiguity matrix. When selecting a vector signal consisting of two orthogonal PCM-signals the choice can be determined by the following considerations.

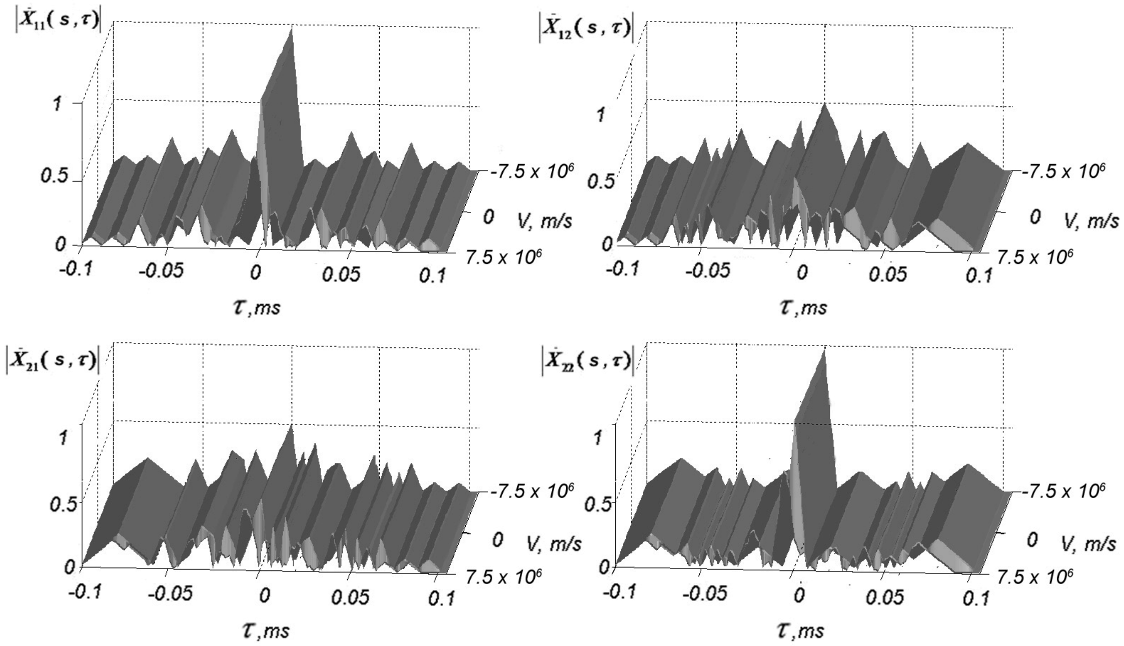

Fig. 4.3 − Absolute value of the normalized wide-band ambiguity matrix $\dot{\mathbf{X}}(s,\tau)$ of orthogonal PCM-signals for a “wide” velocity range (BT=15, T=1 ms).

Rectangular windowed signals have limited use as mother wavelets, because the spectrum of the signal has a *sinc*-form ($\sin^2 x/x^2$), which does not decay quickly. The spectrum of PCM-signals also has a $\sin^2 x/x^2$ form caused by the rectangular sub-pulse. The spectrum vanishes for certain frequencies, meaning that the scaling is not admissible for these frequencies [1].

The vector transmitted signal can be written as a pair of PCM-signals with identical BT-products (see Paragraph 2.2.2). The vector function $\dot{\boldsymbol{\psi}}(t) = \left[\dot{\psi}_1(t) \quad \dot{\psi}_2(t)\right]^T$ should consist of two orthogonal mother wavelets. By analogy with the previous paragraph the sounding signals are proposed to be used as mother wavelets. But the spectrum of a PCM-signal as well as the spectrum of each subpulse has the *sinc*-form. So in general PCM-signals can not be mother wavelets. However, so-called scaled PCM-signals can be used for correlation processing. Therefore the wide-band ambiguity matrix in this paragraph is calculated using corresponding scaled PCM-signals. Scaling of PCM-signals is utilized in the time domain when the duration of signals is changed.

Numerical simulation results of the wide-band and narrow-band ambiguity matrix will be presented here. We use for better visualization PCM-signals with a bandwidth-time product ($\Delta F \cdot T$) value equal to 15. We choose, as in the previous paragraph, T = 1 ms and f_c = 3.315 GHz, the basic parameters in PARSAX.

Figure 4.3 shows the absolute value of the normalized wide-band ambiguity matrix $\dot{\mathbf{X}}(s,\tau)$ of a vector signal base using the proposed PCM-signals. The magnitude of the wide-band

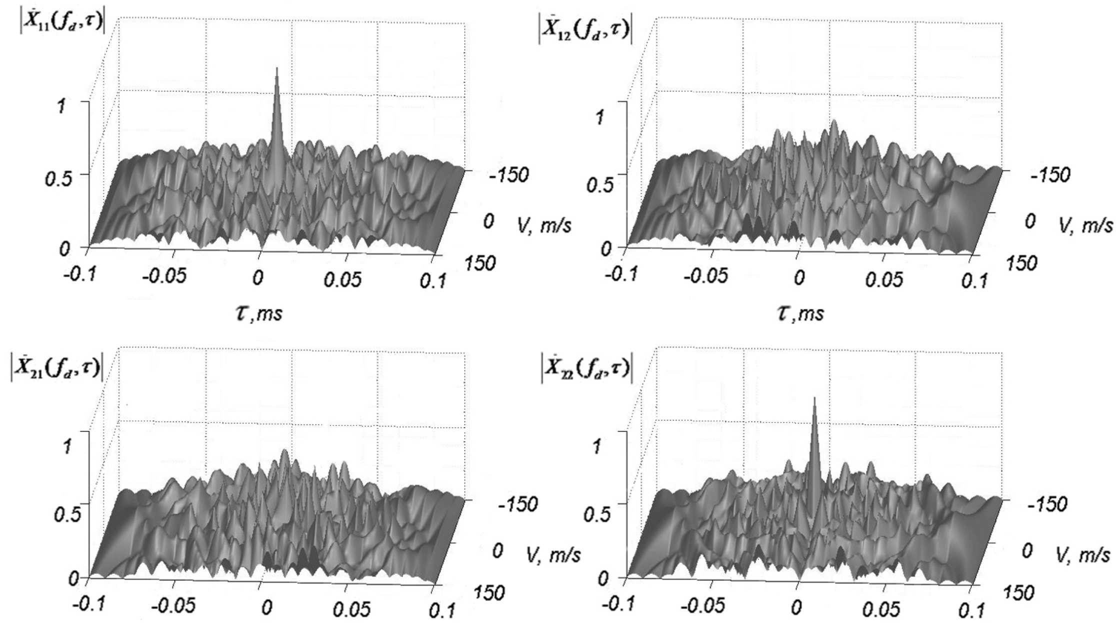

Fig. 4.4 − Absolute value of the normalized narrow-band ambiguity matrix $\dot{\mathbf{X}}(f_d,\tau)$ of orthogonal PCM-signals for a “narrow” velocity range (BT=15, T=1 ms, f_c =3.315 GHz).

ambiguity matrix peaks at (s, τ) = (1, 0). The main-lobe of the auto-ambiguity functions ($\dot{X}_{11}(s,\tau)$, $\dot{X}_{22}(s,\tau)$) which remains over a large range of velocities shows that fast-moving objects can be detected. However, the long duration of the main-lobe along the Doppler frequency (velocity) axis results in a bad velocity resolution for the wide-band correlation processing

.

Fig. 4.4 shows the absolute value of the normalized narrow-band ambiguity matrix $\dot{\mathbf{X}}(f_d,\tau)$ of a vector signal base for PCM-signals. The magnitude of the narrow-band ambiguity matrix peaks at (f_d, τ) = (0; 0).

The form of the auto-ambiguity functions, $\dot{X}_{11}(f_d,\tau)$, $\dot{X}_{22}(f_d,\tau)$ (Fig. 4.4) shows for PCM-signals a good resolution along both delay (range) and Doppler frequency (velocity) axes. Nevertheless, it should be noted again that the possibility of fast-moving object detection should be considered together with the wide-band signal model because the narrow-band approximation works satisfactorily only when BT-product and/or the radial velocity of the observed objects are limited.

The side-lobe levels in the wide-band ($\dot{X}_{11}(s,\tau)$, $\dot{X}_{22}(s,\tau)$) and narrow-band ($\dot{X}_{11}(f_d,\tau)$, $\dot{X}_{22}(f_d,\tau)$) auto-ambiguity functions and the cross-correlation levels in the wide-band ($\dot{X}_{12}(s,\tau)$, $\dot{X}_{21}(s,\tau)$) and narrow-band ($\dot{X}_{12}(f_d,\tau)$, $\dot{X}_{21}(f_d,\tau)$) cross-ambiguity functions for PCM-signals (Fig. 4.3, 4.4) are bigger than the levels for LFM-signals (Fig. 4.1, 4.2) while all other factors being equal. It means a less dynamic distinguishing in the received signals when PCM sounding signals are used compared to LFM-signals.

4.2.2 Range Estimation Error in Correlation Processing

The radar target range is determined by the time delay between the received signal and the radiated signal. If the radar and the observed object are non-moving, the signal roundtrip travel time is constant and equal to $\tau = 2 \cdot R/c$, where R is the distance between radar and object, c is the light velocity. When the target and/or the radar are moving, the roundtrip time delay is varying and depends on the radial velocity of the observed object.

In the narrow-band case the object velocity determines the Doppler frequency (see Table 4.1). If the carrier frequency of the vector sounding signal is a tone (as for PCM-signals) Eq. 4.1 can be used directly. But narrow-band processing will lead to additional restrictions in polarimetric radar, which uses a vector sounding signal consisting of the pair of LFM-signals with equal durations and opposite slopes. There is then an ambiguity in determining the range of the object and its velocity (respectively, time delay and Doppler frequency).

The carrier frequency of the vector sounding LFM signal (Eq. 4.7) varies within the frequency sweep. The target motion shifts the frequency interval of the received signal relative to the transmitted signal with a value f_d. For LFM-signals, this shifting of the ambiguity function along frequency axis may be interpreted as a shift along the time (range) axis and vice versa. So the motion of a radar target causes errors in range. Furthermore the narrow-band ambiguity functions of two LFM-signals with opposite slopes have opposite knife-shaped ridges and their shifts for the same moving target can be interpreted like the presence of another non-existent target. So in polarimetric radars with simultaneous measurement of scattering matrix elements using orthogonal LFM-signals and narrow-band correlation processing we should keep in mind that the radial velocity of the observed targets is then strictly limited [4, 8]. For overcoming this limitation, wide-band correlation processing is needed. We know that in case of wide-band processing the target velocity is defined by the scale factor (see Table 4.1) of the received signal. The scale factor does not depend on the kind of modulation and other parameters of the sounding signal.

We therefore consider the ambiguity in range and velocity (time delay, τ, and scale factor, s) for wide-band correlation processing. When the object and/or transmitter/receiver are moving the roundtrip travel time can be expressed as [1]:

$$\tau(t,V) = \tau_0 + \frac{2\cdot V}{c+V}\left(t-\tau_0\right), \tag{4.9}$$

where τ_0 equals to $\frac{2\cdot R}{c}$ and R is the true distance to the object. With

$$V \cong \frac{(1-s)\cdot c}{2}. \tag{4.10}$$

we obtain the roundtrip travel time:

$$\tau(t,s) = \tau_0 + \frac{2\cdot(1-s)}{3-s}\left(t-\tau_0\right), \tag{4.11}$$

where τ_0 corresponds to the true radar object distance. The error in range detection (time delay) to the object depends on velocity (scale factor) and equals to

$$\tau_e(t,s) = \frac{2(1-s)}{3-s}\left(t-\tau\right). \tag{4.12}$$

In accordance with Eq. 4.2 we again can conclude that in radar with wide-band correlation processing the radar-object range error caused by its motion does not depend on type and polarization of the sounding signals. Therefore the error in range measurement is the same for both channels of polarimetric radar with simultaneous measurement of scattering matrix elements. It means that in case of a compound radar object its motion can not be interpreted by the presence of other non-existent objects and that the radial velocity of radar objects in the wide-band model is not strictly limited anymore.

4.3 De-ramping Processing

De-ramping processing has not been designed for observing moving objects when the motion can not be neglected (fast moving radar objects) over the time interval of a single measurement. However, radar scenes include moving objects most often.

As for correlation processing we introduced in last Section two models for the received signal, namely the narrow-band model and the wide-band model. It is recalled here that the differences of the wide-band and narrow-band models manifest themselves when fast moving radar objects are under observation.

De-ramping processing of signals coming from moving objects is similar for both polarimetric radar channels and for both sophisticated sounding signals. So for clarity sake the observed object motion is explained for one sophisticated signal only. This explains why the spectra of cross-correlation signals are not shown in the figures, which will be presented in the two next paragraphs.

4.3.1 Narrow-band De-ramping Processing

In the narrow-band model the scale factor s is approximated by a Doppler shift f_d (see Section 4.1). This approximation assumes that all frequencies in the signals are shifted equally.

We now consider the narrow-band de-ramping processing in the following example where an FM-CW radar observes four point objects (*1*, *2*, *3*, *4*). Fig. 4.5-a shows the time frequency representation of the received signals. All objects are located at the same radial range corresponding to the roundtrip time delay τ. One object is stable (its radial velocity equals to zero, $V_1 = 0$), one object moves towards the radar ($V_2 < 0$) and two objects move away from the radar with different radial velocities ($V_4 > V_3 > 0$).

The time frequency representation of the de-ramped signals in the time-frequency plane for the narrow-band model is shown in Fig. 4.5-b. The solid gray lines show the limits of the analyzed time-frequency region (from $\tau_{\max}$ to T in time and from 0 to $f_{b\max}$ in frequency). If the sinusoidal beat signal corresponding to a fast-moving radar object falls outside these limits (e.g. Signal 4 in Fig. 4.5-a) it will not be detected, meaning signal 4 is absent in Fig. 4.5-b.

The main parameters in narrow-band de-ramping processing are given below.

Potential range resolution. According to Fig. 4.5-b the de-ramped signals defined by the moving objects are sine beat signals occupying the whole analyzed time interval $(T - \tau_{\max})$. As is known the range resolution in the de-ramping procedure is determined by the sine-signal duration (Eq. 3.19). So according to the narrow-band model the range resolution for the de-ramping processing does not depend on the observed object motion.

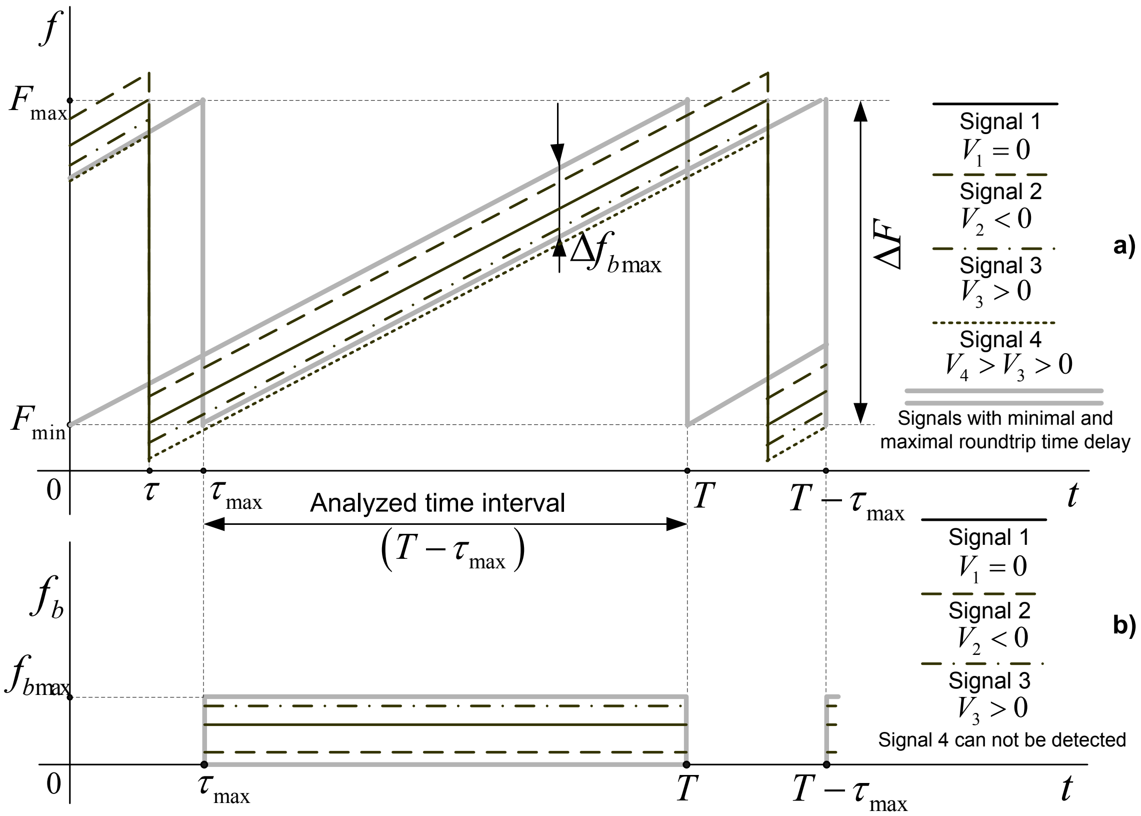

Fig. 4.5 – Narrow-band model: time-frequency representation of a) the received signals; b) the de-ramped signals.

Frequency shift of the received signals. According to the narrow-band signal model described in Section 4.1 the signal scattered by the moving object obtains a frequency shift (Doppler shift). This shift depends on both the radar object velocity V and the carrier frequency f_c of the vector sounding signal (Eq. 4.1). The frequency bandwidths of the four considered signals (Fig. 4.5) are shifted, but their values do not change:

$$\Delta F_1 = \Delta F_2 = \Delta F_3 = \Delta F_4 = \Delta F.$$

Additional time shift of the received signals. The roundtrip time delay for the narrow-band model doesn't depend on the object velocity. So there is no additional time shift for the narrow-band model. However, we should be aware that the Doppler shift of the scattered signal results in a range error.

Range error. The Doppler shift changes the actual frequency of the useful sine signals. So according to Eq. 3.14 the range definition error (R_e) can be written as

$$R_e = \frac{T \cdot f_d}{\Delta F} \cdot \frac{c}{2}, \tag{4.13}$$

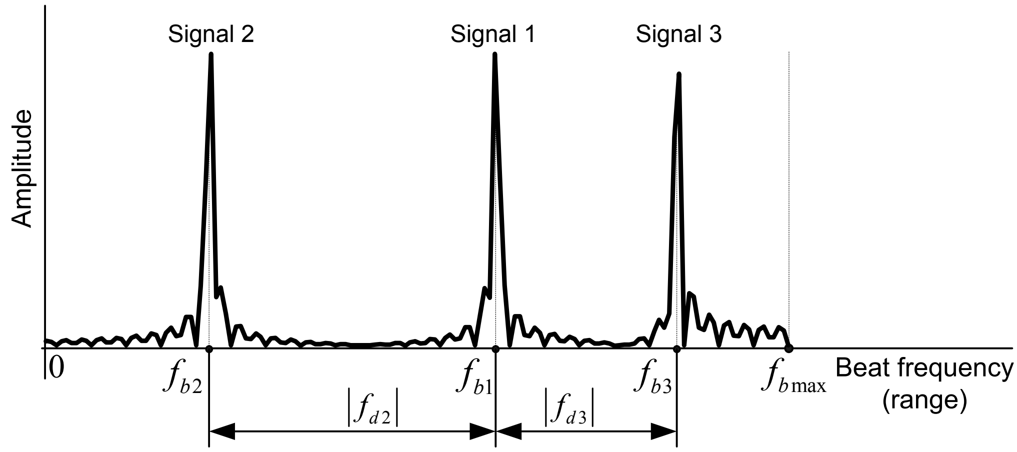

Fig. 4.6 – Spectra of the de-ramped signals (Fig. 4.5.b) the narrow-band model.

where f_d is the Doppler frequency (the difference between the true beat frequency and the estimated one), T is the radar duty cycle, ΔF is the sounding signals bandwidth, c is the light velocity. When the radar object moves towards the radar (and/or the radar moves to the observed object) the Doppler shift is positive and the estimated range will be more than the true range.

Fig. 4.6 shows the de-ramped signals corresponding to Fig. 4.5-b. All objects are located at the same range. The first object is stable, its Doppler shift is equal to zero ($f_{d1} = 0$) and its beat frequency, f_{b1} (which is negative for an up-going slope), corresponds to the true range. The second object moves towards the radar, its Doppler shift is positive ($f_{d2} > 0$) and the resulting calculated beat frequency becomes less than the true beat frequency ($|f_{b2}| = |f_{b1} + f_{d2}| < |f_{b1}|$). So the estimated range of the second object will be less than the true one. By contrast the signal determined by the third object has a negative Doppler shift ($f_{d3} < 0$) and its resulting beat frequency is less than the true beat frequency ($|f_{b3}| = |f_{b1} + f_{d3}| > |f_{b1}|$). The fourth signal (see Fig. 4.5) can not be detected. Although all three detected signals have the same energy (amplitude and duration) the amplitudes of their spectra may be different because of the mutual influence of the signals' spectra via the side-lobes.

4.3.2 Wide-band De-ramping Processing

Fig. 4.7-a shows the time-frequency representation of the received signals for FM-CW radar when four point objects in the same range are observed. One object is stable (its scale factor equals to unity, $s_1 = 1$), one object moves towards the radar ($s_2 > 1$) and two objects move away from the radar with different radial velocities which determine the different scale factors s_3 and s_4 ($s_4 < s_3 < 1$).

The time frequency representation of the de-ramped signals on the time-frequency plane for the wide-band model is shown in Fig. 4.7-b. The gray lines show the limits of the analyzed time-frequency region (from $\tau_{\max}$ to T in time and from 0 to $f_{b\max}$ in frequency).

The de-ramped signals in the wide-band model (Fig. 4.7-b) learn the following. The de-ramped signal defined by the fastest moving objects may still be present in the analyzed time-frequency region. The signal may be beyond the analyzed region partially or completely. Detection of target 4 depends on this time-frequency interval.

The main parameters of the wide-band de-ramping processing are given next.

Potential range resolution for the wide-band model. According to Fig. 4.7-b the de-ramped signals defined by the moving objects are LFM-signals which can occupy the analyzed time interval totally or partially. In case of a moving radar object the range resolution is derived from the corresponding LFM-signal contributing to the de-ramped signal spectrum. The object motion broadens the spectra of the de-ramped signal from a sine-spectrum to a LFM-signal spectrum. So for the wide-band model the range resolution does depend on the observed object motion.

The comparison of the limited sine signal spectrum width and the corresponding de-ramped

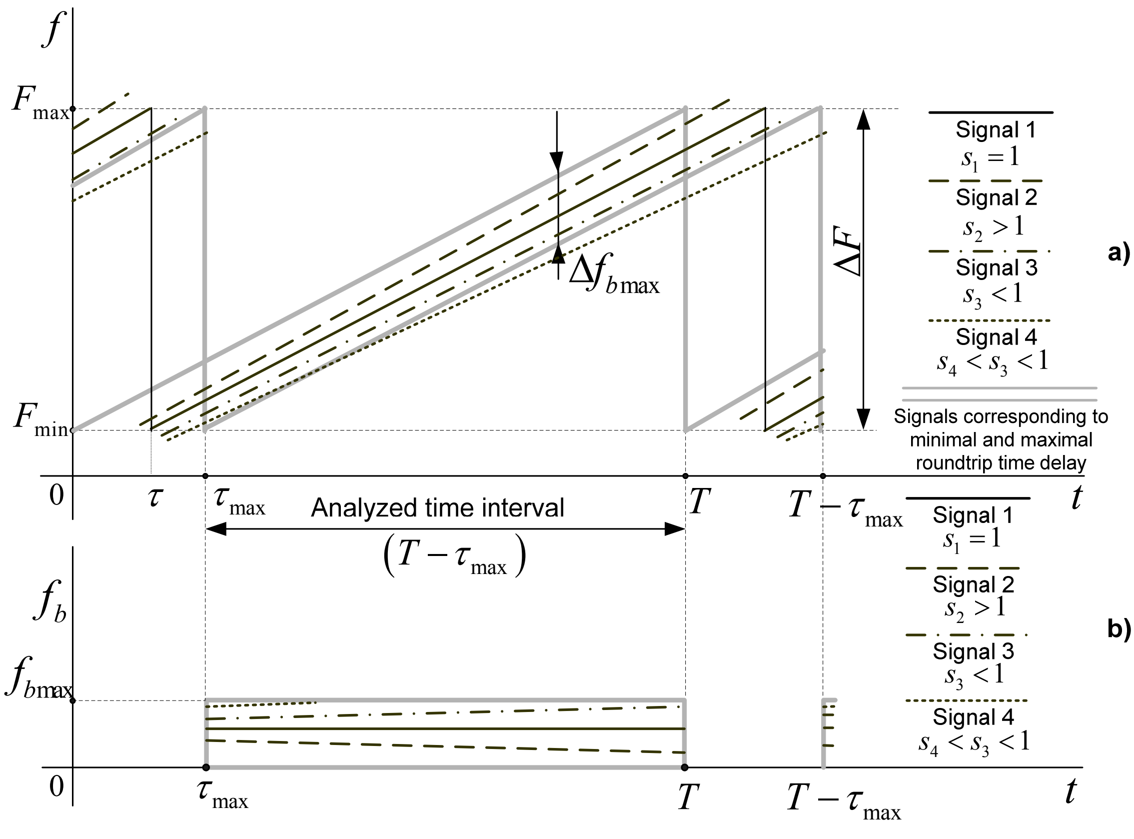

Fig. 4.7 – Wide-band model: time-frequency representation of a) the received signals; b) the de-ramped signals.

LFM-signal spectrum width can give us criteria for de-ramping processing efficiency when moving objects are observed. We note here that the results proposed in this Section show only qualitative but not quantitative bandwidth effects in case of moving objects observations.

Frequency shift of the received signals. A fast-moving radar object changes the spectrum of the LFM-signal according to the scale factor s. All frequencies of the signal scattered by the fast-moving object are multiplied by s. So the bandwidths of the four considered signals (Fig. 4.7) and their extremes in frequencies can be written as

$$\begin{aligned}
&F_{1\min} = s_1 \cdot F_{\min}, \quad F_{1\max} = s_1 \cdot F_{\max} \quad => \quad \Delta F_1 = s_1 \cdot \Delta F, \qquad \Delta F_1 = \Delta F, \\
&F_{2\min} = s_2 \cdot F_{\min}, \quad F_{2\max} = s_2 \cdot F_{\max} \quad => \quad \Delta F_2 = s_2 \cdot \Delta F, \qquad \Delta F_2 > \Delta F, \\
&F_{3\min} = s_3 \cdot F_{\min}, \quad F_{3\max} = s_3 \cdot F_{\max} \quad => \quad \Delta F_3 = s_3 \cdot \Delta F, \qquad \Delta F_3 < \Delta F, \\
&F_{4\min} = s_4 \cdot F_{\min}, \quad F_{4\max} = s_4 \cdot F_{\max} \quad => \quad \Delta F_4 = s_4 \cdot \Delta F, \quad \Delta F_4 < \Delta F_3 < \Delta F.
\end{aligned}$$

Furthermore, it should be noted that if a part of the received de-ramped signal or the whole signal is outside the analyzed time-frequency region (the gray lines in Fig. 4.7-b), the signal will not be processed.

Additional time shift of the received signals. The additional time shift of the received signals depends on both the radial velocity of the object (V) and the roundtrip time delay (τ) corresponding to the true range [1]. We find

$$\tau_{shift} = \frac{2 \cdot V}{c + V} \cdot \tau, \tag{4.14}$$

where c is the light velocity. A positive radial velocity of the object (the object moves away from the radar) results in a positive additional time shift. So the estimated range will be more far than the true range.

Range definition error. De-ramping processing utilizes a range estimation in frequency domain. So the frequency shift in the de-ramped signals relative to the sine-signal frequency (corresponding to the true range) can be determined from its difference with the center frequency of the LFM-signal within the limited analyzed time-frequency region (Fig. 4.7-b) .

Fig. 4.8 shows the de-ramped signals corresponding to Fig. 4.7-b. All objects are located at the same range. The first object is stable, its scale factor equals to unity ($s_1 = 1$) and its beat frequency, f_{b1}, corresponds to the true range. The second object moves to the radar and its beat frequency is less than the true beat frequency ($|f_{b2}| > |f_{b1}|$). So the estimated range of the second object will be less than the true one. By contrast the signal determined by the third object has a beat frequency higher than the true beat frequency ($|f_{b3}| < |f_{b1}|$). The fourth signal can not be fully used (part of signal is outside the analyzed time-frequency region); the highest velocity results in the widest spectrum with the smallest amplitude. We note that in case of fast-moving object observations beat-signal spectrum widening takes place.

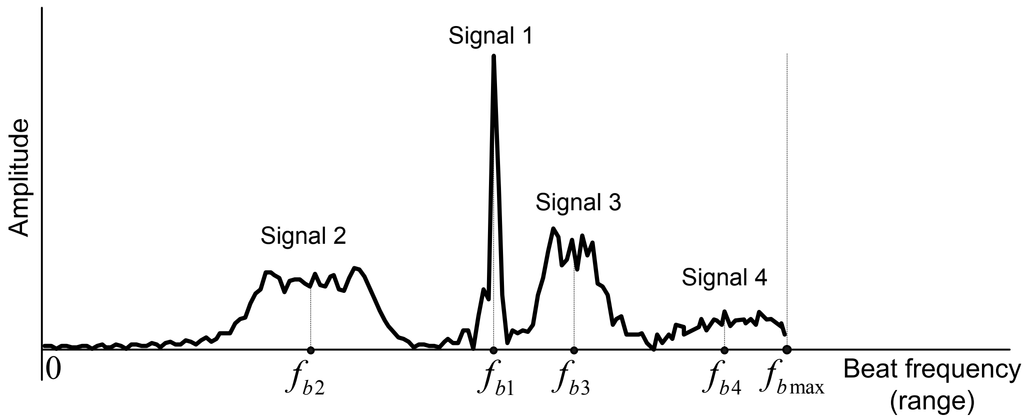

Fig. 4.8 – Spectra of the de-ramped signals (Fig. 4.7.b) for the wide-band model.

The range definition error defined by the object motion can be written:

$$R_e = \frac{T \cdot \Delta f_b}{\Delta F} \cdot \frac{c}{2}, \tag{4.15}$$

where Δf_b is the difference between the true beat frequency and the estimated beat frequency. The error resulting from Eq. 4.15 depends, therefore, on the signal spectra widths. Eq. 4.13 is the particular case of Eq. 4.15, when the beat frequency difference is determined from the Doppler shift.

Finally we remark that the de-ramping processing can be tuned for observing objects with specific radial velocities using the method proposed in Chapter 6 and adaptive signal processing can be applied for suppression of interfering LFM-signals in the de-ramped signal spectra.

4.4 Conclusion

Specific bandwidth effects appearing when fast-moving objects are observed have been analyzed for two types of signal models (narrow-band and wide-band models) and for two techniques of sophisticated signal processing (correlation processing and de-ramping processing). The wide-band correlation processing which is the generalization of the narrow-band allows us to overcome the limitations of the sounding signal BT-product and of the velocity of the observed radar objects. A novel wide-band correlation processing applicable to dual orthogonal polarimetric radar signals has been designed. A new representation of the wide-band de-ramping processing has been developed and the quantitative comparison between the narrow-band and wide-band de-ramping processing has been done. The influence of fast-moving objects has been analyzed for the de-ramped signals in LFM radar and differences between the wide-band signal model and the narrow-band one has been shown.

References

1. L.G. Waiss. “Wavelets and wideband correlation processing”, IEEE SP Magazine, January 1994, pp. 13-32.
2. I. Daubechies, “The Wavelet Transform, Time-Frequency Localization and Signal Analysis”, IEEE Trans. on Information Theory, Vol. 36, No. 5, 1990, pp. 961-1005.
3. O. Roiul and M. Vetterli, “Wavelet and Signal Processing”, IEEE SP Magazine, Vol. 8, No. 4, 1991, pp. 14-38.
4. G.P. Babur, L.P. Ligthart, “Wideband correlation processing in polarimetric radar with compound signals and simultaneous measurement of scattering matrix elements”, Microwaves, Radar and Wireless Communications, 2008. MIKON 2008. 17th International Conference on 19-21 May 2008.
5. M. I. Skolnik, “Introduction to Radar Systems”, 2nd Ed. New York: IEEE, 1981.
6. L. Sibul; L. Ziomek, “Generalized wideband crossambiguity function”, Acoustics, Speech, and Signal Processing, IEEE International Conference on ICASSP '81, Volume 6, Apr 1981, pp. 1239-1242.
7. A. Grossman, J. Morlet, “Decompositions of Hardy Functions into Square Integrable Wavelets of constant shape”, SIAM J. Math. Anal., 15(4), 1984, pp. 723-36.
8. O.A. Krasnov, L.P. Ligthart, Z. Li, P. Lys, F. van der Zwan, “The PARSAX – Full Polarimetric FMCW Radar with Dual-Orthogonal Signals”, Radar Conference, 2008, EuRAD 2008, Oct. 2008, pp. 84-87.

PART 2

ADVANCED PROCESSING IN POLARIMETRIC RADAR WITH CONTINUOUS WAVEFORMS

5. Quasi-Simultaneous Measurement of Scattering Matrix Elements in Polarimetric Radar with Continuous Waveforms Providing High-Level Isolation between Radar Channels

The chapter presents a novel de-ramping technique which provides high-level isolation between branches in FM-CW radar channels. The radar hardware is splitting the received signals with orthogonal polarizations and provides the wanted isolation between polarimetric radar channels. The isolation between the branches in channels is strongly dependent on the time interval when the useful scattered signals, determined from the sounding signals with orthogonal polarizations, occupy the same bandwidth. A pair of LFM-signals having the same form and time shifted relative to each other is proposed in the technique. Because of this time shift useful scattered signals defined with the different sounding signals occupy different bandwidths at every time instant. So de-ramping processing can give the high level of isolation provided with the LPFs used in the de-ramping scheme.

5.1 Problem Statement

Signals with dual orthogonality are needed in polarimetric radar with simultaneous measurement of all scattering matrix elements [1-5]. In FM-CW polarimetric radar the conventional sounding signals are LFM-signals with opposite (up-going and down-going) slopes. Such type of sounding signals allows to split all elements of the scattering matrix and to measure all of them simultaneously during the signals' sweep time (radar duty cycle). However, there are two problems which limit the accuracy in the estimations when de-ramping processing is used.

<u>Problem 1</u>: <u>Side-lobes in the frequency domain</u>. The useful beat signals (tones) are compressed after using the Fourier transform. Their spectra have the information parts (main-lobes) and side-lobes which appear because of the limited time duration of the beat signals, that is the analyzed time interval (see Paragraph 3.3.2). Side-lobes in frequency domain have the same negative influence as side-lobes in time domain have for correlation processing (e.g. matched filtering). They limit the dynamic range of amplitudes of useful received signals.

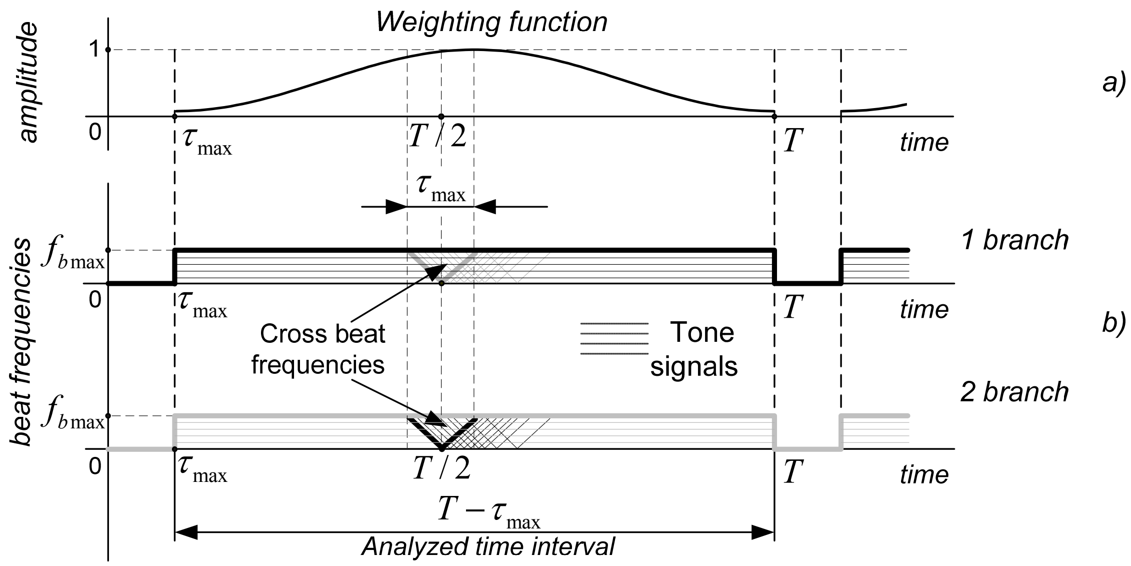

Fig. 5.1 – a) Weighting function (e.g. Hamming function with parameter 0.54) for the beat signals; b) beat-frequency representation of objects per radar channel.

Problem 1 can be solved efficiently using weighting (e.g. the weighting function shown in Fig. 5.1-a) to the beat signal prior to the Fourier transform [6]. However, weighting of beat signals can add to Problem 2 because it decreases the amplitudes of useful beat-signals at the edges and does not change the amplitudes of the interfering (cross-) beat signals (Fig. 5.1-b). We note here that beat frequencies in Fig. 5.1.b correspond to the arbitrary objects and are shown here as an example.

Problem 2: Isolation between the branches within polarimetric radar channels. When the received signals both occupy the same frequency bandwidth and time interval they can have relatively high level of cross-correlation. This time interval is called cross-correlation region (see Paragraph 3.4.2). Although cross-beat frequencies (Fig. 5.1-b) are non-stationary along the analyzed time interval (actually cross-beat frequencies interfere only during a part of the analyzed time interval) their frequencies occupy the whole beat frequency bandwidth ($0...f_{b\max}$). It can limit the accuracy of SM estimations considerably. So the increase of isolation between the branches in FM-CW polarimetric radar is of interest.

Suppression of beat-signals in the middle of the analyzed time interval (Fig. 5.1-b) is unacceptable, because it will limit the beat signals' duration and therefore the radar range resolution (see Paragraph 3.3.2). So a new type of sounding signals which do not result in cross-beat frequencies in FM-CW radar receiver is of interest.

It should be noted that isolation between the two polarimetric radar channels 1 and 2 will not be considered here because this isolation is realized in the radar hardware by careful splitting of the received signals having orthogonal polarizations.

The structure of the chapter is the following. Section 5.2 proposes a new type of vector sounding signal and the corresponding technique providing a high-isolation level between the branches per polarimetric radar channel. The unambiguous range and limitations of the proposed technique are also considered in Section 5.2. Section 5.3 gives the estimation of isolation between branches in PARSAX radar channels when the proposed technique is implemented.

5.2 De-ramping Technique with Quasi-Simultaneous Measurement of Scattering Matrix Elements

5.2.1 Continuous LFM-signals with a Time Shift Relative to Each Other

Continuous LFM-signals having the same form but with a relative time shift are proposed for the de-ramping technique applicable to FM-CW polarimetric radar. A time shift for LFM-signals corresponds to a frequency shift. A time shift between the same LFM-signals of more than the maximum roundtrip time delay, $\tau_{\max}$, can result in high-level isolation between branches in polarimetric radar channels which is then only limited by the amplitude-frequency responses of the LPFs used in the de-ramping filter.

The new type of vector sounding signal (Eq. 2.10) can be written as:

$$\dot{\mathbf{u}}(t) = \begin{bmatrix} \dot{u}_1(t) \\ \dot{u}_2(t) \end{bmatrix} = \begin{bmatrix} \dot{u}_1(t) \\ \dot{u}_1(t - t_{shift}) \end{bmatrix}, \tag{5.1}$$

where $\dot{u}_1(t)$ is an LFM-signal (e.g. with up-going slope) transmitted with the first (horizontal) polarization, $\dot{u}_2(t) = \dot{u}_1(t - t_{shift})$ is the shifted LFM-signal with the second (vertical) polarization and t_{shift} is the time shift between the continuous LFM-signals. The sounding signals are shown in Fig. 5.2-a with the solid lines (black and gray respectively). In the context of a prior uncertainty concerning the radar object we consider that the maximum roundtrip time delay of received signals is equal to $\tau_{\max}$ (radar parameter).

Fig. 5.2.a also shows the frequency plot of received signals at maximum range (determined by the radar system) in both branches of one radar channel (dashed black and gray lines) where $\tau_{\max}$ is the maximum allowed time delay. The frequency plots of the de-ramped received signals (beat signals) are represented in Fig. 5.2.b-e. In the Figure T is the duty cycle of the radar, ΔF means the frequency excursion, $f_{b\max}$ is the maximum beat frequency of the de-ramped signals and f_{diff} is the frequency difference between useful signals in the radar channel branches at every time instant. Amplitudes of cross-beat signals (Fig. 5.2.d-e) are equal to zero in case of ideal LPF's used in the de-ramping scheme (Fig. 5.3).

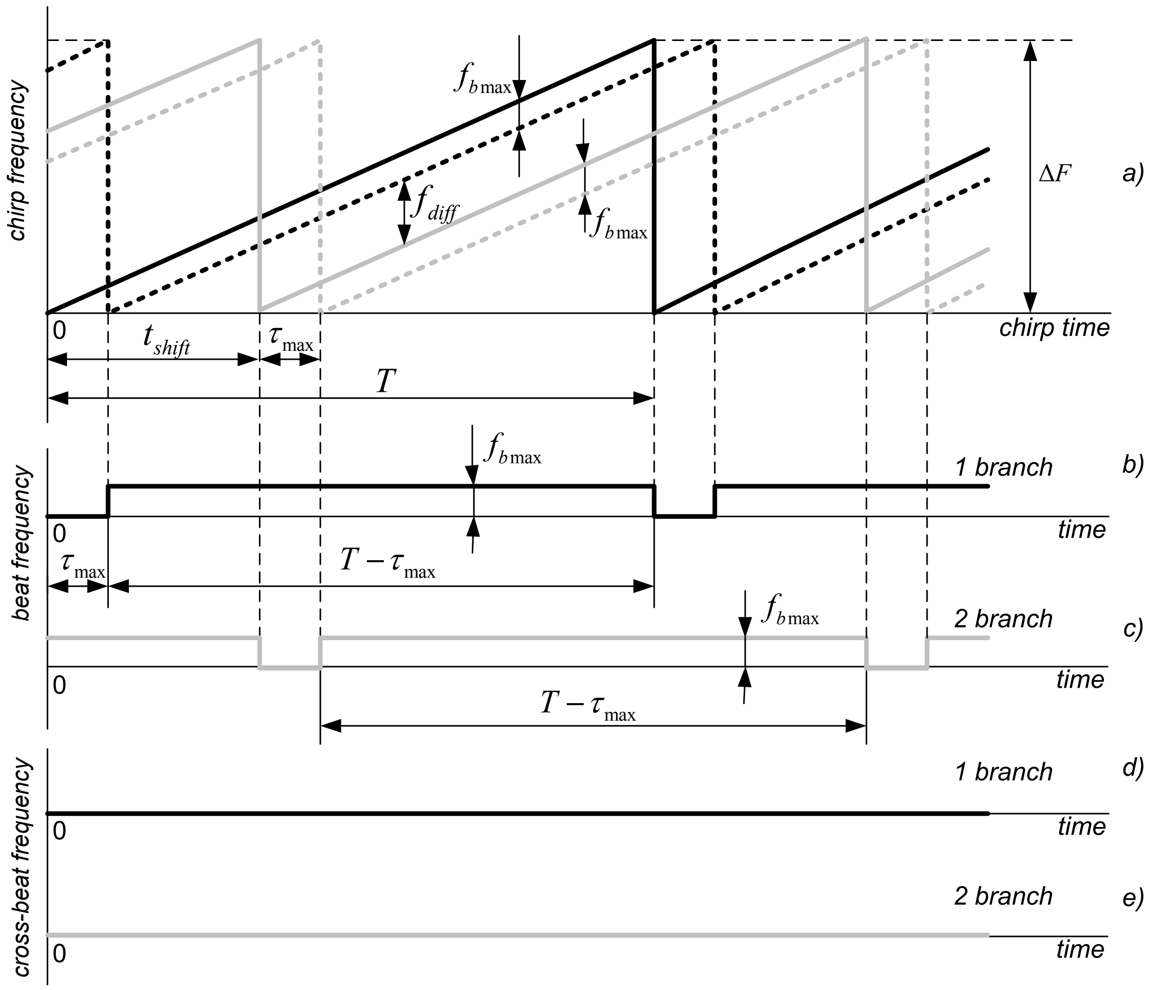

Fig. 5.2 – Frequency plot of continuous LFM-signals with a relative time shift and their beat frequencies in case of ideal LPFs in the branches of one polarimetric radar channel.

For real LPFs used in the de-ramping chain, the isolation between branches per polarimetric radar channel is dependent on:

1. the amplitude-frequency responses per branch;
2. the frequency difference, f_{diff}, between the useful signals in the radar channel branches.

The isolation between branches in PARSAX radar channels is estimated in Section 5.3.

Fig. 5.3 shows the simplified scheme for the de-ramping filter when two continuous LFM-signals with relative time shift are used. The scheme is almost identical to the general de-ramping scheme (Fig. 3.6). However the blocks utilizing Fast Fourier Transform (FFT) are different for both branches (FFT 1 and FFT 2) because they utilize Fourier transforms in different time intervals shifted relative to each other, similar to the way the sounding LFM-signals are shifted.

For estimating all scattering matrix elements each received signal ($\dot{x}_1(t), \dot{x}_2(t)$) is mixed with replicas of the transmitted waveforms ($\dot{u}_1(t)$, $\dot{u}_1(t-t_{shift})$). The de-ramping technique

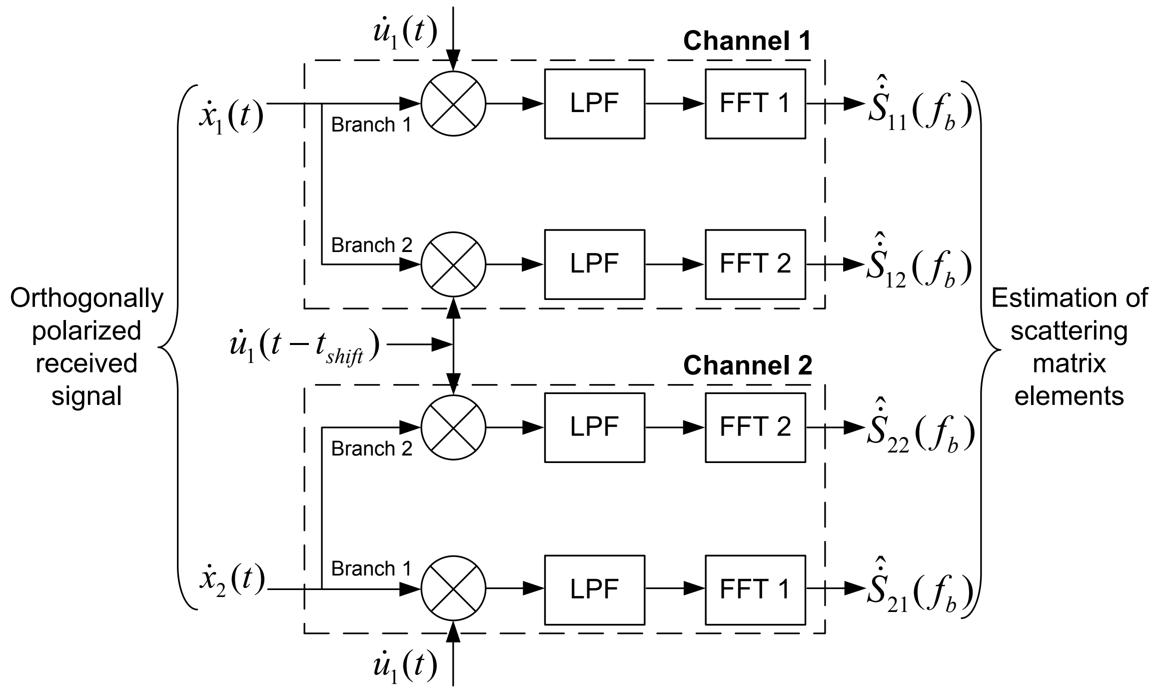

Fig. 5.3 – Simplified scheme for de-ramping filter when two continuous LFM-signals with a relative time shift are used.

proposed in this section is based on the transformation of de-ramped (beat) signals (after low-pass filtering) into the frequency domain (using FFT). This technique provides the resulting spectra as function of beat frequencies (f_b), which correspond to range profiles for all four complex elements of the scattering matrix; we obtain

$$\begin{bmatrix} \hat{\dot{S}}_{11}(f_b) & \hat{\dot{S}}_{12}(f_b) \\ \hat{\dot{S}}_{21}(f_b) & \hat{\dot{S}}_{22}(f_b) \end{bmatrix} = \begin{bmatrix} FFT1\left\{LPF\left(\dot{x}_1(t)\cdot\dot{u}_1^*(t)\right)\right\} & FFT2\left\{LPF\left(\dot{x}_1(t)\cdot\dot{u}_1^*(t-t_{shift})\right)\right\} \\ FFT1\left\{LPF\left(\dot{x}_2(t)\cdot\dot{u}_1^*(t)\right)\right\} & FFT2\left\{LPF\left(\dot{x}_2(t)\cdot\dot{u}_1^*(t-t_{shift})\right)\right\} \end{bmatrix}, \quad (5.2)$$

where $t \in \left[\tau_{\max}...T\right]$.

5.2.2 Unambiguous Range Estimation

The ambiguity in range estimation appears when a signal defined by one duty cycle of the radar and scattered from a far-located object can coincide in time with a signal defined by the next duty cycle and scattered from a near-located object. Since FM-CW radar with continuous waveforms receives scattered signals continuously, the unambiguous range (R_1) is ultimately determined by the maximum unambiguous time delay equal to the radar duty cycle (T). In this ultimate case the unambiguous range, which is marked with index “1” in Fig. 5.4, equals to

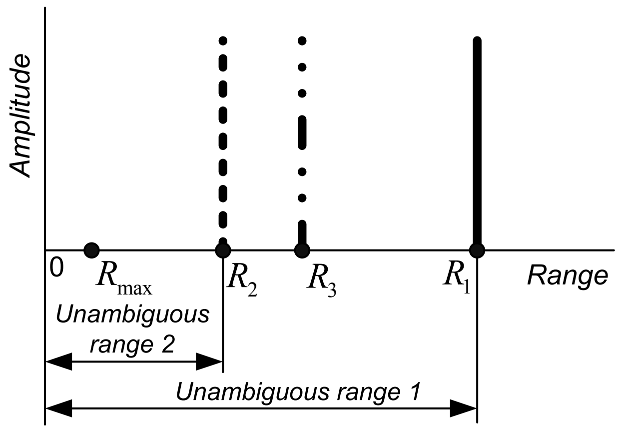

Fig. 5.4 – Unambiguous ranges for de-ramping processing, general case.

$R_1 = \dfrac{c \cdot T}{2}$. When the same LFM-signal with a time shift is used as second vector sounding signal component, the maximum unambiguous time delay changes. The corresponding ultimate unambiguous range, which is marked with indices "2" and "3" in Fig. 5.4, becomes the minimum of $R_2 = \dfrac{c \cdot t_{shift}}{2}$ for $\tau_{\max} < t_{shift} \le \dfrac{T}{2}$ or $R_3 = \dfrac{c \cdot (T - t_{shift})}{2}$ for $\dfrac{T}{2} < t_{shift} < (T - \tau_{\max})$.

It can be seen from Fig. 5.4 that the maximum ultimate unambiguous range for the here-proposed technique will be obtained for a time shift between sounding LFM-signals which is equal to half of the signals' repetition period (Fig. 5.5). The maximum range ($R_{\max}$) is marked in Fig. 5.4-5.5 for FM-CW radar with $\tau_{\max}/T = 0.1$.

For the here-proposed technique we face the following contradiction in any situation. On the one hand, a small time shift t_{shift}, is desirable, because the estimations of SM elements should be

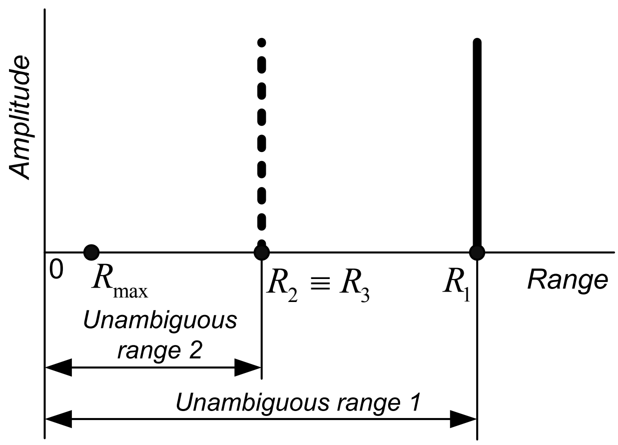

Fig. 5.5 – Ultimate unambiguous ranges for de-ramping processing in case $t_{shift} = T/2$.

close to simultaneous measurement estimations. On the other hand, a small time shift can limit the ultimate unambiguous range. So a compromise should be found when the here-proposed technique is utilized.

5.2.3 Limitations of the Here-Proposed Technique

The technique proposed in this chapter has a number of limitations to the type of used sounding signals. A first limitation is:

1. Quasi-simultaneity of measurements.

We know that the vector sounding signal components (two sounding signals with orthogonal polarizations) are utilized for estimation of the scattering matrix columns. Since sounding LFM-signals with the same form but with a time shift are used as vector sounding signal components, the estimations of SM columns are calculated at different but overlapping time intervals (see Fig. 5.2.b-c). So the proposed technique utilizes quasi-simultaneous measurements of SM elements. In case of fast moving or fast-fluctuating radar targets the impact of this quasi-simultaneous approach should be estimated.

A second limitation also concerns the time shift between the continuous LFM sounding signals in connection to the unambiguous range (see Paragraph 5.2.2).

2. Unambiguous range.

The time shift limits the ultimate unambiguous range for FM-CW polarimetric radar. For the proposed technique this range is determined not by the signals' repetition period but by the minimal time shift between the sounding signals. So the maximum ultimate range for the proposed technique equals to half of the sweep time. It should be noted that the ultimate range is in general much more than the maximum observed range defined by the maximum time delay (maximum beat frequency).

The third limitation is general for FM-CW radar using sounding LFM-signals and is given here for the completeness.

3. Non-linearities in the beat signals.

Sometimes the sounding signal modulation can not be provided as ideal linear, and a frequency non-linearity is present in the transmitted signal. In this case the received de-ramped signals (beat signals) also have non-linearities which cause range resolution degradation in FM-CW radar. From earlier research we know that the range resolution degradation is greater for larger observed range [7]. So non-linearities in the beat signals are not desirable in modern high-resolution radar as in the PARSAX system.

The described problem was solved in IRCTR TU Delft. A novel algorithm was developed, which completely removes the effects of non-linearities in the beat signals, independently of range and Doppler [7-9]. As for the here-proposed de-ramping technique the attention should be paid to the bandwidths of the LPFs by taking possible deviations in the transmitted signal into consideration.

Despite the de-ramping technique with quasi-simultaneous measurement of SM elements has the here-considered limitations, it may provide high-level isolation between branches per FM-CW polarimetric radar channel. A concrete verification for the PARSAX radar is presented in next Section.

5.3 PARSAX Isolation Estimation

We here consider the possibility of using the de-ramping technique proposed in the previous section for the IRCTR-PARSAX radar system.

The proposed de-ramping technique provides an isolation independent on the observed radar target; just the amplitude-frequency responses of the LPFs (see Fig. 5.3) determine the isolation between branches in each FM-CW polarimetric radar channel.

For simulation purposes linear-phase equi-ripple filters were chosen. Such kind of filter is desirable because it has a maximum deviation from the ideal filter which is lowest when we compare this type of filter with other linear-phase FIR filters of the same order. Equi-ripple filters are ideally suited for applications in which a specific tolerance must be met, such as when we should design a filter with a tolerance with respect to a given minimum stop-band attenuation or a given maximum pass-band ripple.

Fig. 5.6 shows the amplitude-frequency response of the equi-ripple filter. f_p and f_s mean pass-band frequency and stop-band frequency respectively.

The following considerations were taken into account for the modelling:

a. The pass-band frequency (f_p) of the equi-ripple filter is known and equal to the maximum frequency of the beat signal ($f_{b\max}$).
b. The stop-band frequency (f_s) and in particular the ratio of the stop-band frequency to the pass-

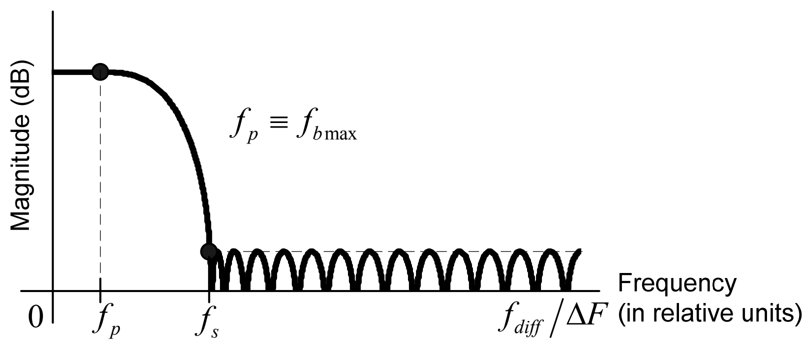

Fig. 5.6 − Amplitude-frequency response function of an equi-ripple filter.

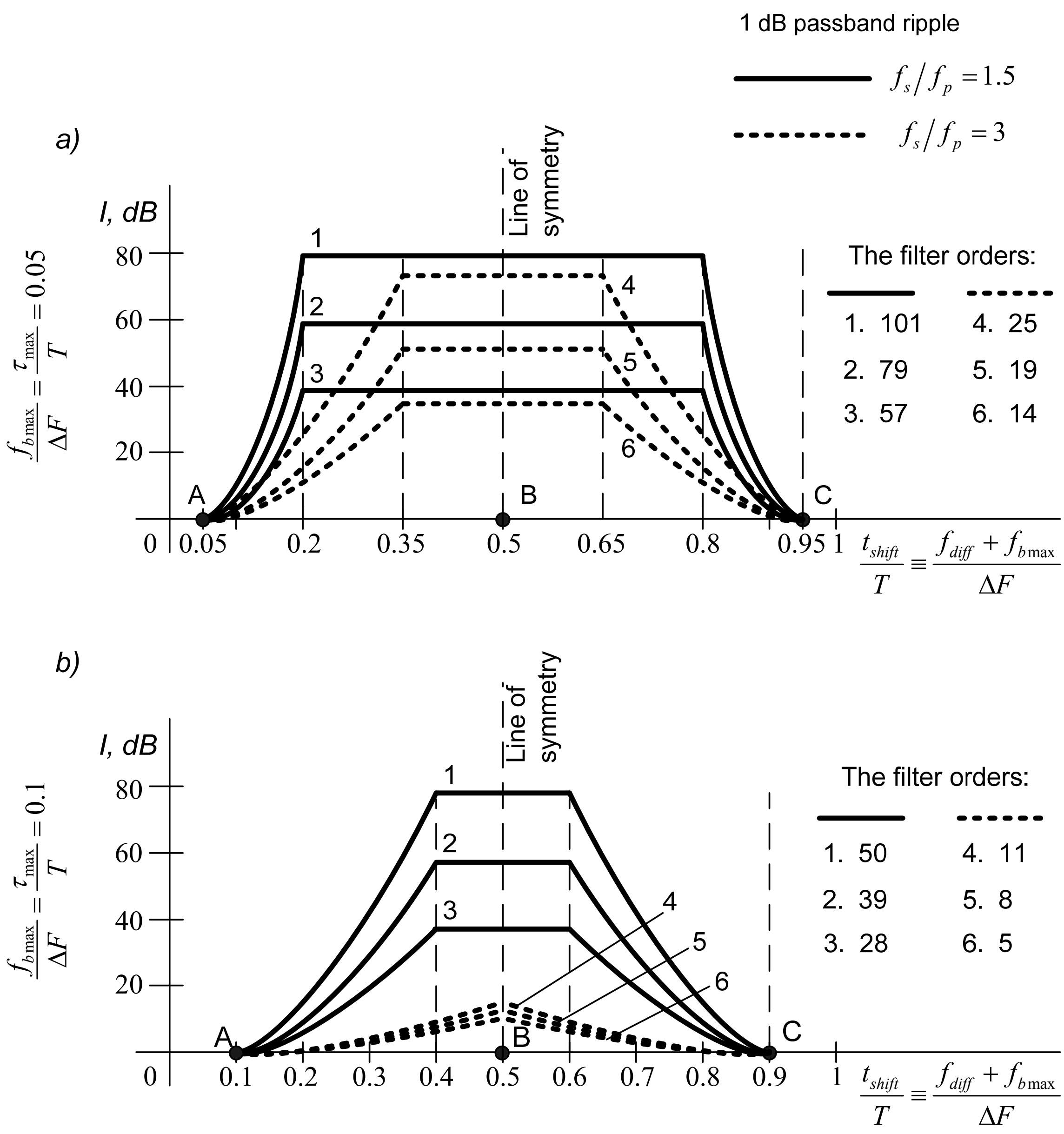

Fig. 5.7 − De-ramping isolation when LFM-signals with a relative time shift are used in combination with an equi-ripple filter with different parameters; a) $\tau_{\max} = 0.05 \cdot T$ and b) $\tau_{\max} = 0.1 \cdot T$.

band frequency (f_s/f_p) was chosen as parameter.

For simulation the pass-band ripple (which is a design parameter) of the equi-ripple filter is equal to 1 dB for all low-pass filters included in the de-ramping scheme.

The maximum roundtrip time delay $\tau_{\max}$ for the PARSAX radar is equal to 0.1 ms, while the sweep time of LFM-signals is 1 ms (see Table A.1). So the ratio $\frac{\tau_{\max}}{T}$, as parameter in the modeling, equals to 0.1. For comparison of modeling results, we also calculated the isolation for $\frac{\tau_{\max}}{T} = 0.05$.

Fig. 5.7 can be used for choosing the time shift (t_{shift}) between the sounding signals having different polarization, assuming a required isolation level. The figures are presented for two ratios f_s/f_p of stop-band to pass-band frequency, that is 1.5 and 3. Fig. 5.7.a and 5.7.b show the isolation for two maximum time delays of the received signal, for $0.05 \cdot T$ and $0.1 \cdot T$ respectively. Points A-C in Fig. 5.8 correspond to:

$$A \rightarrow \frac{f_{b\max}}{\Delta F} \equiv \frac{\tau_{\max}}{T} \quad B \rightarrow \frac{\Delta F}{2 \cdot \Delta F} \equiv \frac{T}{2 \cdot T} \equiv 0.5 \quad C \rightarrow \frac{\Delta F - f_{b\max}}{\Delta F} \equiv \frac{T - \tau_{\max}}{T},$$

$\tau_{\max} = 0.1 \cdot T$.

Fig. 5.7 can also be used for our choice of time shift (t_{shift}) between sounding signals with different polarization. For example when a maximum time delay of $0.1 \cdot T$ and an equi-ripple filter of order 50 with $f_s/f_p = 1.5$ are selected an isolation of 78 dB is feasible for $t_{shift} = (0.4...0.6) \cdot T$. The isolation determined from the LPFs in the radar system can thus be very high.

5.4 Conclusion

This chapter has described a novel technique for continuous "quasi-simultaneous" measurement of SM elements in FM-CW polarimetric radar. The simulation results have shown that very high isolation levels are achievable. Moreover the proposed technique retains the advantages of application of sounding signals with continuous waveforms. Limitations of the proposed technique have also been considered in this chapter.

References

1. D. Giuli, L. Facheris, M. Fossi, and A. Rossettini, "Simultaneous Scattering Matrix Measurement through Signal Coding," in Record of the IEEE 1990 International Radar Conference, 1990, pp. 258-262.
2. D. Giuli, M. Fossi, and L. Facheris, "Radar Target Scattering Matrix Measurement through Orthogonal Signals," IEE Proceedings, Part F. Radar and Signal Processing, vol. 140, Aug. 1993, pp. 233-242.

3. D. Giuli, L. Facheris, M. Fossi, A. Rossettini, “Simultaneous scattering matrix measurement through signal coding,” Radar Conference, 1990., Record of the IEEE 1990 International 7-10 May 1990.
4. G.P. Babur, L.P. Ligthart, “Wideband correlation processing in polarimetric radar with compound signals and simultaneous measurement of scattering matrix elements” Microwaves, Radar and Wireless Communications, 2008, MIKON 2008.
5. O.A. Krasnov, L.P. Ligthart, Z. Li, P. Lys, F. van der Zwan, “The PARSAX — Full Polarimetric FMCW Radar with Dual-Orthogonal Signals”, Radar Conference, 2008, EuRAD 2008, Oct. 2008, pp. 84-87.
6. J.J.M. de Wit, “Development of an Airborne Ka-Band FM-CW Synthetic Aperture Radar”, Dissertation at Delft University of Technology, 2005.
7. A. Meta, “Signal Processing of FMCW Synthetic Aperture Radar Data”, Dissertation at Delft University of Technology, 2006.
8. A. Meta, P. Hoogeboom, L.P. Ligthart, “Range Non-Linearities Correction in FMCW SAR”, in Proc. IEEE Int. Geoscience and Remote Sensing Symp. IGARSS’06, Denver, CO, USA, July 2006.
9. A. Meta, P. Hoogeboom, L.P. Ligthart, “Range Frequency Non-linearities Correction for FMCW SAR”, European Patent Application, no. 06076057.6, May 2006.

6. Flexible De-Ramping Processing

This chapter presents a novel flexible de-ramping processing applicable for linear FM-CW radars. By utilizing special supporting signals the here-proposed technique allows for solving three tasks which can affect the FM-CW radar performance, namely a change in signal bandwidth, shift of beat frequency bands, and selection of range interval among the observed ranges for high-range resolution. The first task provides a varying of radar range resolution without considerable receiver upgrade and offers therefore flexibility of this technique. Shifting the beat signals' bandwidth (the second task) provides flexibility in filters because the filtering of beat signals can then take place at preferred frequencies. The third task allows for an observation of a part of the full radar range, namely the selection of range interval by using flexibility in localization of the beat signals' bandwidth, while in addition there is no need to change the amplitude-frequency responses of the used filters.

6.1 Flexible De-ramping Principle

Flexible de-ramping for linear FM-CW radar may execute the following tasks:

1. change of the received signal bandwidth without range resolution decrease;
2. shift in the beat frequency band.
3. selection of range interval with high range resolution.

The reasons for use of flexible de-ramping processing are the following:

The first task arises from our wish to improve existing FM-CW radar systems in the sense that when the sweep frequency of the sounding LFM-signal is increased for better range resolution, a change of the whole radar receiver is not desirable. In such a case the decrease of the received signal sweep frequency is eligible.

The second task is associated with the potential integrating of a low-pass filter (LPF) or band-pass filter (BPF) applied to the mixed signal in the FM-CW radar receiver.

The third task takes place when only a part of the estimated ranges is of interest, e.g. when the approximate range of wanted objects under observation is known.

For explanation of flexible de-ramping processing we start from the de-ramping basics explained before (see Paragraph 3.3.2). The typical de-ramping processing can be described in three steps

1. Multiplication of the received signal and transmitted signal replica;
2. Low-pass filtering;
3. Fourier Transform (FT).

Since a Fourier Transform is utilized in practice as Fast Fourier Transform, we use FFT hereinafter.

In this section the flexible de-ramping principle is first explained for a single-channel LFM-CW radar (Fig. 6.1). Flexible de-ramping for polarimetric radar with simultaneous measurement of scattering matrix elements is considered in the next section of this chapter.

The sounding LFM-signal having an up-going slope (see Paragraph 2.2.1) for example, can be written as

$$\dot{u}_1(t) = \exp\left[j \cdot 2\pi \cdot \left(\frac{k_1}{2} \cdot t^2 + f_1 \cdot t \right) + \varphi_1 \right], \quad t \in [0...T], \tag{6.1}$$

where k_1 (called sweep rate; dimension 1/sec^2) is a positive constant which determines the frequency deviation (ΔF_1) of the sounding signal, f_1 and φ_1 are the initial frequency and phase of the sounding signal. Flexible de-ramping for a sounding LFM-signal having down-going slope is utilized in a similar way and is considered in the next section when describing the vector sounding signal.

For estimation of the reflection coefficients as function of range (beat frequency) the received signal, $\dot{x}(t)$, is mixed with the replica of the transmitted waveform, $\dot{u}_1(t)$, as illustrated in Fig. 6.1. An FFT is applied to the so-obtained beat signals after demodulation and low-pass filtering. The resulting spectrum as function of beat frequency (f_b) for each ramp corresponds to the estimation of reflection coefficients as function of beat frequency:

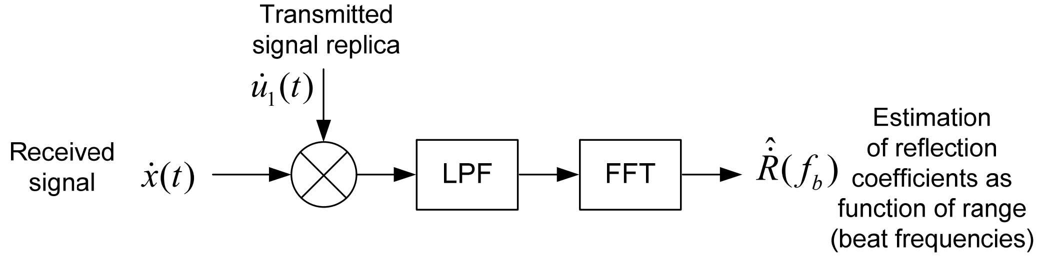

Fig. 6.1 – Simplified scheme for a typical de-ramping filter in a “standard” single-channel LFM-CW radar.

$$\hat{\dot{R}}(f_b) = FFT\left[LPF\left[\dot{x}(t)\cdot \dot{u}_1(t)\right]\right], \tag{6.2}$$

where the FFT is calculated for signals within the time interval $\left[\tau_{\max}...T\right]$; $\tau_{\max}$ is the maximum time delay for the received signals and T is the duty cycle of the FM-CW radar.

The delayed copy of the signal can be written as

$$\dot{u}_1(t-\tau) = \exp\left[j\cdot 2\pi\cdot \left(\frac{k_1}{2}\cdot(t-\tau)^2 + f_1\cdot(t-\tau)\right) + \varphi_1 \right], \tag{6.3}$$

where the roundtrip time delay, τ, can vary over the interval $\left[0...\tau_{\max}\right]$. The multiplication of the transmitted signal and its delayed copy gives the sum signal (with sum frequencies) and difference signal (with difference frequencies). The sum signal is filtered out by the LPF and the difference signal containing beat frequencies is of interest.

The multiplication of the transmitted signal and its delayed replica after low-pass filtering can be written as

$$\dot{u}_1(t-\tau)\cdot \dot{u}_1(t) = \exp\left[j\cdot 2\pi\cdot \left(-k_1\cdot\tau\cdot t + \frac{k_1}{2}\cdot\tau^2 - f_1\cdot\tau \right)\right]. \tag{6.4}$$

The beat frequency is proportional to the echo signal roundtrip time delay, τ, determining the radar object range (the beat frequency corresponds to the first item in the exponential term of Eq. 6.4). The two other terms are constants.

The FM-CW radar receiver has a fixed beat frequency bandwidth Δf_b for a definite maximum time delay $\tau_{\max}$. The increase of sounding signal bandwidth leads to the proportional increase of the beat frequency bandwidth and, therefore, to the range resolution increase (see Eq. 3.13). However a sounding signal bandwidth increase can demand the corresponding decrease of the received signal bandwidth if the existing radar hardware re-use is desirable. The received signal bandwidth can be utilized if we apply flexible de-ramping processing. Problems concerning the observed range limitations due to increasing the sounding LFM-signal bandwidth and the impact are described in [2].

A possible block-diagram for FM-CW radar using flexible de-ramping processing is shown in Fig. 6.2. We note that two blocks for sounding signal bandwidth increase and received signal bandwidth decrease were added to the existing FM-CW radar hardware. ΔF_1 is the bandwidth of the signal produced by the existing radar transmitter. It determines the beat frequency bandwidth Δf_{b1} according to Eq. 3.13. ΔF_2 corresponding to the modified (increased) sounding signal bandwidth, which results into the increased range resolution. The corresponding beat frequency bandwidth is Δf_{b2}. We choose $\Delta F_2 > \Delta F_3$, where ΔF_3 corresponds to the bandwidth of the

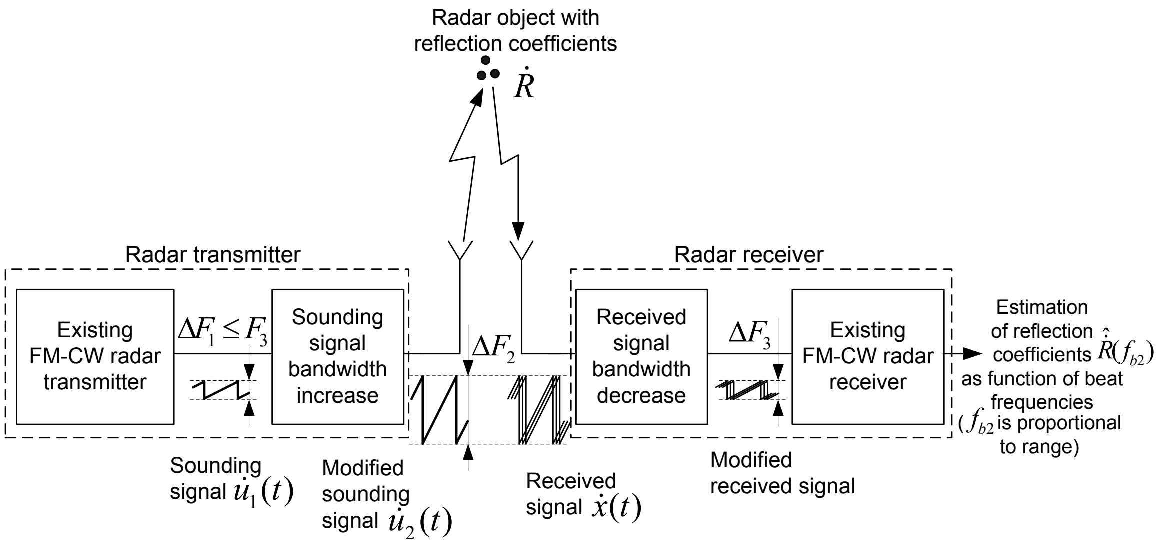

Fig. 6.2 – Possible diagram for FM-CW radar using flexible de-ramping processing.

existing radar hardware of both transmitter and receiver. The condition $\Delta F_1 \leq \Delta F_3$ gives us some freedom in the LFM-sounding signal within the existing transmitter hardware bandwidth.

The bandwidth increase and bandwidth decrease of LFM-signals, can be organized by using stretched processing [1]. The stretching is provided via a supporting signal, $\dot{v}\,(t)$, which is an LFM-signal with strict constraints on selected waveform parameters:

$$\dot{v}(t) = \exp\left[j \cdot 2\pi \cdot \left(\frac{k_0}{2} \cdot t^2 + f_0 \cdot t \right) + \varphi_0 \right], \quad t \in [0...T]; \tag{6.5}$$

where k_0, f_0 and φ_0 are the sweep rate, initial frequency and initial phase, respectively. It is noted that a slow-down for an up-going LFM-signal occurs when the sweep rate k_0 is positive [1].

Flexible de-ramping processing can be described in four steps (Fig. 6.3):

1. Stretching of the received signal using a supporting LFM-signal;
2. Multiplication of the stretched received signal with a modified transmitted signal;
3. Low-pass or band pass filtering;
4. Fast Fourier Transform.

The first and second step can be joined in practice. However, for better describing the various processing aspects proposed in this chapter they are considered separately.

6.1.1 Change of the Received Signal Bandwidth (First Variant)

The first variant of the flexible de-ramping scheme is shown in Fig. 6.3.

The multiplication of the received signal and supporting signal results into the stretching of the received signal. It changes the received signal bandwidth. It can be used as follows. It is known that the sounding LFM-signal bandwidth determines the FM-CW radar range resolution (see Paragraph 3.3.2). So for better range resolution a larger sounding signal bandwidth is wanted. In this case flexible de-ramping can be implemented when such a resolution change is desirable; however a hardware upgrade of the radar receiver is not eligible. So if a larger range resolution is needed (e.g. for the PARSAX radar), a sounding signal with a larger bandwidth is used together with a slow-down supporting signal and the radar receiver needs only an additional stretching block. So flexible de-ramping processing gives the flexibility to radar for obtaining different (e.g. larger) range resolutions without significant radar receiver upgrades.

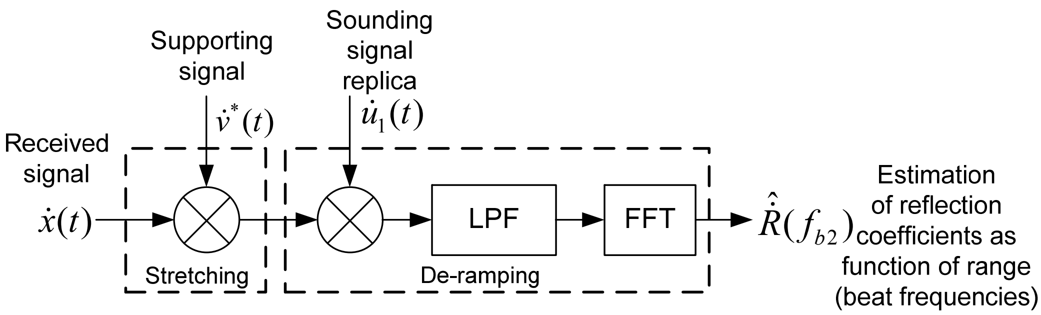

Fig. 6.3 – Simplified scheme for a flexible de-ramping filter. Variant 1.

In analogy with Eq. 6.2 the resulting spectrum ($R(f_{b2})$) as function of beat frequencies (f_{b2}) for the ramps of interest, corresponds to the estimated range profile and is calculated from:

$$\hat{\dot{R}}(f_{b2}) = FFT\left[LPF\left[\left(\dot{x}(t)\cdot\dot{v}^*(t)\right)\cdot\dot{u}_1(t)\right]\right], \tag{6.6}$$

where *LPF* means low-pass filter and the FFT is utilized for the multiplied signals after filtering over the $\left[\tau_{\max}...T\right]$-interval. The transmitted signal $\dot{u}_1(t)$ with parameters k_1, f_1, φ_1 and the existing radar receiver bandwidth $\Delta F_3 = \left[F_{3\min}...F_{3\max}\right]$ are considered to be known. The parameters k_0, f_0, φ_0 of the supporting signal $\dot{v}(t)$ occupying the bandwidth $\Delta F_0 = \left[F_{0\min}...F_{0\max}\right]$ (the initial frequency f_0 is equal to the minimum signal frequency $F_{0\min}$) will be discussed now. The localization of the signals' bandwidths is shown in Fig. 6.4.

Fig. 6.4 shows the stretching of the received signal, namely its bandwidth decrease, which is based on the following considerations. The frequency band of an arbitrary LFM-signal with definite duration is determined from its sweep rate. So the sweep rate change provided by the supporting signal affects the frequency band in the receiver. Therefore, for the sweep rate of the supporting signal k_0 is of interest.

The signal received by the modified FM-CW radar occupies the bandwidth $\Delta F_2 = \left[F_{2\min}...F_{2\max}\right]$ (the initial frequency f_2 is equal to the minimum signal frequency $F_{2\min}$). The frequency band of the received signal in the time interval of interest (see the geometry of Fig. 6.4) can be written as

$$\Delta F_2 = k_2 \cdot T = k_2 \cdot \left(T - \tau_{\max}\right) + k_2 \cdot \tau_{\max}, \tag{6.7}$$

where $\tau_{\max}$ is the maximum roundtrip time delay determined from the maximum object range. Considering the fact that $f_{b2} = k_2 \cdot \tau$, Eq. (6.7) can be rewritten as

$$\Delta F_2 = k_2 \cdot \left(T - \tau_{\max}\right) + \Delta f_{b2}, \tag{6.8}$$

where Δf_{b2} is the width of the beat frequency band.

Stretching does not change the width of the beat frequency band Δf_{b2}. So, in analogy with Eq. 6.7 the frequency band of the stretched signal in the time interval of interest ($T - \tau_{\max}$) becomes

$$\Delta F_3 = k_3 \cdot \left(T - \tau_{\max}\right) + \Delta f_{b2} = (k_2 - k_0) \cdot \left(T - \tau_{\max}\right) + \Delta f_{b2}. \tag{6.9}$$

Parameter k_0 for conversion of ΔF_2 into ΔF_3 can be calculated from

$$k_0 = k_2 - \left(\frac{\Delta F_3 - \Delta f_{b2}}{T - \tau_{\max}}\right). \tag{6.10}$$

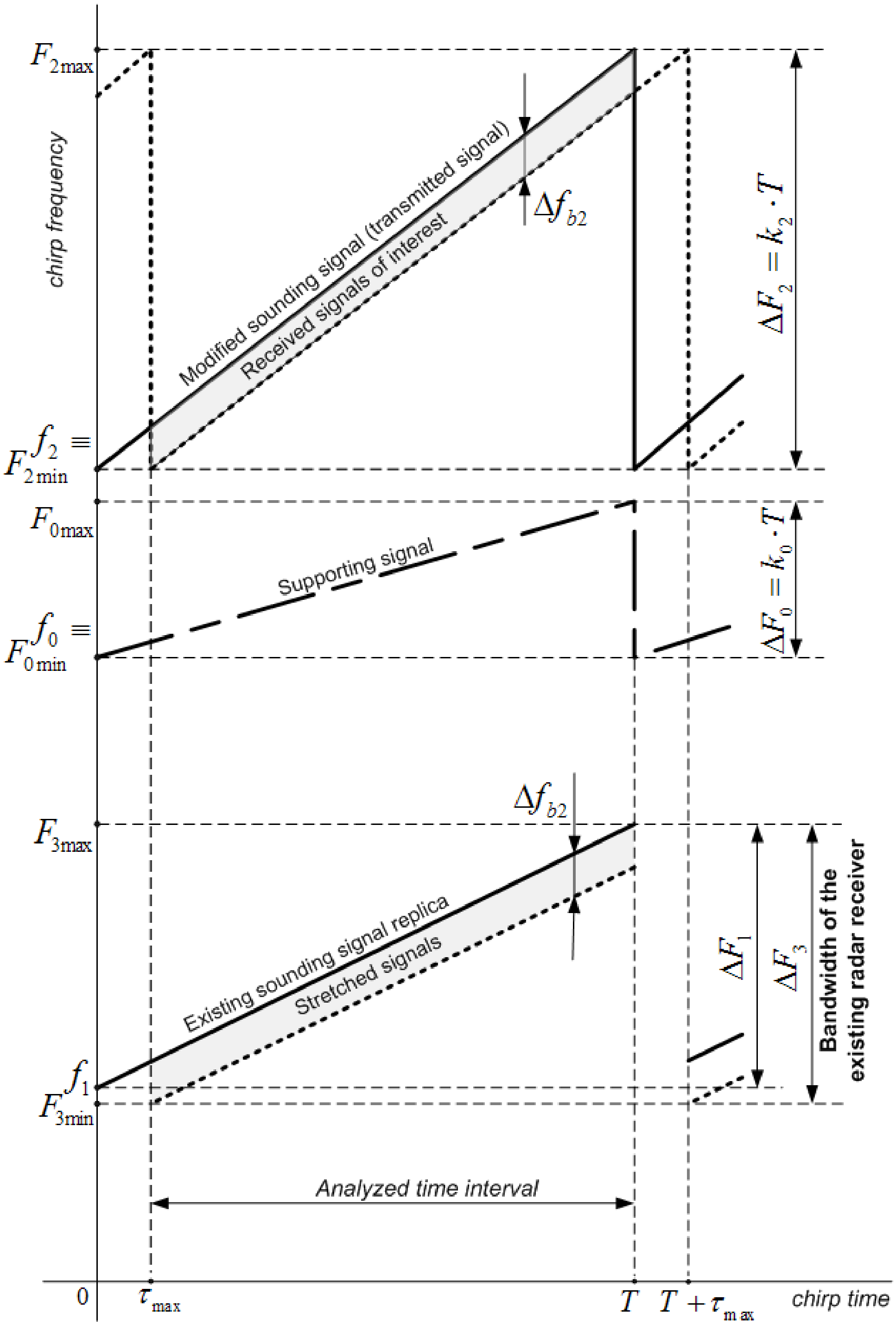

Fig. 6.4 – Time-frequency representation of the signals in the FM-CW radar receiver.

The sweep rate of the supporting signal (k_0) defines its slope, which next determines the stretched signal bandwidth (ΔF_2). The initial frequency (f_0) of the supporting signal affects the shift for the stretched signal along the frequency axis. On the basis of the geometry given in Fig. 6 the boundaries of the stretched signals, $F_{3\min}$ and $F_{3\max}$, at the corresponding time points ($\tau_{\max}$ and T) can be calculated as follows

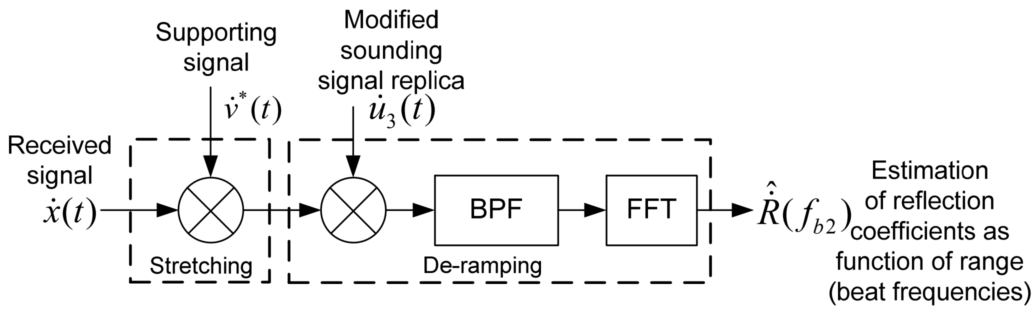

Fig. 6.5 – Simplified scheme for flexible de-ramping filter. Variant 2.

$$F_{3\min} = (k_2 \cdot \tau_{\max} + f_2) - (k_0 \cdot \tau_{\max} + f_0) - \Delta f_{b2},$$
$$F_{3\max} = (k_2 \cdot T + f_2) - (k_0 \cdot T + f_0). \tag{6.11}$$

From Eq. 6.11 the initial frequency of the supporting signal can then be derived

$$f_0 = \tau_{\max} \cdot \left(k_2 - k_0\right) + f_2 - \Delta f_{b2} - \mathrm{F}_{3\min}, \tag{6.12}$$

or

$$f_0 = T \cdot \left(k_2 - k_0\right) + f_2 - \mathrm{F}_{3\max}. \tag{6.13}$$

The third parameter of the supporting signal, the initial phase, φ_0, is not of great importance and must be taken into account during radar calibration.

We note here that in the modified FM-CW radar receiver the received signals can occupy a bandwidth more than ΔF_3 over the time interval $\left[0...T\right]$; however, the goal of flexible de-ramping processing is to obtain stretched signals within the bandwidth ΔF_3 over the time interval $\left[\tau_{\max}...T\right]$.

Knowing the solution for the first task (change of the received signal bandwidth) we can give the approach for solving the second task.

6.1.2 Shift in Beat Frequency Band (Second Variant)

A second variant of flexible de-ramping scheme is shown in Fig. 6.5. It is noted that the two multipliers in the scheme can also here be replaced by one multiplier. In this case the supporting signal and modified transmitted signal are replaced by one signal. However, for the explanation of the flexible de-ramping principle the scheme is described as presented in the figure below.

In analogy with Eq. 6.6 the resulting spectrum as function of beat frequency (f_{b2}) for the ramps of interest, can be calculated from:

$$\hat{\dot{R}}(f_{b2}) = FFT\left[BPF\left[\left(\dot{x}(t) \cdot \dot{v}^*(t)\right) \cdot \dot{u}_3(t)\right]\right] \tag{6.14}$$

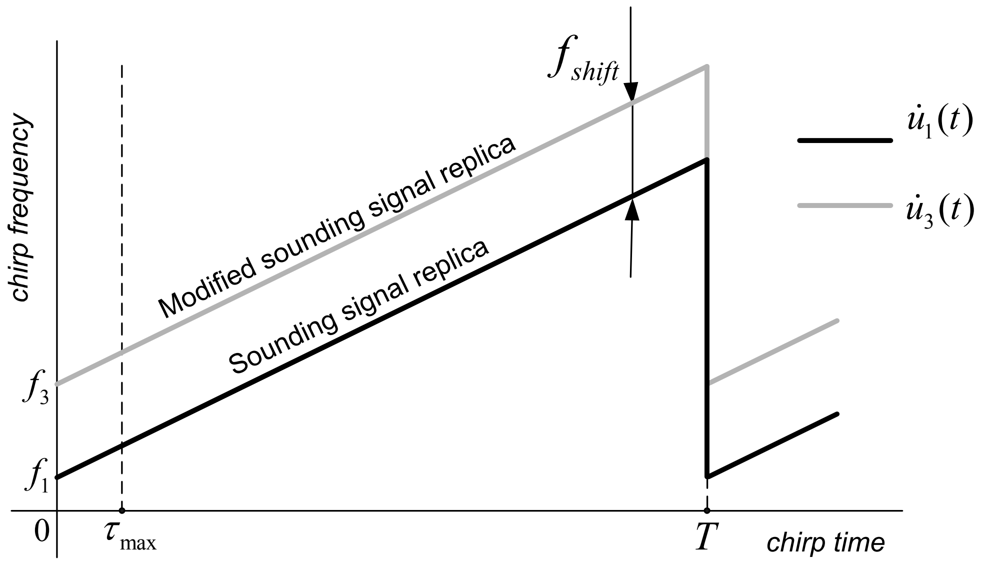

Fig. 6.6 – Frequency variations for signals $\dot{u}_1(t)$ and $\dot{u}_3(t)$.

where *BPF* means band-pass filter. The analyzed time interval is $\left[\tau_{\max}...T\right]$ as before. Eq. 6.14 corresponds to the estimated range profile.

The transmitted signal, $\dot{u}_1(t)$, is modified in the radar receiver for actual de-ramping as follows

$$\dot{u}_3(t) = \dot{u}_1(t) \cdot \exp(j \cdot 2\pi \cdot f_{shift} \cdot t), \tag{6.15}$$

where f_{shift} is a positive shift in beat signal bandwidth along the frequency axis.

Fig. 6.6 shows the frequency variation characteristics for the signals $\dot{u}_1(t)$ and $\dot{u}_3(t)$. The use of signal $\dot{u}_3(t)$ shifts the beat frequency band along the frequency axis depending on the f_{shift} value. The limiting values of the beat frequencies can be written as

$$\begin{aligned} f_{b\min} &= f_{shift}, \\ f_{b\max} &= f_{shift} + \Delta f_{b2}. \end{aligned} \tag{6.16}$$

These values determine the bandwidth of the BPF. We mention here also that f_{shift} is a positive value when the sounding signal is an up-going LFM-signal. When f_{shift} has a negative value, an overlapping of beat frequencies in the resulting spectrum can take place.

When the BPF-bandwidth can not be adjusted to a value equal to the beat frequency band (Δf_b) or when the estimation in a selected radar range (within the allowable maximum range) is needed the third task appears.

6.1.3 Selection of a Range Interval with High Range Resolution (Single-Channel)

The maximum range in FM-CW radar is defined from the maximum time delay, τ, which is determined from the BPF filter bandwidth, Δf_{BPF}, corresponding to the maximum beat frequency band, Δf_b. If the bandwidth of this BPF filter is less than the beat frequency band Δf_{b2} ($\Delta f_{BPF} < \Delta f_{b2}$), the de-ramping processing allows for observing a set of predefined co-determined range profiles. But by using a *variable* beat signal bandwidth shift, f_{shift}, we can observe the *desirable* (by the operator selected) range profiles.

The de-ramping processing scheme for the third task is presented in Fig. 6.7. The mathematical equations for the third task correspond to Eqs. 6.14 to 6.15 obtained for solving the second task except that a variable beat signal bandwidth shift, $f_{shift} \in \left[f_{shift\min} \cdots f_{shift\max} \right]$, will be used.

The wanted performance of the third task (Fig. 6.7.a-b) can be derived from the selected edges of the BPF amplitude-frequency response ($f_{BPF\min}$ and $f_{BPF\max}$) and lead to the beat frequency shift variations:

$$\begin{aligned} f_{shift\min} &= f_{BPF\max} - \Delta f_{b2}, \\ f_{shift\max} &= f_{BPF\min}. \end{aligned} \tag{6.17}$$

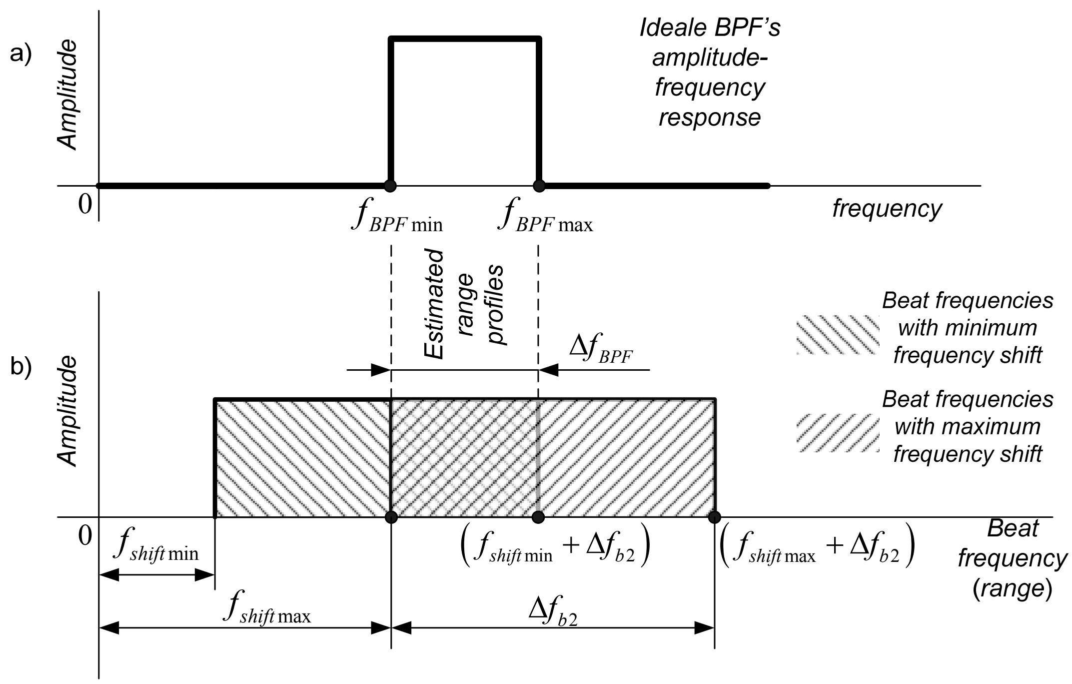

Fig. 6.7 – a) Ideal amplitude-frequency response of the band-pass filter (BPF); b) beat frequencies.

Table 6.1 – Flexible de-ramping mathematics.

Parameter	Expression	Comment
Sweep rate of the supporting signal.	$k_0 = k_2 - \left(\frac{\Delta F_3 - \Delta f_{b2}}{T - \tau_{\max}} \right)$	ΔF_3 is the desirable bandwidth of the stretched received signal (k_2 , Δf_b , T and $\tau_{\max}$ are known parameters).
Initial frequency of the supporting signal.	$f_0 = \tau_{\max} \cdot (k_2 - k_0) +$ $+ f_2 - \Delta f_{b2} - F_{3\min}$ or $f_0 = T \cdot (k_2 - k_0) + f_2 - \mathrm{F}_{3\max}$	$F_{3\min}$ is the lowest frequency of the received stretched signal in the analyzed time interval; $F_{3\max}$ is the highest frequency of the received stretched signal in the analyzed time interval.
The initial phase of the supporting signal.	$\varphi_0 = [0 ... 2 \cdot \pi]$	φ_0 is not of specific interest, but should be taken into account during radar calibration.
Additional shift of the beat signals along the frequency axis.	$f_{shift\min} = f_{BPF\max} - \Delta f_b$ $f_{shift\max} = f_{BPF_{\min}}$	where $f_{BPF\min}$ is the lowest frequency of the BPF amplitude-frequency response; $f_{BPF\max}$ is the highest frequency of the BPF amplitude-frequency response. (When a beat signal shift is desired the LPF in the de-ramping scheme should be replaced by an BPF).

It should be noted again that the third task is a generalization of the second task. In case of equality of the BPF-bandwidth and beat frequency band, $\Delta f_{BPF} = \Delta f_{b2}$, the frequency shift interval is one value and is equal to 0.

The main expressions for flexible de-ramping processing are given in Table 6.1.

6.2 Application of Flexible De-ramping Processing in FM-CW Polarimetric Radar with Simultaneous Measurement of Scattering Matrix Elements

Flexible de-ramping processing can be applied in FM-CW polarimetric radar with simultaneous measurement of scattering matrix elements. Flexibility of the de-ramping technique for polarimetric radar is provided with the use of two supporting signals ($\dot{v}_1(t)$ and $\dot{v}_2(t)$) which are also LFM-signals. Both signals are supposed to be processed with the received signals of horizontal and vertical polarizations correspondently. The supporting signals with corresponding parameters k_0, f_{01}, f_{02}, φ_{01} and φ_{02} are the following:

$$\begin{aligned} \dot{v}_1(t) &= \exp\left[j \cdot 2\pi \cdot \left(\frac{k_0}{2} \cdot t^2 + f_{01} \cdot t \right) + \varphi_{01} \right], \\ \dot{v}_2(t) &= \exp\left[j \cdot 2\pi \cdot \left(-\frac{k_0}{2} \cdot t^2 + f_{02} \cdot t \right) + \varphi_{02} \right], \end{aligned} \qquad (6.18)$$

where the first subscript “0” means the supporting signal, the second subscript (“1”, “2”) means its sequential number. k_0 is the sweep rate, f_{01} and f_{02}, φ_{01} and φ_{02} are the initial frequencies and initial phases of the supporting signals occupying the bandwidth $\Delta F_0 = \left[F_{0\min} ... F_{0\max} \right]$.

The vector sounding signal components (two LFM-signals) can be written as

$$\begin{aligned} \dot{u}_{11}(t) &= \exp\left[j \cdot 2\pi \cdot \left(\frac{k_1}{2} \cdot t^2 + f_{11} \cdot t \right) + \varphi_{11} \right], \\ \dot{u}_{12}(t) &= \exp\left[j \cdot 2\pi \cdot \left(-\frac{k_1}{2} \cdot t^2 + f_{12} \cdot t \right) + \varphi_{12} \right], \end{aligned} \qquad (6.19)$$

where the first subscript “1” means the sounding signal, the second subscript means polarization of the vector sounding signal component (“1” − horizontal, “2” − vertical). k_1 is the sweep rate, f_{11} and f_{12}, φ_{11} and φ_{12} are the initial frequencies and initial phases of the transmitted signals correspondently. The vector sounding signals are described as two LFM-signals with opposite slopes

$$\begin{aligned} f_{11} &= F_{3\max} - \Delta F_1, \\ f_{12} &= F_{3\min} + \Delta F_1, \end{aligned} \qquad (6.20)$$

where ΔF_1 is the frequency band of both signals. We remember that the existing radar hardware bandwidth is marked as $\Delta F_3 = \left[F_{3\min} ... F_{3\max} \right]$. So the first sounding signal component occupies $\Delta F_1 = \left[f_{11} ... F_{3\max} \right]$, the second sounding signal component occupies $\Delta F_1 = \left[F_{3\min} ... f_{12} \right]$, $\Delta F_1 \le \Delta F_3$.

In FM-CW polarimetric radar the same tasks (change of the received signal bandwidth, shift of the beat frequency band or selection of the range interval) as for the single-channel radar can take place. The approaches for solving these tasks in dual-channel (polarimetric) radar are considered in this section.

6.2.1 Reduction of the Received Signal Bandwidth

The first task should be applied when for example the sampling of the received signals with a bandwidth ΔF_2 is impossible, but it can be realized with the reduced bandwidth ΔF_3. In this case the use of two multipliers in every branch of the radar receiver (Fig. 6.8) is the solution. The beat frequency bandwidth Δf_{b2} stays the same for the received signals and for the signals with reduced bandwidth.

The resulting spectrum as function of beat frequency (f_{b2}) for the ramps of interest corresponds to the estimated range profile. We find

$$\begin{aligned}
\hat{\dot{S}}_{11}(f_{b2}) &= FFT\left[LPF\left[\left(\dot{x}_1(t)\cdot\dot{v}_1^*(t)\right)\cdot\dot{u}_{11}(t)\right]\right],\\
\hat{\dot{S}}_{21}(f_{b2}) &= FFT\left[LPF\left[\left(\dot{x}_1(t)\cdot\dot{v}_2^*(t)\right)\cdot\dot{u}_{12}(t)\right]\right],\\
\hat{\dot{S}}_{22}(f_{b2}) &= FFT\left[LPF\left[\left(\dot{x}_2(t)\cdot\dot{v}_2^*(t)\right)\cdot\dot{u}_{12}(t)\right]\right],\\
\hat{\dot{S}}_{12}(f_{b2}) &= FFT\left[LPF\left[\left(\dot{x}_2(t)\cdot\dot{v}_1^*(t)\right)\cdot\dot{u}_{11}(t)\right]\right],
\end{aligned} \tag{6.21}$$

where *LPF* means low-pass filter over the $\left[0...\Delta f_{b2}\right]$ pass-band. The FFT is utilized for the multiplied signals after filtering over the $\left[\tau_{\max}...T\right]$ time interval for every duty cycle of the polarimetric FM-CW radar.

Fig. 6.9 shows the stretching of the received signal $\dot{x}_1(t)$ for horizontal polarization, which is processed in Channel 1, in case of a bandwidth decrease. Stretching of the received signal $\dot{x}_2(t)$ for vertical polarization, which is processed in Channel 2, is done in the same way and will not be considered separately.

First, the received signal $\dot{x}_1(t)$ containing LFM-signals with up-going and down-going slopes is fed into two branches of the radar channel (Fig. 6.8). Branch 1 is meant for information extraction from received LFM-signals with up-going slope, Branch 2 does the same for received LFM-signals with down-going slope (Fig. 6.9.a).

The first supporting signal in Channel 1 is used for slow-down the up-going LFM-signals in the first branch, the second supporting signal does the same according to down-going LFM-signals (Fig. 6.9.b)

Stretching of the signals results in decreased bandwidths of the useful signals (Fig. 6.9.c), which belong to the bandwidth of the existing radar receiver. So a considerable receiver upgrade may not be needed.

When the sounding signals are LFM-signals with opposite slopes (Eq. 6.18) the sweep rates of the supporting signals can be calculated as follows. The frequency band of the received signal in the time interval of interest $\left[\tau_{\max}...T\right]$ can be written as

$$\Delta F_2 = k_2 \cdot T = k_2 \cdot \left(T - \tau_{\max}\right) + \Delta f_{b2}. \tag{6.22}$$

Stretching does not change the width of the beat frequency band Δf_{b2}. So, in analogy with Eq. 6.22, the frequency band of the stretched signal in the time interval of interest ($T - \tau_{\max}$) becomes

$$\Delta F_3 = k_1 \cdot \left(T - \tau_{\max}\right) + \Delta f_{b2} = (k_2 - k_0) \cdot \left(T - \tau_{\max}\right) + \Delta f_{b2}. \tag{6.23}$$

From both equations the parameter k_0 for conversion from ΔF_2 into ΔF_3 can be calculated

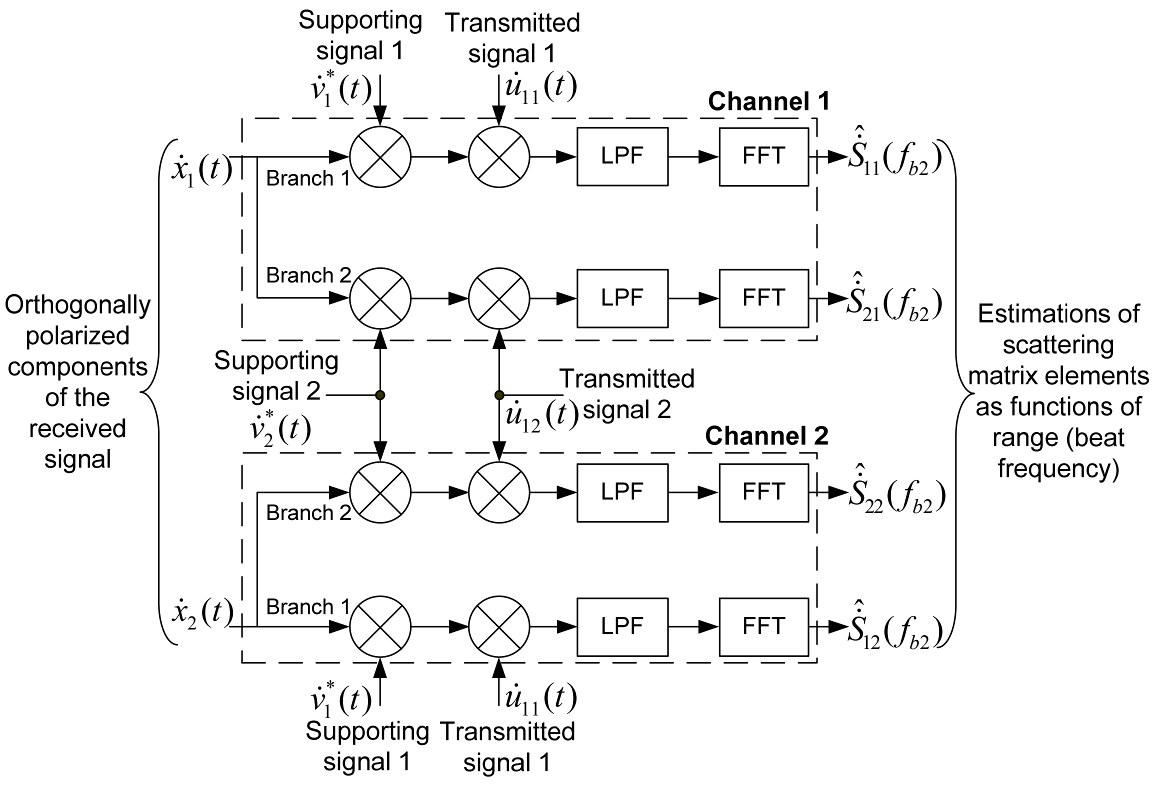

Fig. 6.8 – Simplified scheme of the flexible de-ramping filter for the FM-CW polarimetric radar receiver. Variant 1.

$$k_0 = k_2 - \left(\frac{\Delta F_3 - \Delta f_{b2}}{T - \tau_{\max}} \right). \tag{6.24}$$

On the basis of the geometry of Fig. 6.9 the boundaries of the stretched signals, $F_{3\min}$ and $F_{3\max}$, can be found. We derive

$$F_{3\min} = (k_2 \cdot \tau_{\max} + f_{21}) - (k_0 \cdot \tau_{\max} + f_{01}) - \Delta f_{b2}, \tag{6.25}$$

and

$$F_{3\max} = (-k_2 \cdot \tau_{\max} + f_{22}) - (-k_0 \cdot \tau_{\max} + f_{02}) + \Delta f_{b2}. \tag{6.26}$$

When the lower boundary $F_{3\min}$ for the existing radar receiver is known the initial frequencies of the supporting signals is calculated with use of Eq. 6.25 and become

$$f_{01} = f_{21} - \left[F_{3\min} + \Delta f_{b2} - \left(k_2 - k_0 \right) \cdot \tau_{\max} \right]. \tag{6.27}$$

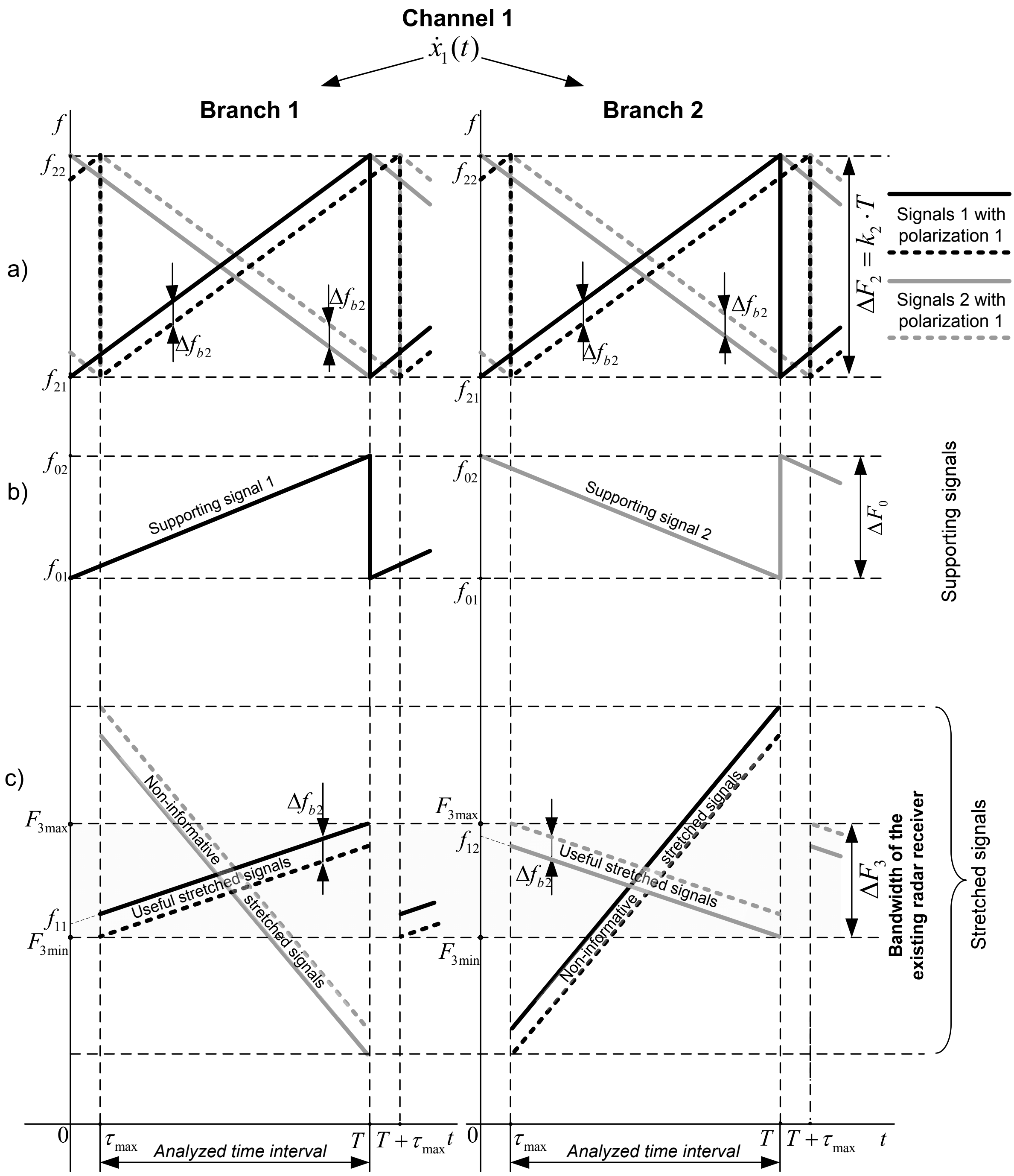

Fig. 6.9 – a) Frequency plot of continuous LFM-signals with opposite slopes; b) supporting signals; c) stretched signals in the time interval of interest.

With the upper boundary, $F_{3\max}$, known, the initial frequency of the second supporting signal is calculated with use of Eq. 6.26 and becomes

$$f_{02} = f_{22} - \left[F_{3\max} - \Delta f_{b2} + (k_2 - k_0) \cdot \tau_{\max}\right]. \tag{6.28}$$

Next we go to the solution of the second task for FM-CW polarimetric radar.

6.2.2 Shift in the Dual-Channel Beat Frequency Band

The second variant of flexible de-ramping filter for FM-CW polarimetric radar is shown in Fig. 6.10. As before, BPF means band-pass filter.

The second task for polarimetric radar is like the already-given approach for a single-channel radar (see Section 6.1.2). The task can be fulfilled by introducing a sinusoidal signal to the sounding signal.

The sounding vector signal components, $\dot{u}_{11}(t)$ and $\dot{u}_{12}(t)$, are modified in the radar receiver for de-ramping by

$$\begin{aligned} \dot{u}_{31}(t) &= \dot{u}_{11}(t) \cdot \exp(j \cdot 2\pi \cdot f_{shift} \cdot t), \\ \dot{u}_{32}(t) &= \dot{u}_{12}(t) \cdot \exp(j \cdot 2\pi \cdot \left(-f_{shift}\right) \cdot t), \end{aligned} \tag{6.29}$$

where $\dot{u}_{31}(t)$ and $\dot{u}_{32}(t)$ are the modified transmitted signals, the first subscript "*3*" means the modified sounding signals for the second task. f_{shift} is the beat signal bandwidth shift for signals related to the up-going and down-going LFM-signals. The beat frequency shift is a positive value

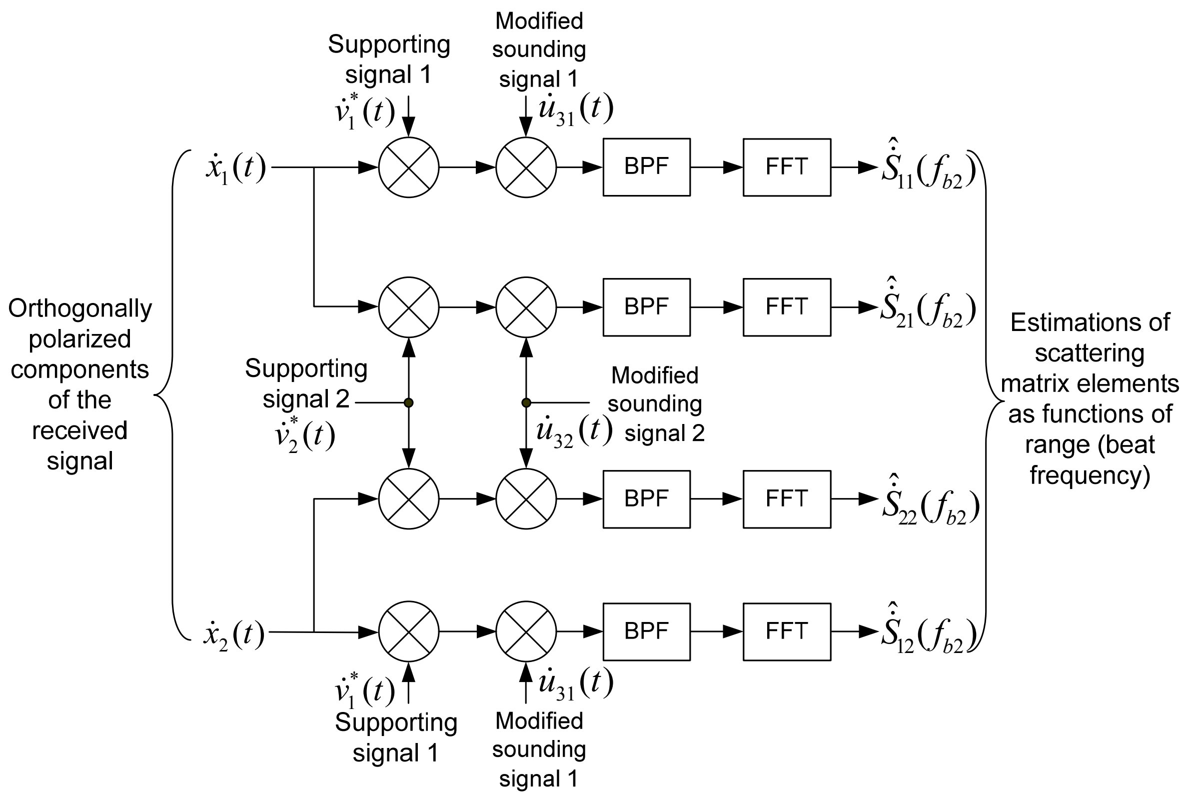

Fig. 6.10 – Simplified scheme of the flexible de-ramping filter for FM-CW polarimetric radar. Variant 2.

for processing of up-going LFM-signals and negative for down-going LFM-signals.

The resulting spectrum as function of beat frequency (f_{b2}) for the ramps of interest corresponds to the estimated range profile and can be found from

$$\begin{aligned}
\hat{\dot{S}}_{11}(f_{b2}) &= FFT\left[BPF\left[\left(\dot{x}_1(t)\cdot\dot{v}_1^*(t)\cdot\dot{u}_{31}(t)\right)\right]\right],\\
\hat{\dot{S}}_{21}(f_{b2}) &= FFT\left[BPF\left[\left(\dot{x}_1(t)\cdot\dot{v}_2^*(t)\right)\cdot\dot{u}_{32}(t)\right]\right],\\
\hat{\dot{S}}_{22}(f_{b2}) &= FFT\left[BPF\left[\left(\dot{x}_2(t)\cdot\dot{v}_2^*(t)\right)\cdot\dot{u}_{32}(t)\right]\right],\\
\hat{\dot{S}}_{12}(f_{b2}) &= FFT\left[BPF\left[\left(\dot{x}_2(t)\cdot\dot{v}_1^*(t)\right)\cdot\dot{u}_{31}(t)\right]\right],
\end{aligned} \tag{6.30}$$

where BPF means band-pass filter. The FFT is utilized for the multiplied signals after filtering over the $\left[\tau_{\max}...T\right]$ -interval for every duty cycle of FM-CW radar, as discussed before.

The limiting values of the beat frequencies can be written as

$$\begin{aligned}
f_{b\min} &= f_{shift},\\
f_{b\max} &= f_{shift} + \Delta f_{b2},
\end{aligned} \tag{6.31}$$

where Δf_{b2} is the beat frequency band. These limiting values in Eq. 6.31 determine the BPF pass-band.

When a vector sounding signal including two LFM signals with opposite slopes is used we should take into account the influence of the cross (LFM) signals, which appear in the de-ramped signals. So the time-frequency representation of signals is of interest when a shift in the beat frequency band is utilized.

Fig. 6.11 shows the flexible de-ramping processing of the received signal ($\dot{x}_1(t)$) with horizontal polarization, which is processed in Channel 1, in case of a shift in the beat frequency band. The modified transmitted signals ($\dot{u}_{31}(t)$ and $\dot{u}_{32}(t)$) have negative ($-f_{shift}$) and positive (f_{shift}) frequency shifts (Fig. 6.11.a). The useful de-ramped signals (namely tone signals) are processed in the intermediate frequency band $\left[f_{shift}...\left(f_{shift}+\Delta f_{b2}\right)\right]$ (Fig. 6.11.b). The cross (LFM) beat signals occupy a large part of the time interval along the analyzed time axis corresponding to the tone signals' bandwidth.

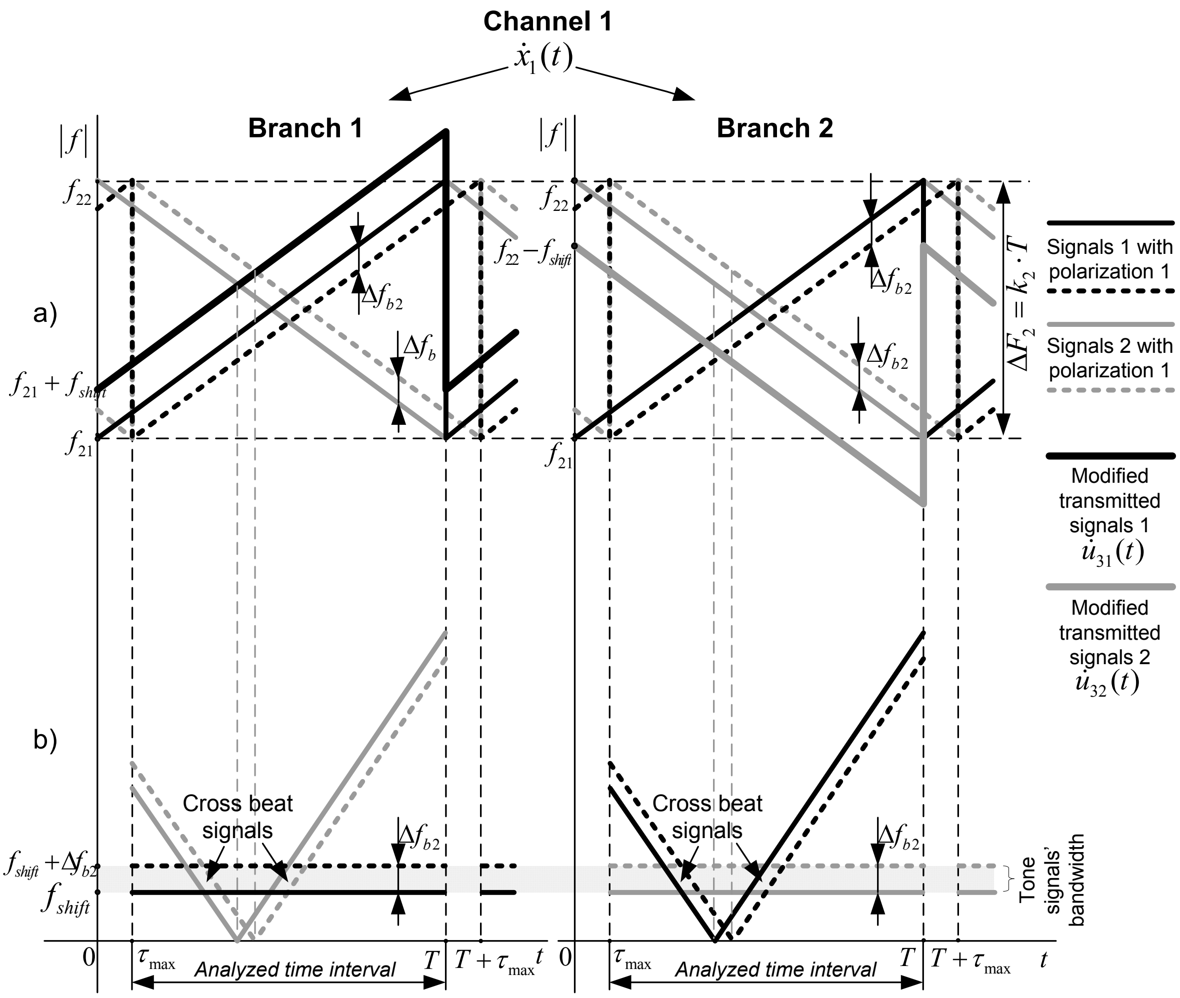

Fig. 6.11 – a) Frequency plot of continuous LFM-signals with opposite slopes and the modified transmitted signals; b) time-frequency representation of the de-ramped signals.

The geometry of Fig. 6.11.b, namely the time-frequency representation of the cross beat signals, hints the way how to decrease cross beat signals existing in the tone signals bandwidth to a 50% impact. For realizing such decrease the frequency shift (f_{shift}) of the supporting signals should satisfy the following condition:

$$f_{shift} \geq \Delta F_2/2 - 2 \cdot k_2 \cdot \tau_{\max} + f_{b2} \quad \text{or} \quad f_{shift} \geq \Delta F_2/2 - \Delta f_{b2},. \qquad (6.32)$$

Eq. 6.32 is defined from the geometry of the cross beat signals having a sweep rate equal to $2 \cdot k_2$.

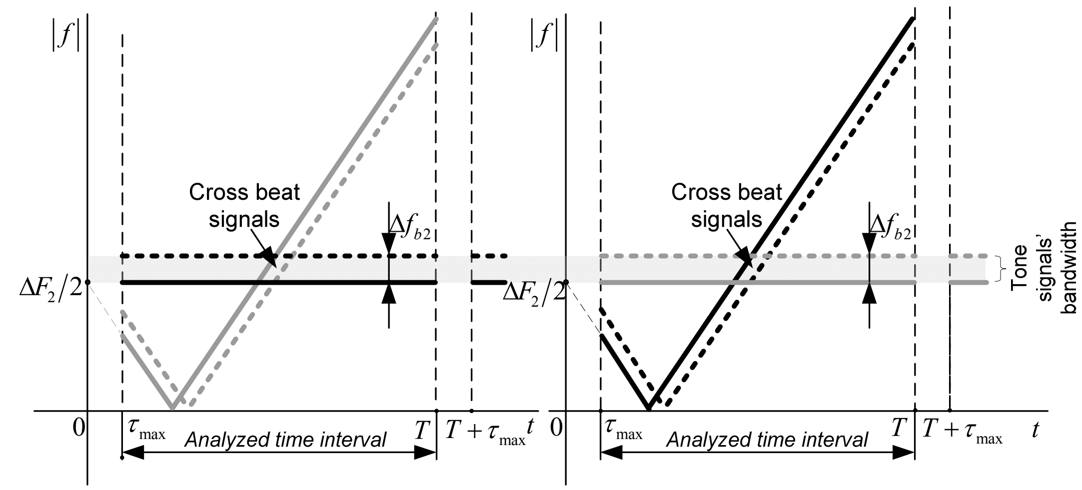

Fig. 6.12 – Time-frequency representation of the de-ramped signals in case of $f_{shift} = \Delta F_2/2$.

Fig. 6.12 shows the time-frequency representation of the de-ramped signals in case $f_{shift} = \Delta F_2/2$.

Once again we note that if the execution of the mentioned first task is not needed two series multipliers in the chains of the flexible de-ramping filter can be replaced by one multiplier. Therefore every branch of the de-ramping filter for the FM-CW polarimetric radar (Variant 3) has then only one multiplier (Fig. 6.13).

For the scheme shown in Fig. 6.13 the modified sounding signals marked with the first subscript "4" are calculated from

$$\begin{aligned} \dot{u}_{41}(t) &= \dot{u}_{11}(t) \cdot \dot{v}_1^*(t) \cdot \exp(j \cdot 2\pi \cdot f_{shift} \cdot t), \\ \dot{u}_{42}(t) &= \dot{u}_{12}(t) \cdot \dot{v}_2^*(t) \cdot \exp(j \cdot 2\pi \cdot \left(-f_{shift}\right) \cdot t), \end{aligned} \tag{6.33}$$

where $\dot{u}_{11}(t)$ and $\dot{u}_{12}(t)$ are the components of the vector sounding signals, f_{shift} is the (beat signal) bandwidth shift.

The resulting spectrum as function of beat frequency (f_{b2}) for the ramps of interest corresponds to the estimated range profile and are derived from

$$\begin{aligned} \hat{\dot{S}}_{11}(f_{b2}) &= FFT\left[BPF\left[\dot{x}_1(t) \cdot \dot{u}_{41}(t)\right]\right], \\ \hat{\dot{S}}_{21}(f_{b2}) &= FFT\left[BPF\left[\dot{x}_1(t) \cdot \dot{u}_{42}(t)\right]\right], \\ \hat{\dot{S}}_{22}(f_{b2}) &= FFT\left[BPF\left[\dot{x}_2(t) \cdot \dot{u}_{42}(t)\right]\right], \\ \hat{\dot{S}}_{12}(f_{b2}) &= FFT\left[BPF\left[\dot{x}_2(t) \cdot \dot{u}_{41}(t)\right]\right]. \end{aligned} \tag{6.34}$$

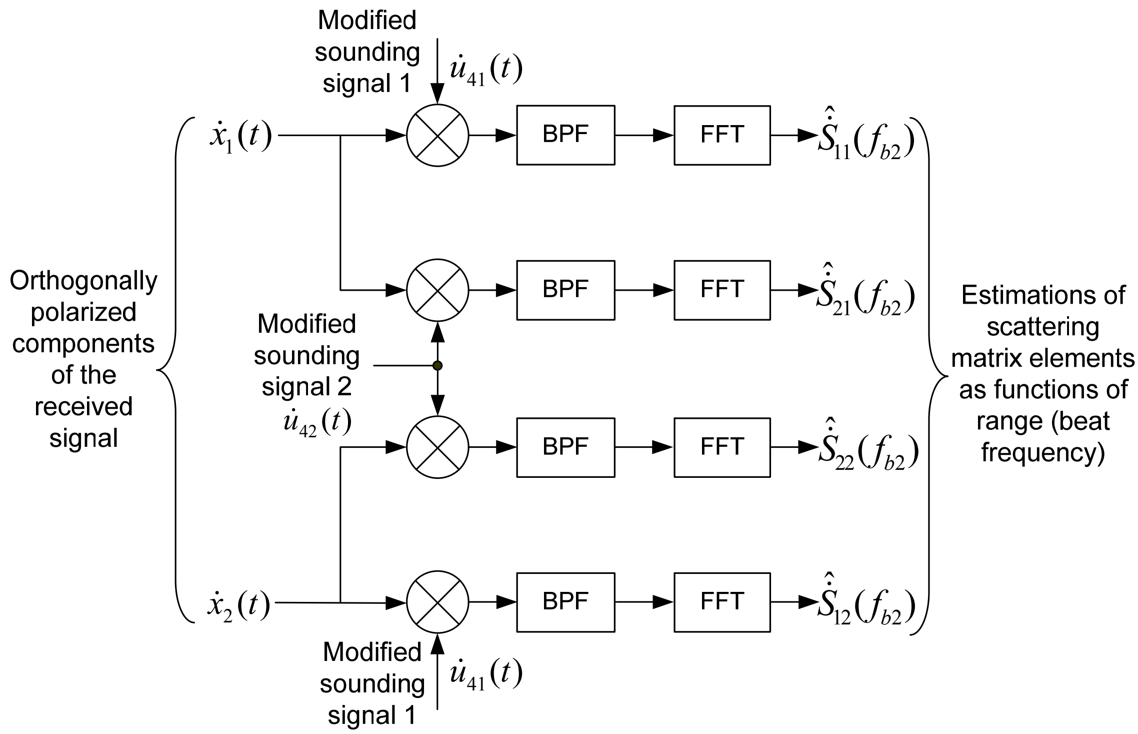

Fig. 6.13 – Simplified scheme of the flexible de-ramping filter for FM-CW polarimetric radar. Variant 3.

When the BPF-bandwidth is less than the corresponding frequency bands or when the estimation of a part of radar ranges (within the maximum radar range) is needed the third task is needed.

6.2.3 Selection of a Range Interval with High Range Resolution (in Dual-Channel Polarimetric Radar)

Executing the third task solution is done according the geometry of Fig. 6.7.a-b. The dual-channel beat frequency shift is supposed to be variable.

Assuming that in the BPFs signals can pass in the frequency band $\left(f_{BPF1\min}...f_{BPF1\max}\right)$ the required boundaries for the frequency shifts can be calculated as:

$$\begin{aligned} f_{shift\min} &= f_{BPF\max} - \Delta f_{b2}, \\ f_{shift\max} &= f_{BPF\min}. \end{aligned} \tag{6.35}$$

So the equations for the third task solution for FM-CW polarimetric radar are the same as for the FM-CW single-channel radar.

We note an additional advantage of selecting a range interval with high range resolution in case of FM-CW polarimetric radar with simultaneous measurement of SM elements. When the

Table 6.2 – Flexible de-ramping mathematics for polarimetric radar.

Parameter	Expression	Comment
Sweep rate of the supporting signals.	$k_0 = k_2 - \left(\dfrac{\Delta F_3 - \Delta f_{b2}}{T - \tau_{\max}}\right).$	ΔF_3 is the desirable bandwidth of the stretched received signal (k_2, Δf_{b2}, T and $\tau_{\max}$ are known radar parameters).
Initial frequencies of supporting signals.	$f_{01} = f_{21} - \left[F_{3\min} + \Delta f_{b2} - (k_2 - k_0)\cdot\tau_{\max}\right].$ and $f_{02} = f_{22} - \left[F_{3\max} - \Delta f_{b2} + (k_2 - k_0)\cdot\tau_{\max}\right].$	$F_{3\min}$ is the lowest frequency of the received stretched signal in the analyzed time interval; $F_{3\max}$ is the highest frequency of the received stretched signal in the analyzed time interval.
Initial phases of the supporting signals.	$\varphi_{01} = [0...2\cdot\pi]$, $\varphi_{02} = [0...2\cdot\pi]$.	φ_{01} and φ_{02} are not of interest for flexible de-ramping, but should be taken into account during radar calibration.
Additional shift of beat signals along the frequency axis.	$f_{shift\min} = f_{BPF\max} - \Delta f_{b2}$, $f_{shift\max} = f_{BPF\min}$.	$f_{BPF\min}$ and $f_{BPF\max}$ are the lowest and highest frequencies in the BPF amplitude-frequency response correspondently; (When a beat signal shift is desired the LPF in the de-ramping scheme should be replaced by the BPF).

BPF-bandwidth is less then the beat frequency bandwidth ($\Delta f_{BPF} < \Delta f_b$) the lengths of cross-beat frequencies after filtering in the analyzed time interval will also be less. So the energy of cross-beat signals will be lowered and therefore their negative influence on estimations of SM-elements will be diminished.

The main expressions of the flexible de-ramping processing for polarimetric radar are given in Table 6.2.

6.2.4 PARSAX Implementation

This paragraph presents the numerical simulation of de-ramping processing in the FM-CW polarimetric radar PARSAX. Numerical simulation of de-ramping processing for a single-channel radar will not be considered because the results for polarimetric radar elucidates optimally the efficiency of the proposed technique.

As is known the PARSAX radar has a central frequency (f_c) 3.315 GHz, maximum frequency deviation (ΔF) 50 MHz, sweep time (T) 1 ms, maximum time delay ($\tau_{\max}$) 0.1 ms, beat frequency bandwidth (Δf_b) 5 MHz (see Table A.1). The sounding signal can be considered as quasi-monochromatic and having one spectral component because it is located in a narrow frequency band.

When a larger range resolution is desirable, the sounding signal bandwidth (ΔF_2) is increased. Assume an ΔF_2 equal to 300 MHz and a minimum frequency of the sounding signal (f_{21}) equal to 9.70 GHz, its maximal frequency (f_{22}) becomes 10.00 GHz. In so doing the PARSAX radar receiver is operating over a vector sounding signal bandwidth (ΔF_3) equal to 50 MHz and its initial frequency is equal to 3.29 GHz. It means $F_{3\min} = 3.29$ GHz and $F_{3\max} = 3.34$ GHz for stretched signals in the analyzed time interval $\left[\tau_{\max}...T\right]$.

Sweep rates for a vector sounding signal (k_2) is calculated (see Paragraph 2.2.1) from

$$k_2 = \frac{\Delta F_2}{T} = \frac{300 \cdot 10^6}{1 \cdot 10^{-3}} = 300 \cdot 10^9 .$$

The new beat frequency band corresponding to ΔF_2 is calculated from Eq. 3.13

$$\Delta f_{b2} = k_2 \cdot \tau_{\max} = 300 \cdot 10^9 \cdot 0.1 \cdot 10^{-3} = 30 \cdot 10^6 \text{ Hz}.$$

The supporting signals ($\dot{v}_1(t)$ and $\dot{v}_2(t)$) are used for stretching of the received signals. The parameters (k_0 , f_{01} and f_{02}) of the supporting signals are of interest. By knowing the frequency boundaries ($F_{2\min}$, $F_{2\max}$) for stretched signals, the sweep rate (k_0) can be calculated from Eq. 6.24:

$$k_0 = k_2 - \left(\frac{\Delta F_3 - \Delta f_{b2}}{T - \tau_{\max}} \right) = 300 \cdot 10^9 - \left(\frac{50 \cdot 10^6 - 30 \cdot 10^6}{1 \cdot 10^{-3} - 0.1 \cdot 10^{-3}} \right) = 277.78 \cdot 10^9 .$$

Likewise the initial frequencies of supporting signals are calculated according to Eq. 6.27-28:

$$\begin{aligned} f_{01} &= f_{21} - \left[F_{3\min} + \Delta f_{b2} - \left(k_2 - k_0\right) \cdot \tau_{\max} \right], \\ f_{02} &= f_{22} - \left[F_{3\max} - \Delta f_{b2} + \left(k_2 - k_0\right) \cdot \tau_{\max} \right]. \end{aligned}$$

$$f_{01} = 9.70 \cdot 10^9 - \left[3.29 \cdot 10^9 + 30 \cdot 10^6 - \left(300 \cdot 10^9 - 277.78 \cdot 10^9\right) \cdot 0.1 \cdot 10^{-3} \right] \approx 6.382 \text{ GHz},$$
$$f_{02} = 10.00 \cdot 10^9 - \left[3.34 \cdot 10^9 - 30 \cdot 10^6 + \left(300 \cdot 10^9 - 277.78 \cdot 10^9\right) \cdot 0.1 \cdot 10^{-3} \right] \approx 6.688 \text{ GHz}.$$

Phases of supporting signals are not of interest here because in any case they are taken into account in the radar calibration process.

The transmitted signals ($\dot{u}_{11}(t)$ and $\dot{u}_{12}(t)$) are used for de-ramping processing (Fig. 6.8, 6.14). Their sweep rate k_1 and initial frequencies f_{11} and f_{12} are calculated as follows. When the parameters of the supporting signals are known the sweep rate (k_1) and initial frequencies (f_{11} and f_{12}) of the transmitted signals can be calculated as follows:

$$k_1 = k_2 - k_0 = 300 \cdot 10^9 - 277.78 \cdot 10^9 = 22.22 \cdot 10^9.$$

The initial frequencies are calculated according to Eq. 6.20:

$$f_{11} = F_{3\max} - k_1 \cdot T = 3.34 \cdot 10^9 - 22.22 \cdot 10^9 \cdot 1 \cdot 10^{-3} \approx 3.318 \cdot 10^9 \text{ Hz};$$

$$f_{12} = F_{3\min} + k_1 \cdot T = 3.29 \cdot 10^9 + 22.22 \cdot 10^9 \cdot 1 \cdot 10^{-3} \approx 3.312 \cdot 10^9 \text{ Hz}$$

So the up-going and down-going transmitted signals ($\dot{u}_{11}(t)$ and $\dot{u}_{12}(t)$) occupy the bandwidths $\left[3.318 \cdot 10^9 \text{ to } 3.340 \cdot 10^9\right]$ Hz and $\left[3.290 \cdot 10^9 \text{ to } 3.312 \cdot 10^9\right]$ Hz consequently.

An example of this Paragraph is shown in a simplified scheme of a flexible de-ramping filter (Fig. 6.14) allowing a reduction of the received signal bandwidth. We note that the filter scheme

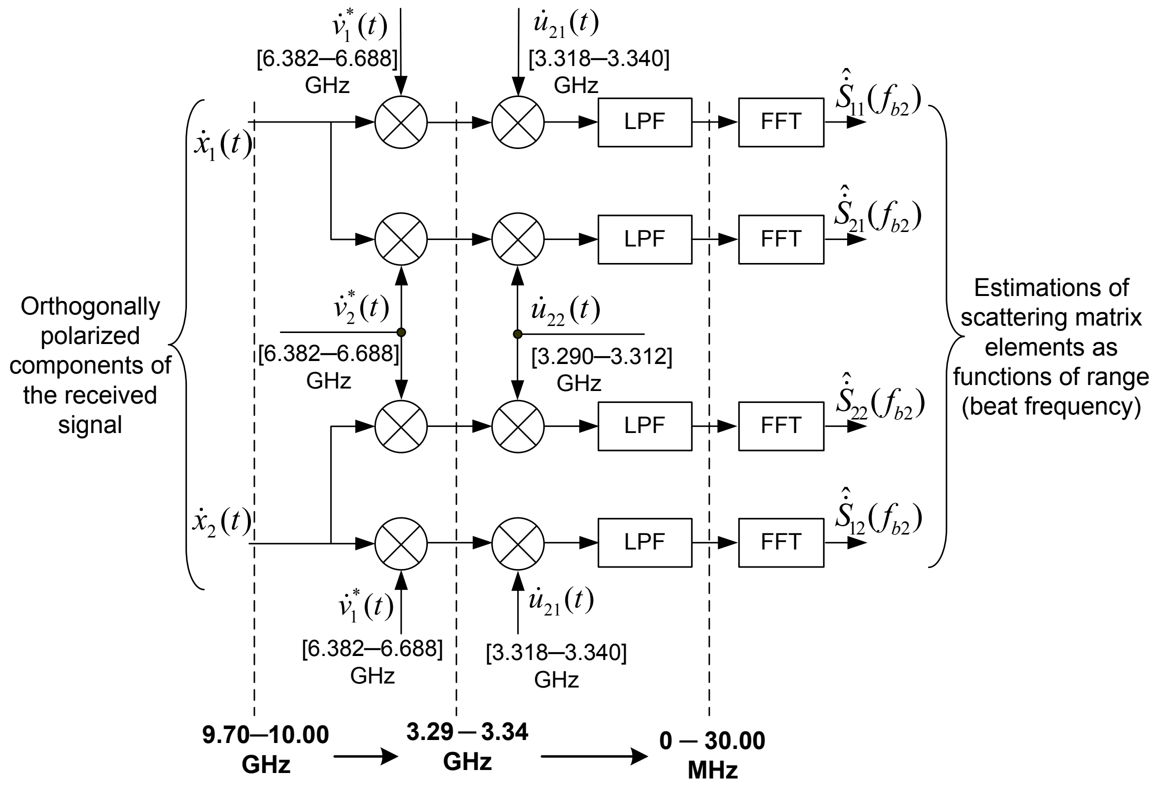

Fig. 6.14 – Simplified scheme of a flexible de-ramping filter for the PARSAX radar receiver.

for the PARSAX radar receiver is simplified for the better visibility of the numerical simulation and do not contain here such blocks like low noise amplifiers, band-pass filters and analog-to-digital convertors.

6.3 Conclusion

This chapter has proposed a novel flexible de-ramping processing applicable to received signals for both single channel and dual-channel (polarimetric) radar. The proposed technique does not limit FM-CW radar receiver hardware with the sounding signal parameters. Flexible de-ramping uses the special supporting signal which helps to change the received signals' bandwidth, shift beat frequency band and select the range interval (beat frequencies) from the total range. Particularly, the example for flexible de-ramping processing developed within the work of this thesis for PARSAX implementation has been presented.

References

1. W.J. Caputi, "Stretch: A Time-Transformation Technique", IEEE Transactions on Aerospace and Electronic Systems, Volume AES-7, Issue 2, March 1971, pp. 269-278.
2. G. Babur, O. Krasnov, L.P. Ligthart, "High Range Resolution FM-CW Radar Utilizing Flexible De-Ramping Processing", IEEE Transactions on Aerospace and Electronic Systems, submitted.

7. Cross-Correlation Decrease in FM-CW Polarimetric Radar with Simultaneous Measurement of Scattering Matrix Elements

This chapter presents a novel technique for decrease of cross-correlation components existing in the beat-signals when a vector sounding signal is used. The knowledge about the location of the cross-correlation components is used and the amplitudes of the beat signals are suppressed along the part of the analyzed time interval. The here-proposed technique can be utilized in real time and thanks to its high efficiency it allows to achieve a qualitatively new level of polarimetric radar performance for estimations of SM elements.

7.1 Processing Background for FM-CW Polarimetric Radar

The purpose of the technique proposed in this chapter is suppression of cross-correlation components of de-ramped signals. For a better explanation of the proposed processing background the basic scheme of the de-ramping filter (Fig. 7.1) is reminded. As before, LPF means low-pass filter, FFT means fast Fourier transform. De-ramped signals at the key-points *A-D* are under consideration in this chapter.

FM-CW radar signal handling requires understanding of the stages of sounding, propagation, scattering, receiving, and de-ramping processing. The up-going ($\dot{u}_1(t)$) and down-going ($\dot{u}_2(t)$) LFM-signals are transmitted with orthogonal polarizations *1* and *2* (linear horizontal and vertical polarizations). During the processes of propagation and scattering the received signal is created, $\dot{\mathbf{x}}(t) = \left[\dot{x}_1(t) \quad \dot{x}_2(t)\right]^T$. The polarimetric radar purpose is the measurement of the scattering matrix elements ($\dot{S}_{11}$, $\dot{S}_{12}$, $\dot{S}_{21}$, $\dot{S}_{22}$) for all observed ranges. The first component of the received signal with horizontal polarization, $\dot{x}_1(t)$, is used for the estimations $\hat{\dot{S}}_{11}$ and $\hat{\dot{S}}_{21}$, which are utilized in Channel 1. The second component of the received signal with vertical polarization, $\dot{x}_2(t)$, is used for the estimations $\hat{\dot{S}}_{12}$ and $\hat{\dot{S}}_{22}$, which are utilized in Channel 2 (upper dot in the notation means complex value, and a hat $\hat{}$ means the estimation of variable).

The time-frequency distribution of the received signals in the two channels of polarimetric radar with simultaneous measurement of SM elements is shown in Fig. 7.2.a-b. The cross-correlation components for the de-ramping procedure are determined within the regions, in which replicas of the first signal (signals *1*) and replicas of the second signal (signals *2*) occupy the same time and frequency region. The signals are analyzed along the time interval $\left[\tau_{\max}...T\right]$, where $\tau_{\max}$ is maximal time delay corresponding to maximum observed range, T is the radar duty cycle.

De-ramping processing by definition means the transformation of sets of LFM-signals into sine-signals (tones). The frequency of each tone corresponds to the definite roundtrip time delays determined by the corresponding range. Fig. 7.3 shows the time-frequency distribution of the de-ramped signals in the key-points (*A-D*) of the scheme in case of ideal LPFs. There is the unique correspondence between the frequency of tones, f_b, and the observed range, R (see Paragraph 3.4.2). So the maximum beat frequency, $f_{b\max}$, determines the maximum range $R_{\max}$ observed by the radar under design. However beat frequencies of the de-ramped signals do not contain tones and noise only.

They contain also cross-correlation components (cross LFM signals) at the time when the useful (for the definite branch) scattered signals (with up-going or down-going slopes) occupy the same bandwidth.

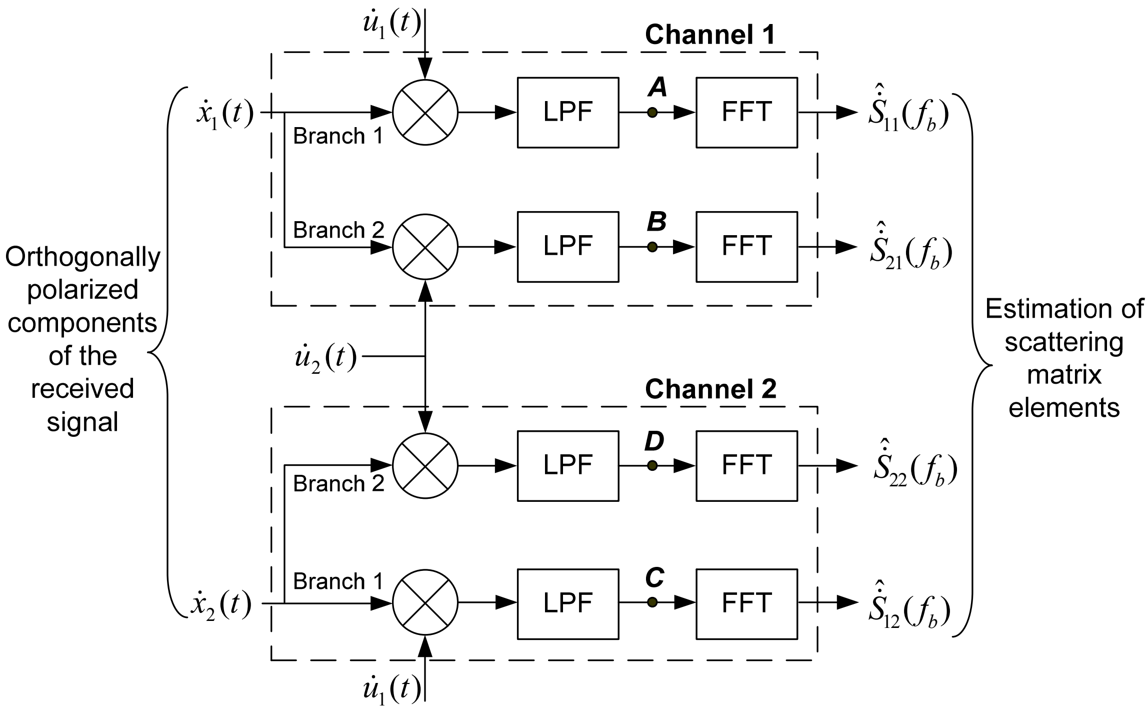

Fig. 7.1 – Basic scheme of the de-ramping filter.

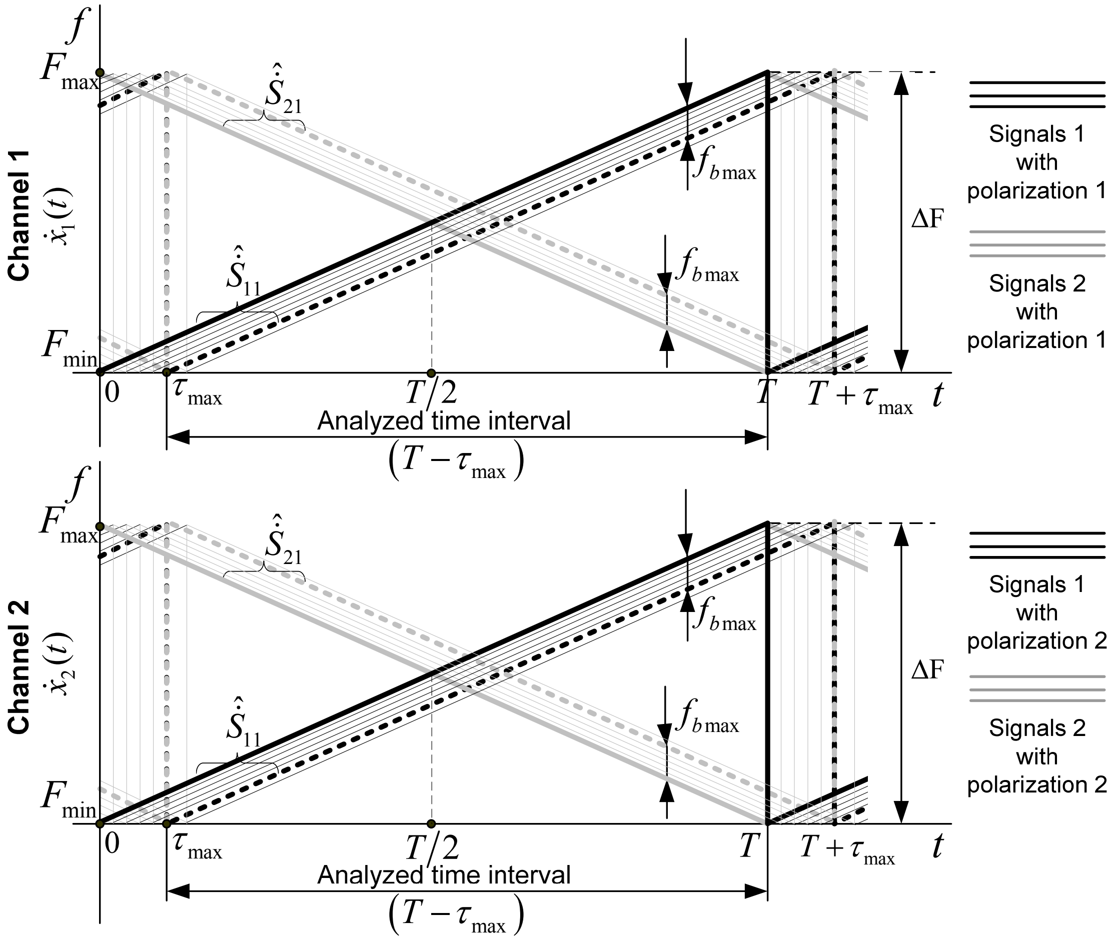

Fig. 7.2 – Time-frequency distribution of the received signals in

a) Channel 1 ($\dot{x}_1(t)$) and b) Channel 2 ($\dot{x}_2(t)$).

The problem is that the FFT is suitable for stationary signals on the analyzed time interval, e.g. for tones. However, cross-correlation components (resulting into existing cross LFM-signals) are not stationary (Fig. 7.3). The locally existing sets of cross LFM-signals (cross-correlation components) may influence the whole analyzed beat-frequency bandwidth, $[0...f_{b\max}]$. Their spectra can have a footprint form (Fig. 7.4). The level of the "footprints" (named also cross-correlation level) can come above the noise level and can be different per observed radar object. The next de-ramped signals' spectra were calculated without any window weighting.

Modeling results presented in this Chapter are presented as time-frequency distributions of the de-ramped signals in the key-points (*A-D*) and their spectra. The modeling parameters conforms with the PARSAX radar system parameters (see Appendix A.1): $T = 1$ ms, $\tau_{max} = 0.1$ ms, $f_{b\max} = 5$ MHz. Short Time Fourier Transform (STFT) has been used for the modeling. Signals scattered from five scatterers having roundtrip time delays less than τ_{max}, and a sixth scatterer with

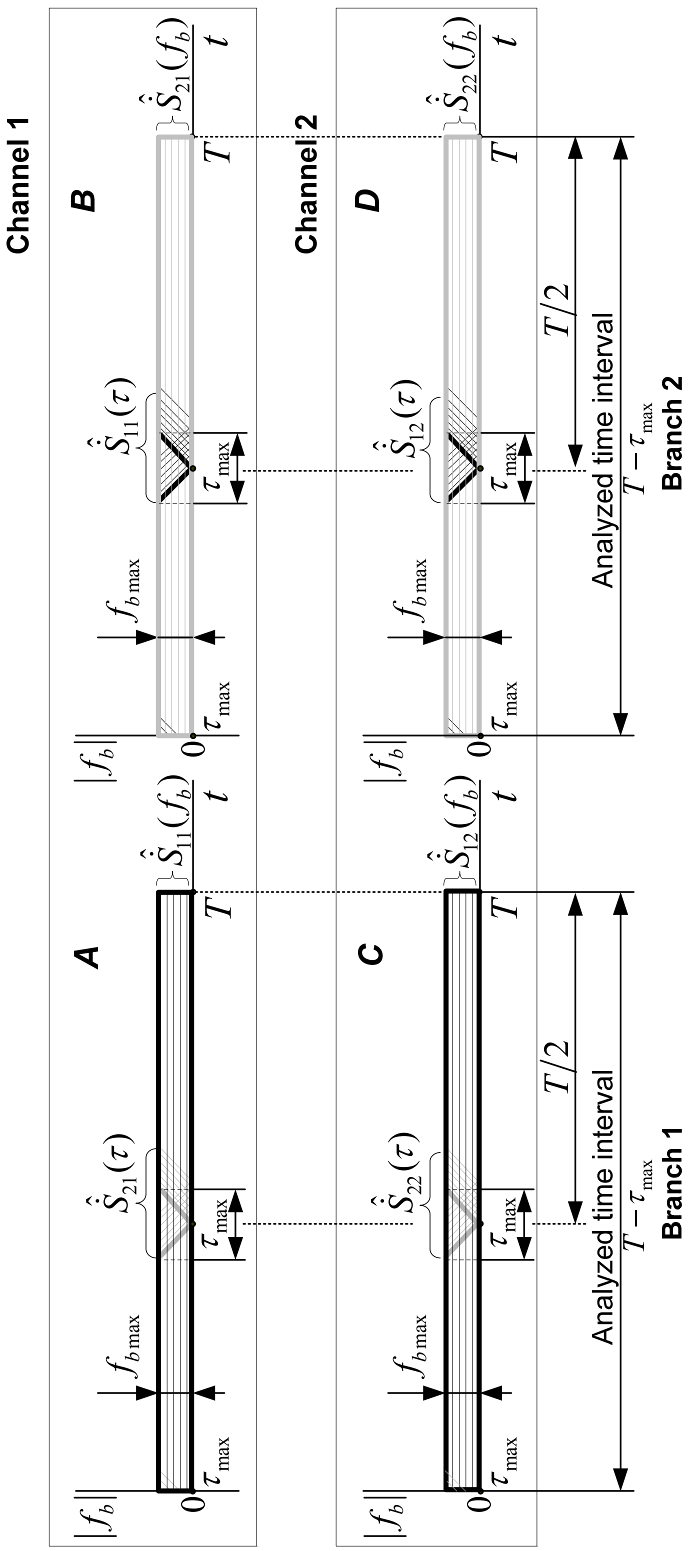

Fig. 7.3 – Time-frequency distribution of the de-ramped signals (key-points *A-D*) used for range profile estimations.

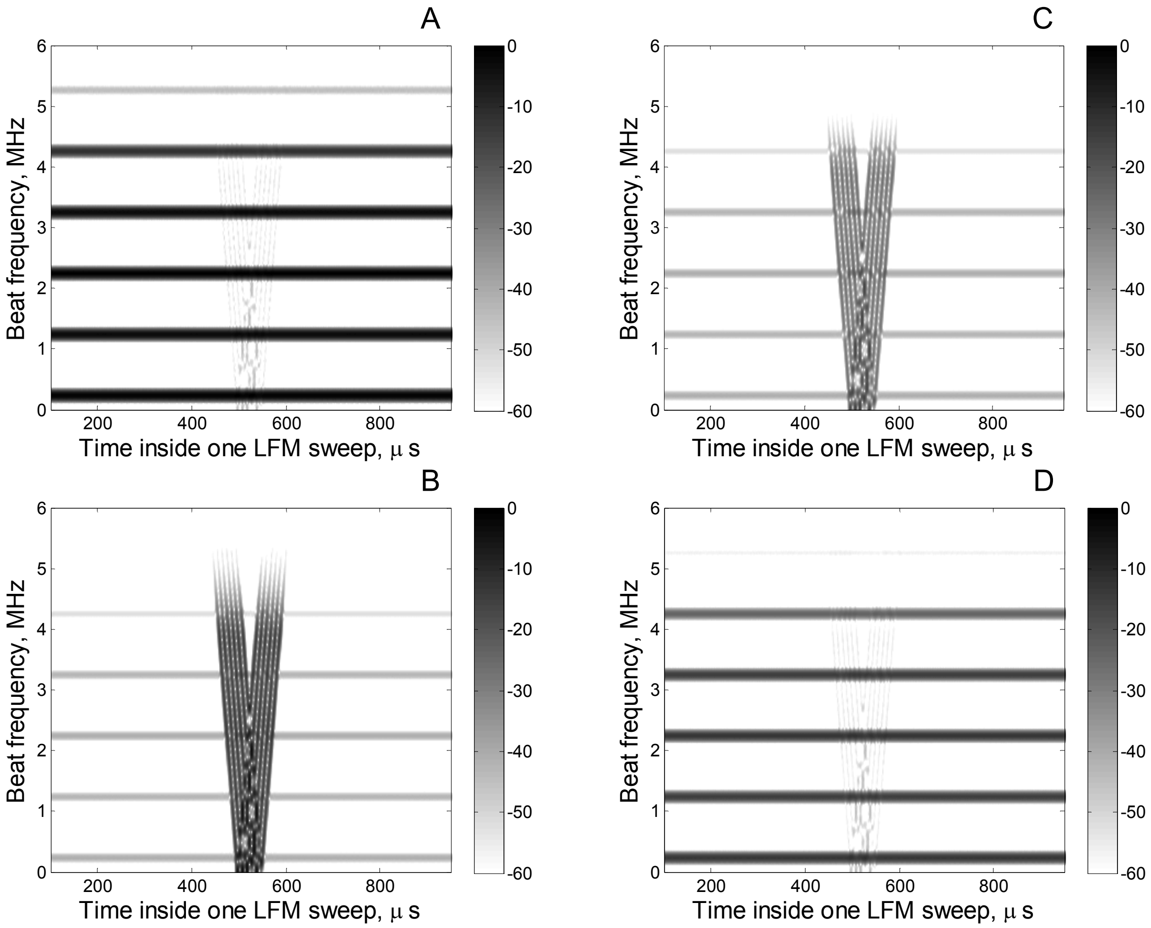

Fig. 7.4 – Time-frequency distribution of the de-ramped signals in the key-points of the branches. 6 scatterers.

a roundtrip time delay a little more than $\tau_{\max}$ are assumed. However, as the LPFs (used in the modeling) are not ideal all six tone signals are visible on the time-frequency plane. Scattering matrices for all scatterers were chosen equal to

$$\dot{\mathbf{S}} = \begin{bmatrix} 1 & 0.1 \\ 0.1 & 0.5 \end{bmatrix}.$$

A Hamming window is applied to the whole analyzed time interval for suppression of the spectra side-lobes defined by the finite duration of the de-ramped signals. The noise of the signals was chosen to be not-present for the purity of the modeling with regard to cross-correlation suppression.

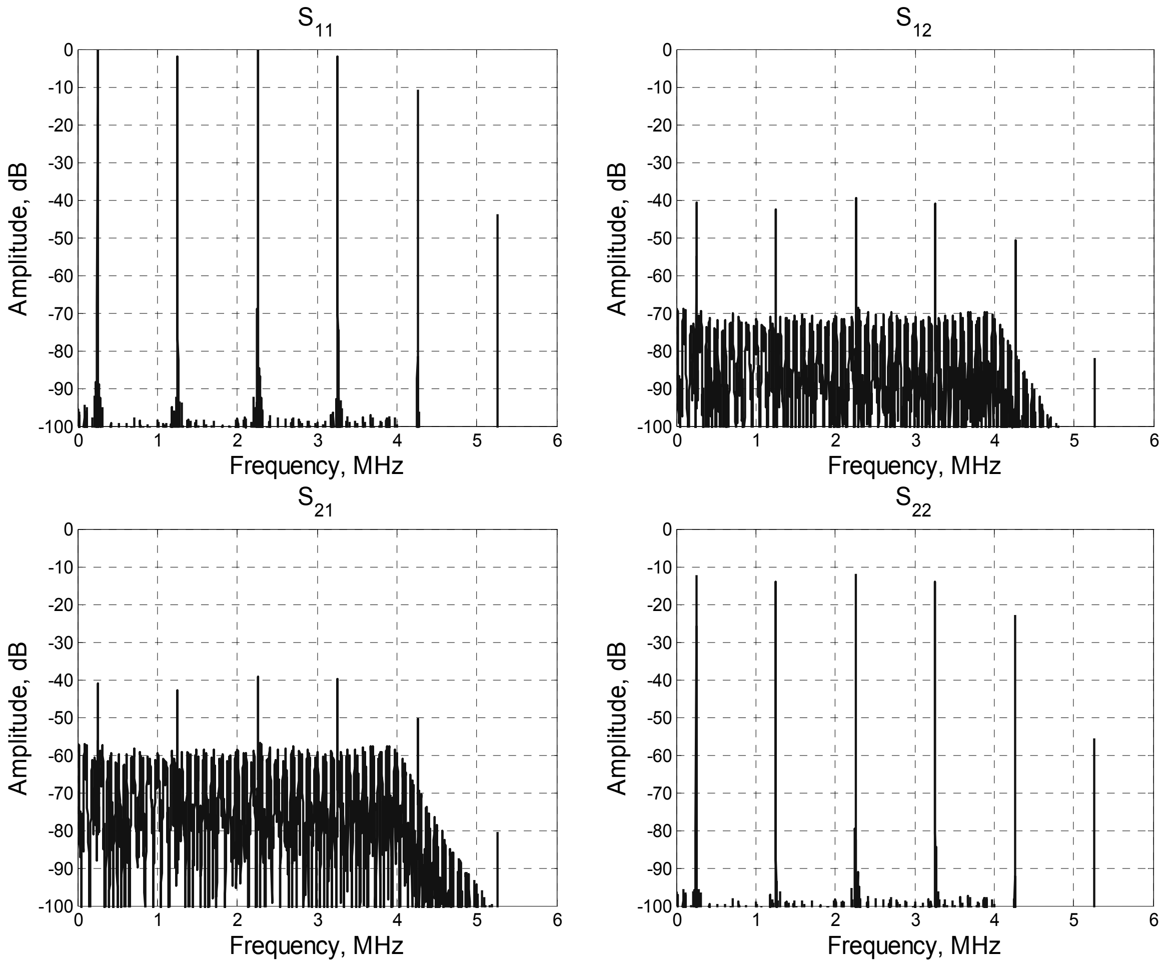

Fig. 7.5 – De-ramped signals spectra used for SM elements estimations. 6 scatterers.

Fig. 7.4 shows the time-frequency distribution of the de-ramped signals in the key-points of the branches. The analyzed time interval is $\left(\tau_{\max}...T\right)=\left(100...1000\right)\mu\text{s}$, the beat frequency band is $\left(0...f_{\max}\right)=\left(0...5\right)\text{MHz}$. As LPFs are not ideal the frequency axes show the frequencies up to 6 MHz. The amplitudes of the signals are normalized and their values from 0 to –100 dB correspond to the grayscale from black to white.

We remark that STFT used for the signals' representation on the time-frequency plane is limited according the uncertainty principle which predicates that the corresponding time and frequency coefficients cannot both be known with arbitrary precision. So the lines in Fig. 7.4 can not be thin both for tones and cross LFM signals.

We can see the peaks corresponding to the useful (tone) signals and the footprints corresponding to cross LFM signals. Significant components shown in Fig. 7.4 at points B and C result into high levels of the footprints of the spectra for estimation $\hat{\hat{S}}_{21}(f_b)$ and $\hat{\hat{S}}_{12}(f_b)$; these high levels limit the dynamic range of the useful signals considerably. The weak cross LFM signals shown in Fig. 7.4 to points A and D results in a very low footprint and influence the estimations $\hat{\hat{S}}_{11}(f_b)$ and $\hat{\hat{S}}_{22}(f_b)$ weakly.

It should be noted that cross-correlation components as well as tones contain information about range profiles. However, information about ranges is not only present in the beat frequencies of tones but also in the time delays (τ) of the cross LFM-signals. So cross-correlation components can be used for range profiles estimation ($\hat{\hat{S}}_{ij}(\tau)$, where $i, j = 1, 2$); this is an interesting aspect which can be investigated in future.

The information contained in the cross-correlation components can be extracted using correlation methods. The combination of correlation methods and de-ramping processing can become another topic for future research.

The novel technique for cross-correlation components' suppression is described in the next Section.

7.2 Suppression of Cross-Correlation Components from the Beat Signals

The proposed technique is based on the fact that cross LFM signals occupy only a part of the analyzed time interval (Fig. 7.6.a). The V-shaped cross correlation components have $\tau_{\max}$-duration and $\left[0...f_{b\max}\right]$-bandwidth (Fig. 7.6.b). The amplitudes of the scattered signals decay with the fourth power of range R (roundtrip time delay τ) due to propagation. So we may assume that the amplitudes of the cross correlation components also decay strongly with range (Fig. 7.6.c). The mutual positions of plots along the X-axes in Fig. 7.6.a-c correspond to each other.

Maximum roundtrip time delay for a cross correlation component (determined by the objects located at $\left(0...R_{\max}\right]$-range) equals to $\tau_{\max}/2$ (not to $\tau_{\max}$ as for useful (tone) signals). It is defined by the fact that the sweep rate of these signals is increased twice after de-ramping processing. So, the cross correlation component duration equals to $\tau_{\max}$ and the maximum roundtrip time delay for cross de-ramped signals equals to $\tau_{\max}/2$. The time interval corresponding to the cross LFM signals presence (i.e. maximum time interval which is dependent on the cut off from the beat signals) becomes:

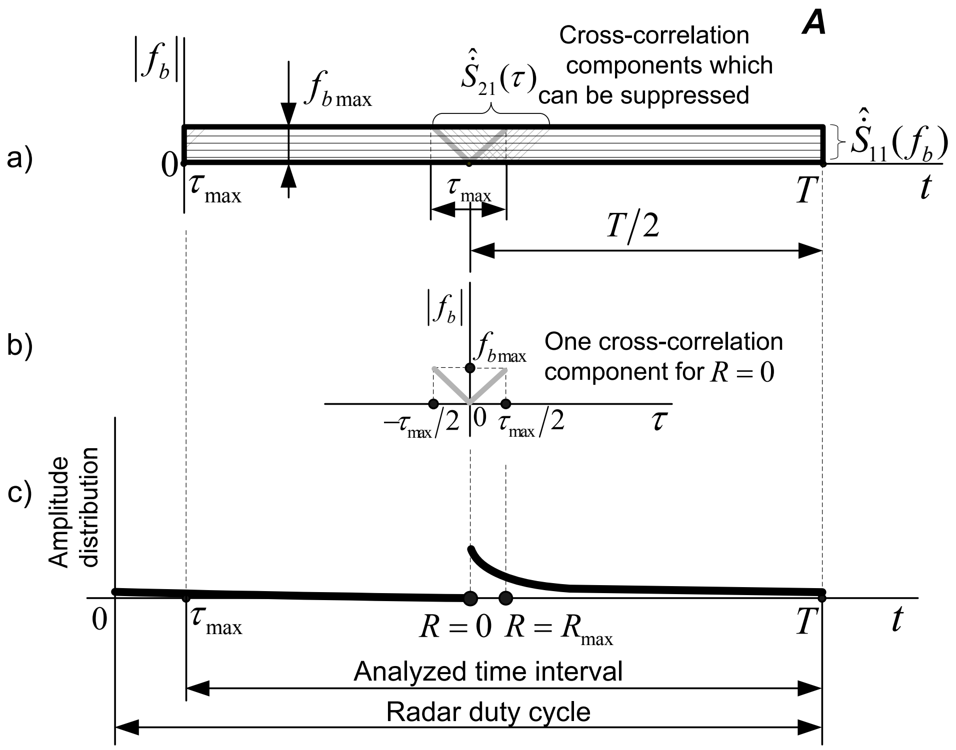

Fig. 7.6 – a) Time-frequency distribution of the de-ramped signals in one of the branches;
b) Time-frequency distribution of one cross-correlation component corresponding to zero roundtrip time delay;
c) Amplitude distribution for cross-correlation components as function of time.

$$t_{cut} = \frac{3 \cdot \tau_{\max}}{2}. \tag{7.1}$$

The time interval for localization of possible cross correlation components is assumed to be connected with the cut off (Fig. 7.7).

The time frequency representation of the beat signals with the cut off time interval is shown in Fig. 7.8. The spectra of the corresponding de-ramped signals is shown in Fig. 7.9. As before, scattering matrices for all scatterers were chosen

$$\dot{\mathbf{S}} = \begin{bmatrix} 1 & 0.1 \\ 0.1 & 0.5 \end{bmatrix}.$$

The noise level is equal to zero.

The suppression of the de-ramped signals' amplitudes (near the middle part of the analyzed time interval, Fig. 7.8) results in the considerable suppression of cross LFM signals' spectra (Fig. 7.9). We note here the increase of the side-lobe level of the tone signals due to the rectangular weighting.

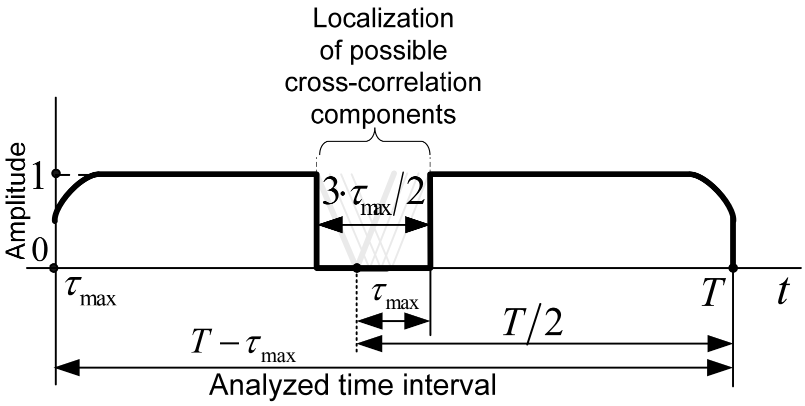

Fig. 7.7 – Rectangular cut-off window applied to the beat signals.

As known, the proposed technique suppresses not only the cross components but also the useful (tone) signals what results in some range resolution decrease and signal energy loss. So narrowing of the time interval for suppression can be of interest.

A time-frequency representation of the beat signals with a narrowed cut off time interval $2\tau_{max}/2$, is shown in Fig. 7.10. The spectra of the corresponding de-ramped signals are visualized in Fig. 7.11.

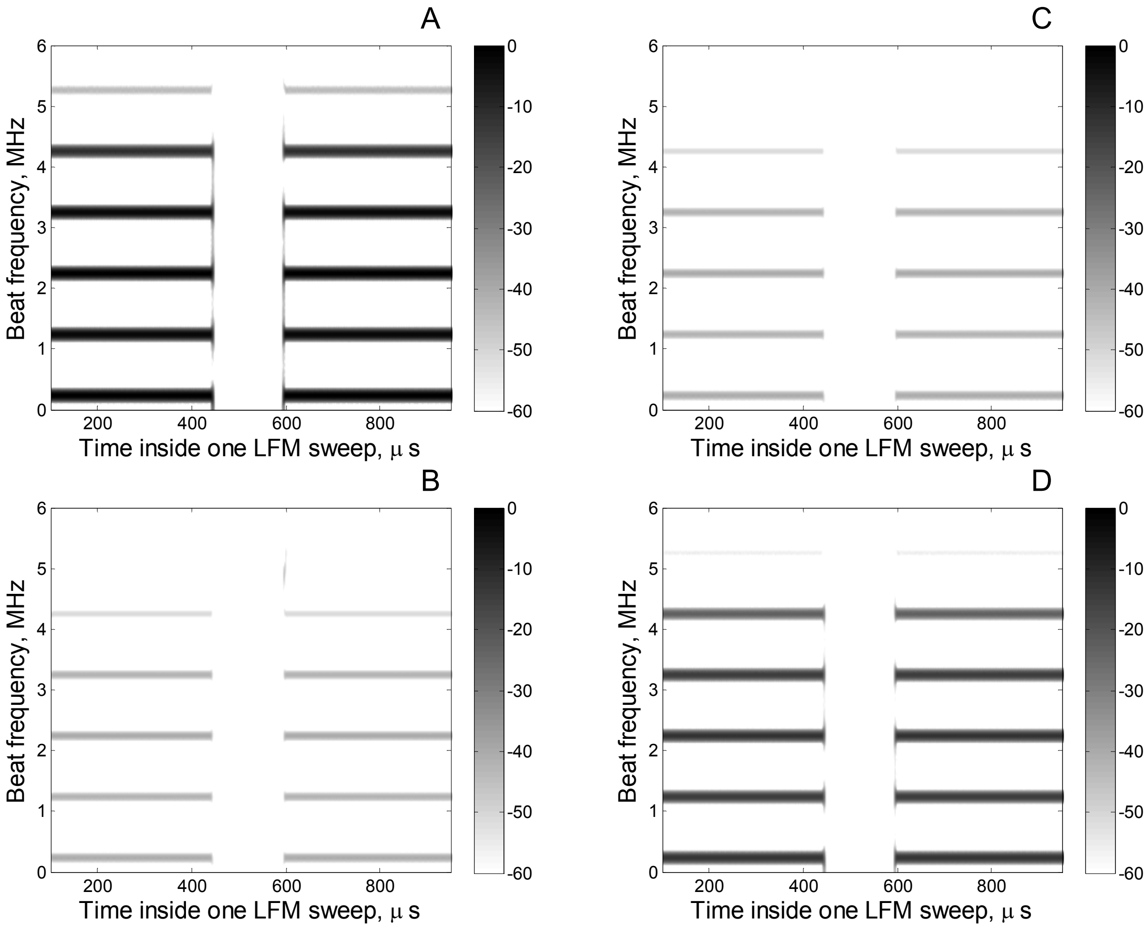

Fig. 7.8 – Time-frequency distribution of the de-ramped signals in the key-points of the branches. The window is rectangular, the cut-off time interval is equal to $3 \cdot \tau_{\max}/2$.

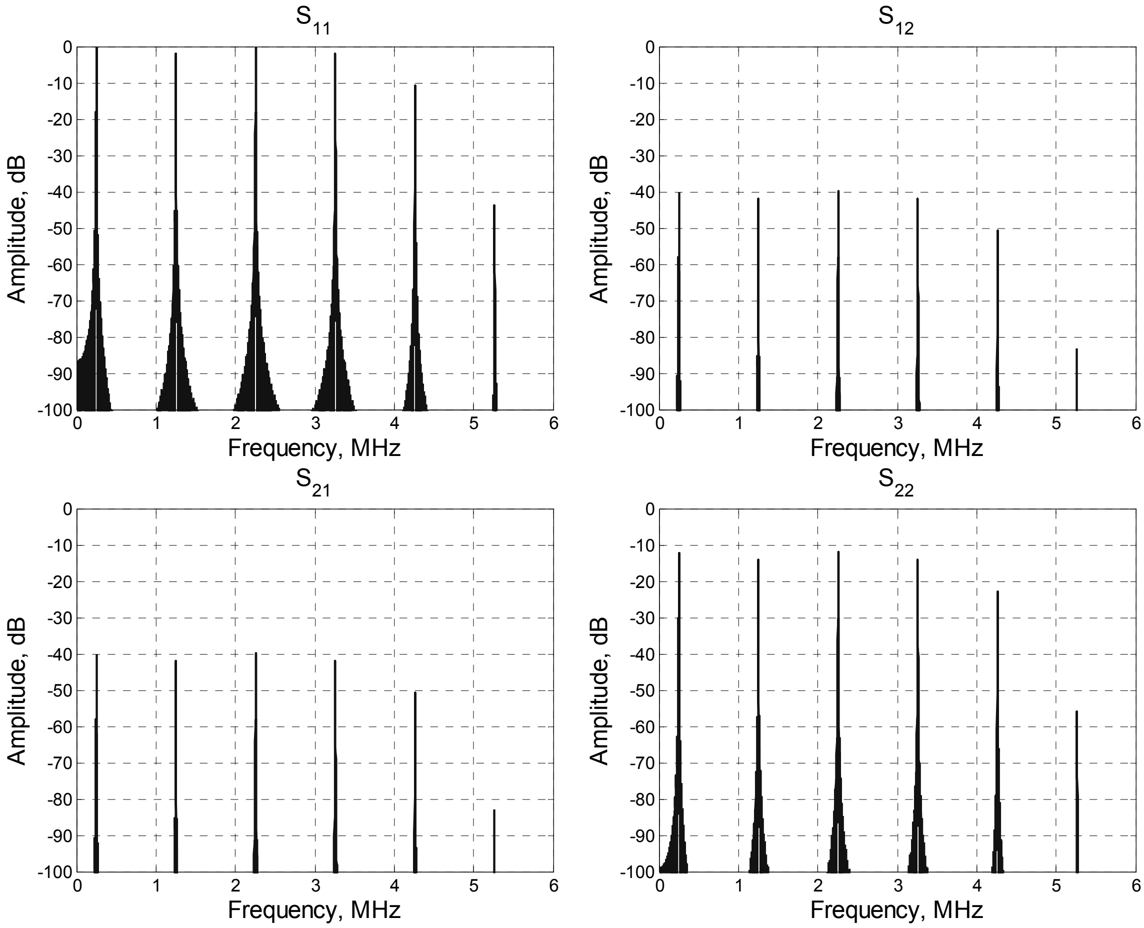

Fig. 7.9 – De-ramped signals spectra used for SM elements estimations. The window is rectangular, the cut-off time interval is equal to $3 \cdot \tau_{\max} / 2$.

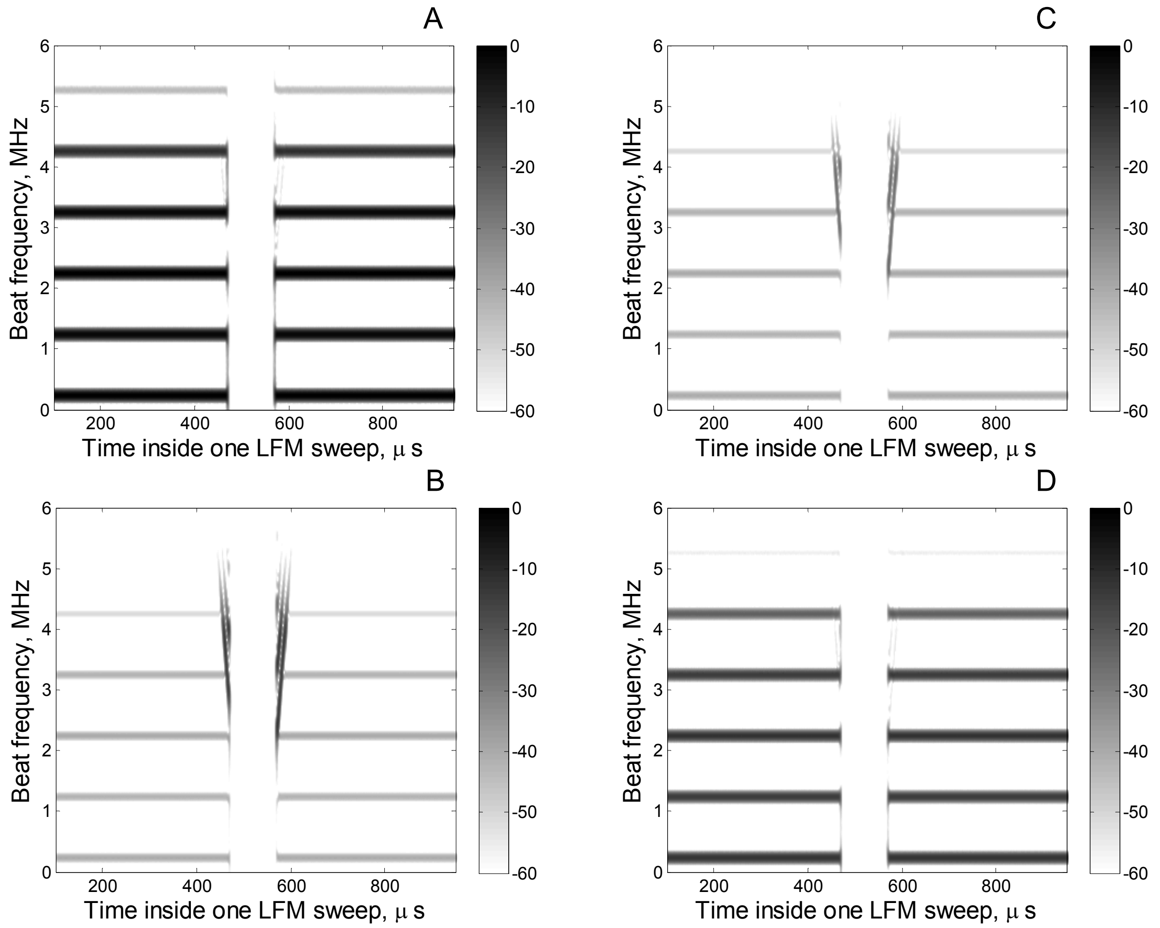

Fig. 7.10 – Time-frequency distribution of the de-ramped signals in the key-points of the branches. The window is rectangular, the cut-off time interval is equal to $2 \cdot \tau_{\max} / 2$.

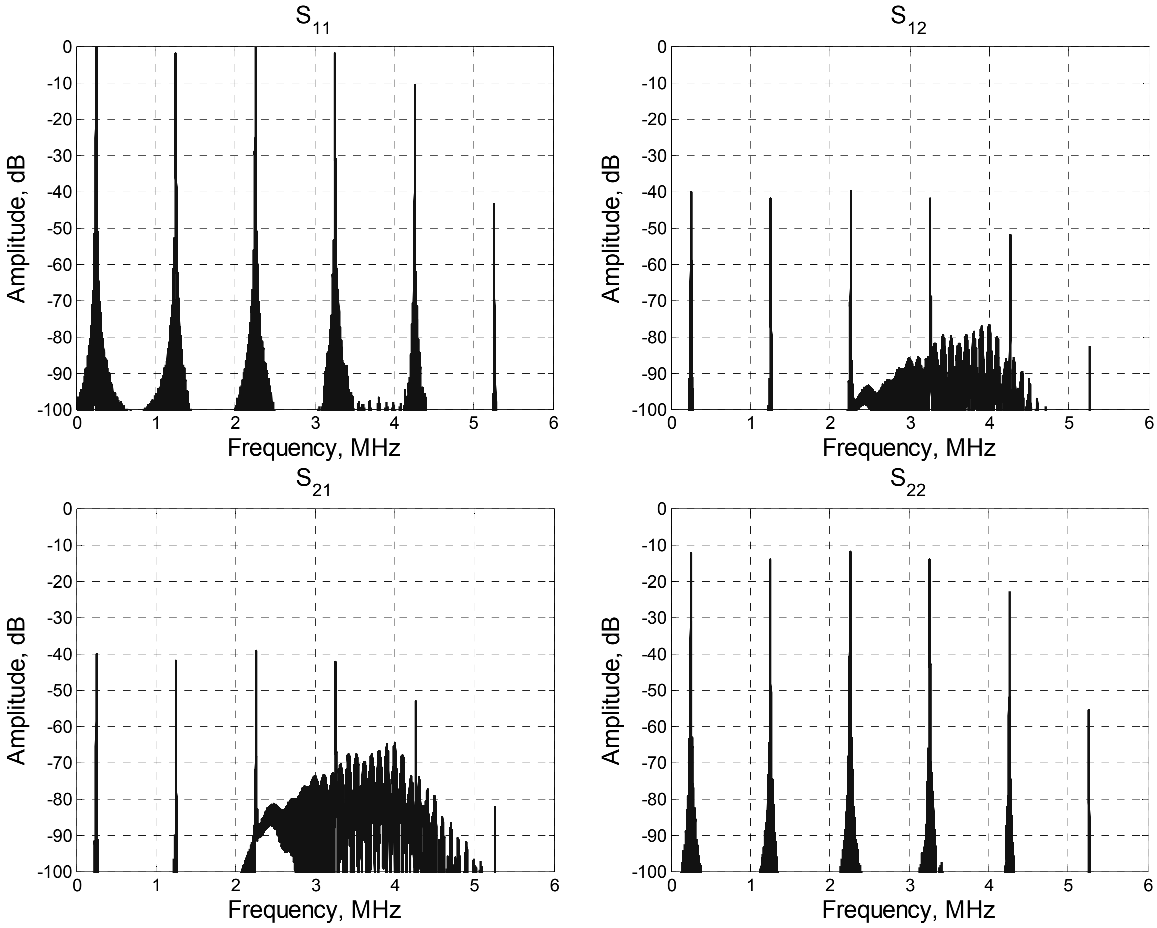

Fig. 7.11 – De-ramped signals spectra used for SM elements estimations. The window is rectangular, the cut-off time interval is equal to $2 \cdot \tau_{\max}/2$.

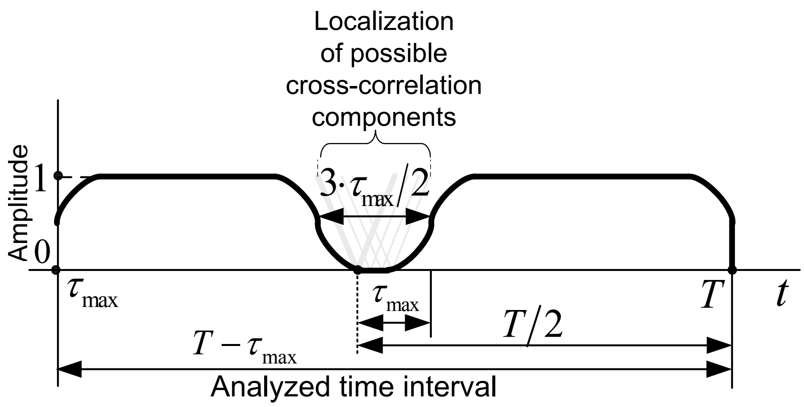

Fig. 7.12 – Smoothed-out window applied to the beat signals.

The footprints are decreased; however, we see the comparatively high level of cross components' spectra for the estimations $\hat{\dot{S}}_{11}(f_b)$ and $\hat{\dot{S}}_{22}(f_b)$ depending on frequency. It is explained by the presence of a remainder, yielding a contribution onto the cross correlation components at high frequencies (Fig. 7.19, points B, C).

Figures 7.9 and 7.11 show that the useful spectral components have a sinc-form and a relatively high level of side-lobes. This increase of side-lobes is determined from the rectangular cut-off of the signals. It is known that for suppression of the side-lobes in the signals' spectra window weighting is usually applied to the beat signals. In this case such smoothed weighting functions as Hamming, cosine, Gauss windows etc. are used. We can try to implement a smoothed-out time window (Fig. 7.12) for improvement of the spectra shown in Fig. 7.9 and 7.11.

Fig. 7.13 and 7.14 show the time-frequency representation of the beat signals with the smoothed-out cut-off time interval shown in Fig. 7.12. The spectra of the corresponding de-ramped signals are shown in Fig. 7.11. The result of the cut-off and the smoothed windowing is a considerable decrease in both the footprints and the side-lobe levels.

The time-frequency representation of the beat signals with a narrowed cut-off time interval is shown in Fig. 7.15 in case of the smoothed-out weighting. The spectra of the corresponding de-ramped signals are shown in Fig. 7.16. Comparatively to the previous example the cross correlation suppression still keeps to be very effective.

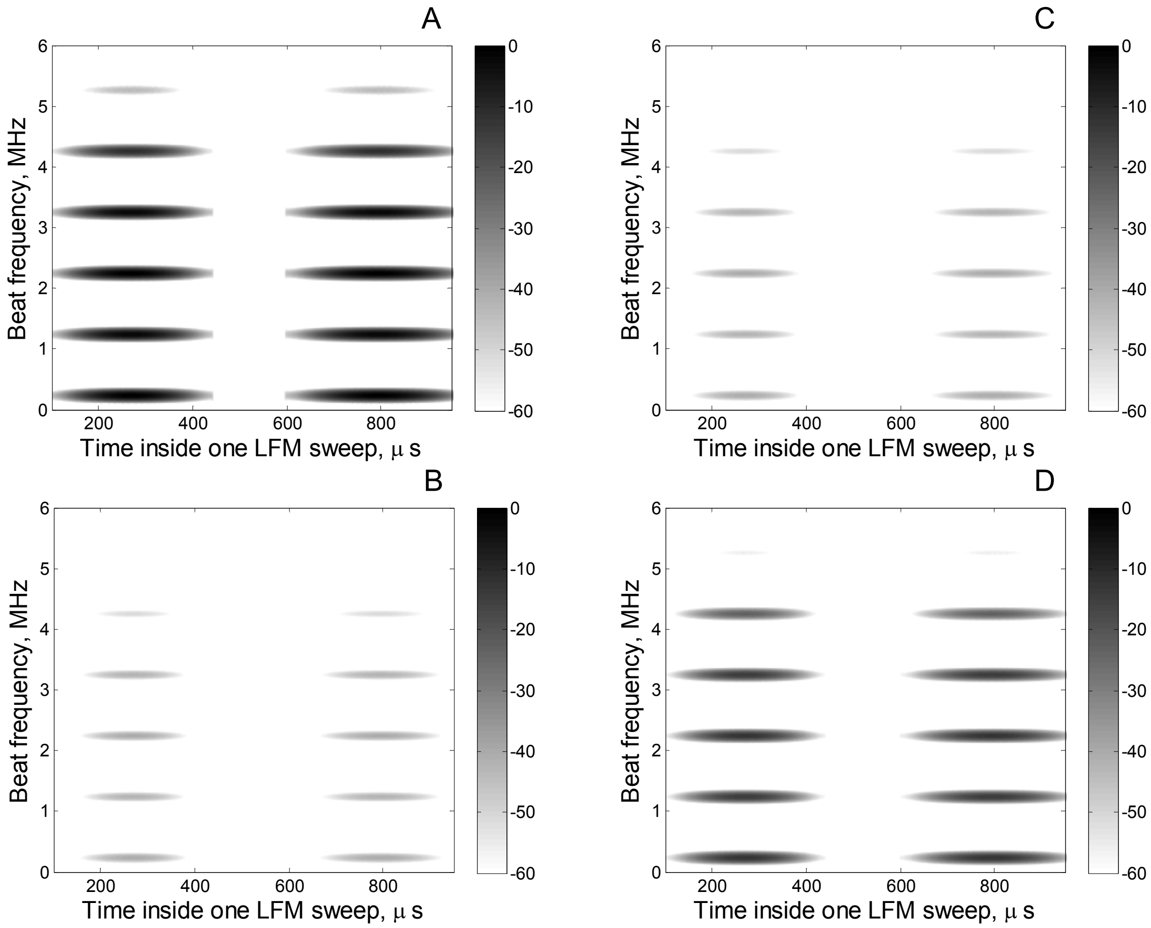

Fig. 7.13 – Time-frequency distribution of the de-ramped signals in the key-points of the branches. The window is smoothed-out, the cut-off time interval is equal to $3 \cdot \tau_{\max}/2$.

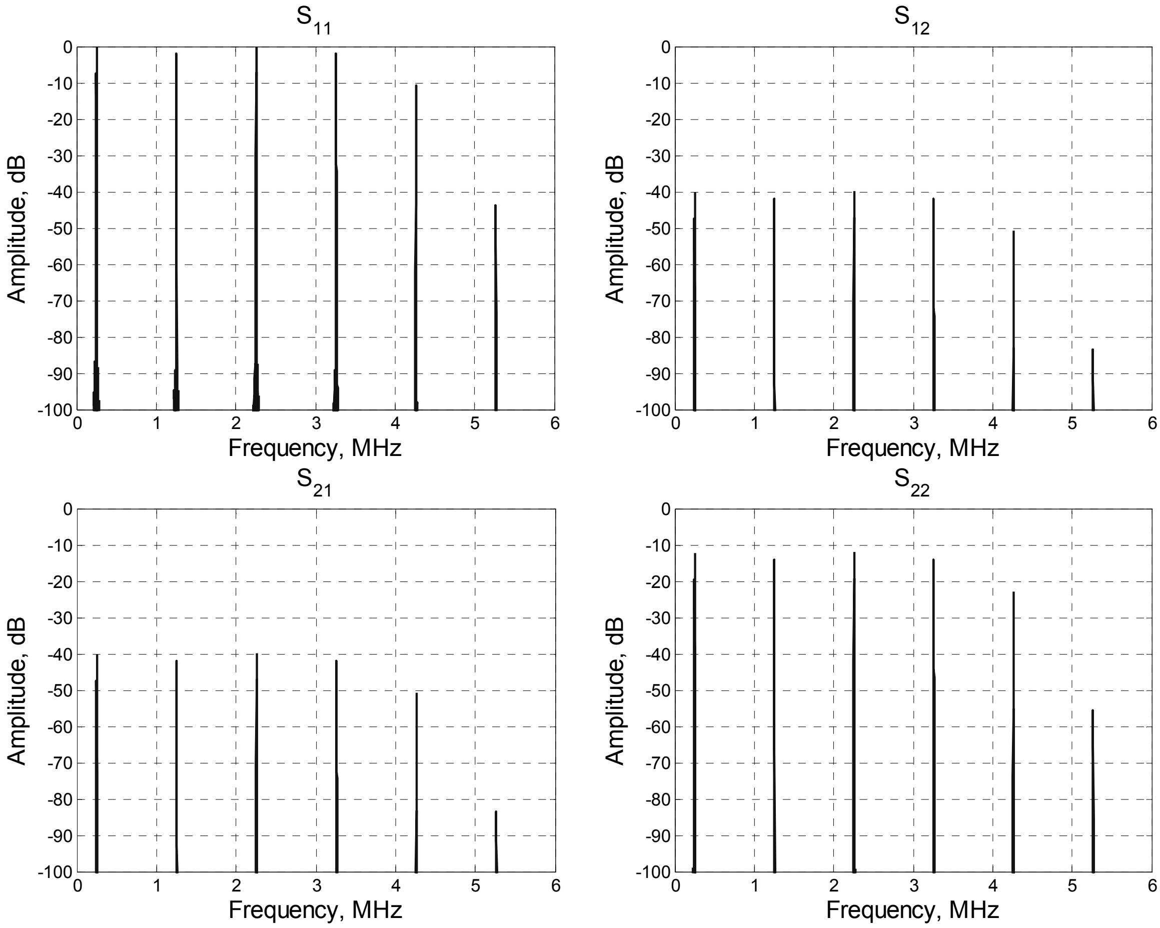

Fig. 7.14 – De-ramped signals spectra used for SM elements estimations. The window is smoothed-out, the cut-off time interval is equal to $3 \cdot \tau_{\max} / 2$.

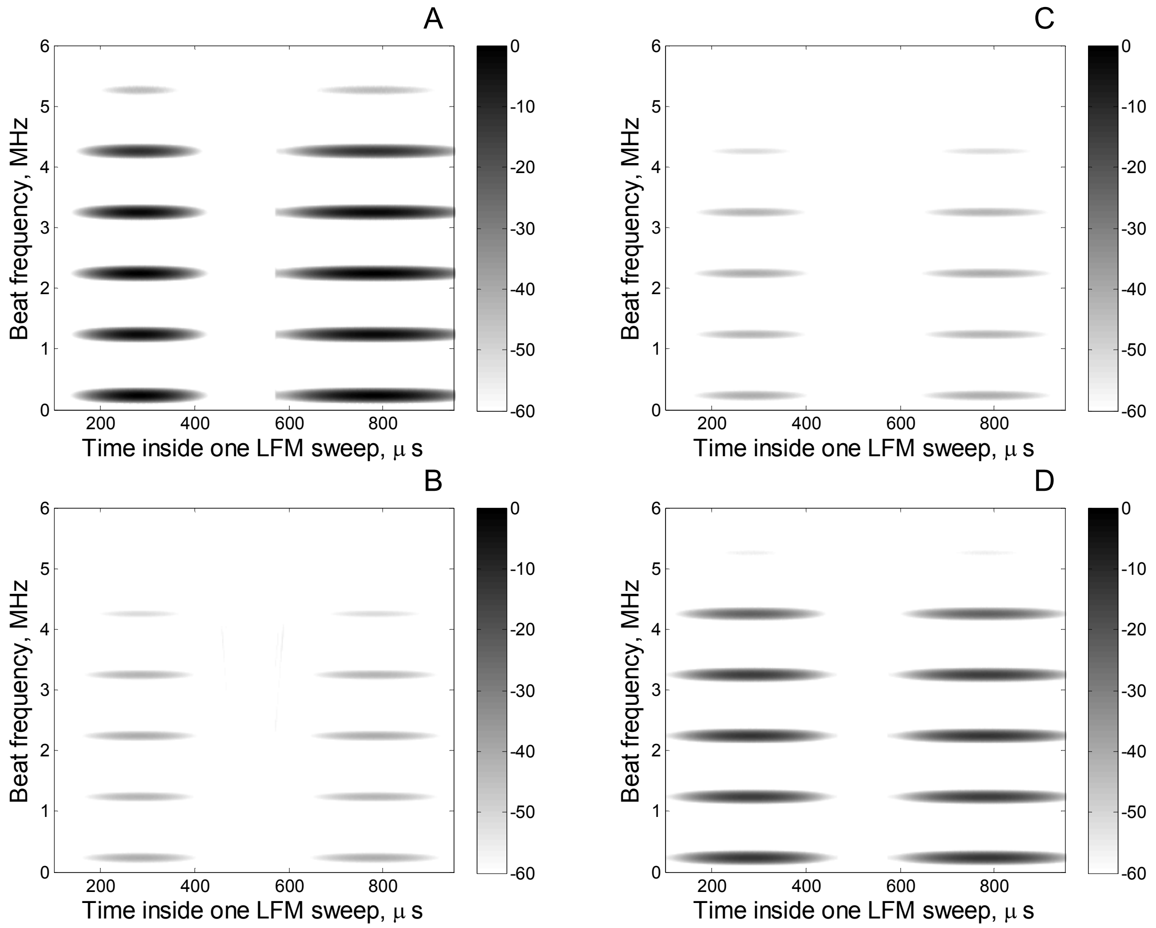

Fig. 7.15 – Time-frequency distribution of the de-ramped signals in the key-points of the branches. The window is smoothed-out, the cut-off time interval is equal to $2 \cdot \tau_{\max} / 2$.

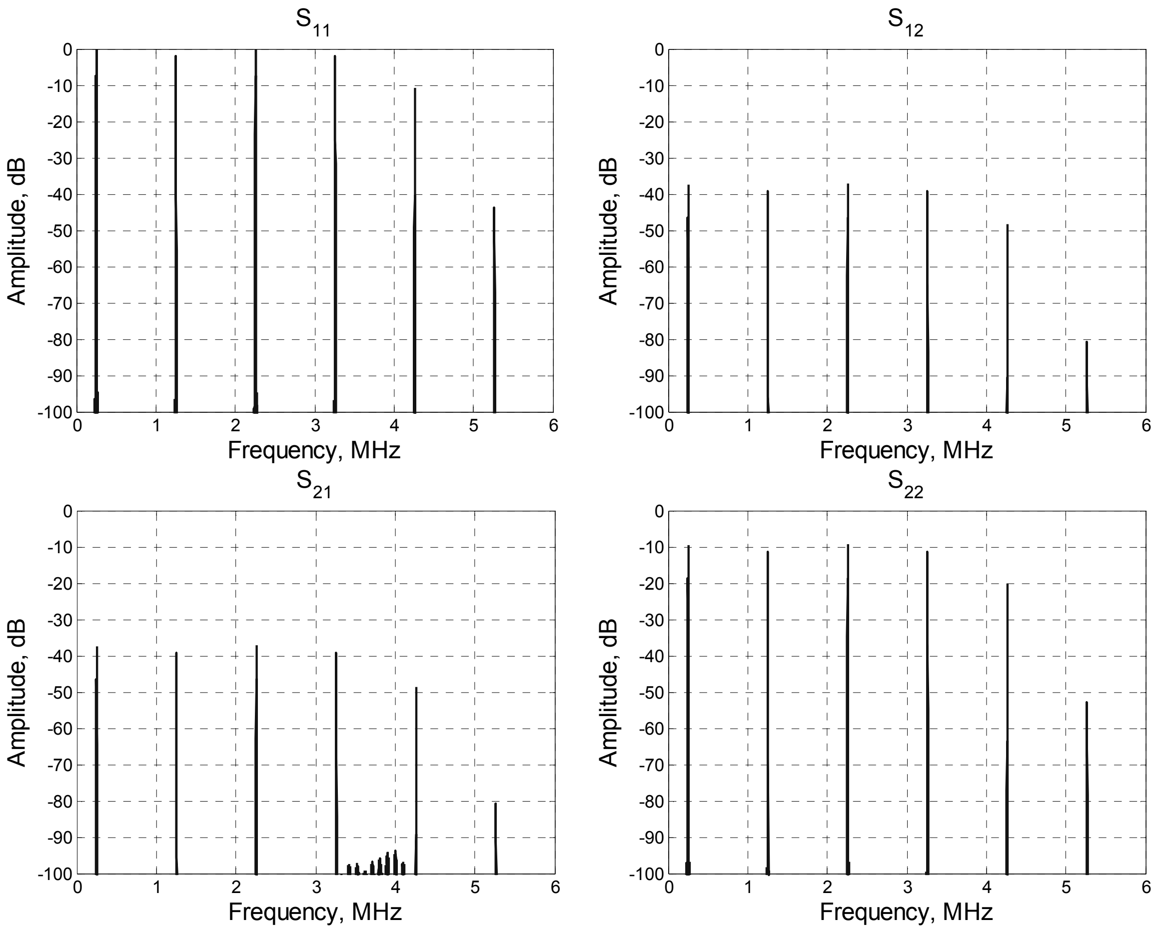

Fig. 7.16 – De-ramped signals spectra used for SM elements estimations. The window is smoothed-out, the cut-off time interval is equal to $2 \cdot \tau_{\max}/2$.

The proposed technique has shown fine results in terms of cross correlation components' suppression. However we should remember two consequences of the technique used:

- Resolution decrease.

  The range resolution in FM-CW radar depends on the analyzed time interval, namely on the tone signals' duration (see Eq. 3.19). As part of this interval is during cut-off, the resulting resolution is decreased.
- Energy of useful signals degradation.

  The energy decrease results into smaller amplitudes of the peaks in the spectra used for SM elements' estimations.

The energy degradation can be calculated for the PARSAX radar parameters (see Appendix A, Table A.1) based on the tone signals duration. The analyzed time interval for the standard de-ramping processing is $\left(T-\tau_{\max}\right)=1.0-0.1=0.9$ ms. The time interval which is selected for maximum cut-off equals to $t_{cut}=3\cdot 0.1/2=0.15$ ms according to Eq. 7.1. After suppression the total duration of tone signals equals to $0.9-0.15=0.75$ ms. So the energy loss is determined by the ratio $0.75/0.9$ what means 1.58 dB. It is of marginal impact for PARSAX. So the advantage of cross correlation suppression outweighs the disadvantage of energy loss.

Based on the modeling results shown in this Section, we can safely say that the cut-off procedure is very effective. However it can be improved if the V-shape of the cross LFM signals is taken into account. Also the information about the cross LFM signals' amplitudes can be obtained from the cross branch in the corresponding radar channel (see Fig. 7.3). So an adaptive suppression of cross LFM signals in the de-ramped signals is a topic for future research.

7.3 Conclusion

This chapter has described a technique to decrease the negative influence of cross-correlation components in an FM-CW polarimetric radar receiver which appears when a vector sounding signal is used. A novel solution has been proposed for improvement of estimations of SM-elements comparing to the standard re-ramping procedure. It allows subtraction of cross-correlation components from the beat signals and re-estimation of SM-elements properly. The modeling results have shown high efficiency of the proposed technique and outstanding improvements achievable in FM-CW polarimetric radar with simultaneous measurements of SM elements have been demonstrated.

8. Conclusions

The results obtained in the thesis have been mainly developed within the PARSAX project. The output of the work can produce a breakthrough in radar polarimetry technology, allowing to achieve a qualitatively new level of polarimetric radar performance and made this technology ready for different applications.

The thesis consists of two parts. The first part is devoted to the theory of dual-orthogonal polarimetric radar signals with continuous waveforms. If the first orthogonality, namely the polarimetric orthogonality, is specified, the choice of the second (extra) orthogonality *is not evident*. Many types of signal orthogonality are considered in the thesis. The concept of sophisticated dual-orthogonal polarimetric radar signals for application in polarimetric radar with simultaneous measurement of scattering matrix elements has been presented in Chapter 2.

As known, the processing of sophisticated signals includes compression utilizing correlation methods or de-ramping processing (only for frequency modulated signals). The overview and comparison of correlation and de-ramping methods for the dual-orthogonal sophisticated signals' processing have been made in Chapter3. *The in this Chapter given novel time-frequency representation of beat signals* in FM-CW polarimetric radar with simultaneous measurement of SM elements *was not available* to the scientific community before.

High-resolution polarimetric radar can observe fast moving objects but specific bandwidth effects may appear. It is known that the Doppler approximation corresponding to the narrow-band signal model will not be appropriate because it restricts the sounding signal BT-product and/or the velocity of the observed radar objects. A novel wide-band correlation processing for overcoming these limitations has been proposed for dual-orthogonal polarimetric radar signals. An additional aspect worthwhile to be mentioned is, that the author has calculated the errors in range estimation when sophisticated sounding signals are used in polarimetric radar with simultaneous measurement of scattering matrix elements. As for de-ramping processing a wideband model of the de-ramped signals *was missing in the literature*. Above mentioned results have been presented in Chapter 4.

The second part of the thesis is devoted to advanced processing in polarimetric radar with continuous waveforms (and with focus on polarimetric FM-CW radar).

Polarimetric radar provides dual orthogonality only for sounding signals. During the processes of sounding and scattering the polarization of the signals can be changed. The received signals with orthogonal polarizations can be splitted into two channels in the antenna system of the radar receiver, while the signals in the channels are splitted into branches making use of the orthogonality of the waveforms. Since the radar duty cycle is finite, such kind of orthogonality can not provide continuous isolation between the branches in the radar receiver channels. A *novel technique* for continuous "quasi-simultaneous" measurement of SM elements in FM-CW polarimetric radar has been proposed in the thesis. The description of the technique and the achievable isolation level have been presented in Chapter 5.

Our new approaches in high-resolution Doppler polarimetric radar can lay the fundaments for increasing the radar performance. A change in signal bandwidth can be desired for improvement of existing FM-CW radar systems in the sense that the sweep frequency of the sounding LFM-signal is increased for better range resolution. Also the shift in the beat frequency band and/or the selection of range interval with high range resolution can be demanded. For this reason, in Chapter 6 *a novel de-ramping processing* is proposed for satisfying these demands for both single-channel and polarimetric radar with simultaneous measurement of SM elements.

The isolation problem in polarimetric FM-CW radar, which has been considered in Chapter 5, can be significant. The author also proposes in Chapter 7 *a novel method* allowing a solution based on a de-ramped signal representation in the time-frequency plane as described in Chapter 3. The isolation between the polarimetric FM-CW radar branches has been defined by the cross-correlation components (cross LFM signals) existing in the beat signals. The possible location of these components has been used and the amplitudes of the beat signals can be suppressed along a part of the analyzed time interval. The description of the proposed technique and the modeling results showing its efficiency have been presented in Chapter 7.

Next we note a number of topics for future research:

1. De-ramping processing with linear superposition of LFM-signals (see Paragraph 2.2.3) using non-linearity correction with the potentials of high isolation between branches in the polarimetric radar receiver.
2. Comparative analysis of the here-presented three de-ramping techniques (see Paragraph 3.4.2) and the corresponding experimental data obtained from PARSAX .
3. Analysis of differences in the wide- and the narrow-band ambiguity matrices (see Paragraph 4.2.1) for different types of sophisticated signals.
4. Investigation of de-ramping processing in case of fast-moving radar objects (wide-band de-ramping processing), see Paragraph 4.3.2. combined with narrowing (and/or reconstructing) the spectra of a fast-moving object by using the flexible de-ramping technique proposed in Chapter 6.

5. Implementation and testing of a performance technique for quasi-simultaneous measurements of SM elements in polarimetric radar with continuous waveforms (see Chapter 5). Analysis of this performance technique should be directed especially to the isolation issue in the radar channels.
6. Flexible de-ramping processing for solving three major radar tasks (Section 6.2) with application in the PARSAX radar system. This topic is important for the PARSAX valorization phase.
7. Use of the flexible de-ramping processing (see Paragraphs 6.2.1 and 6.2.4) upgrading the existing PARSAX radar receiver operating in S-band into an S- and X-band receiver.
8. Implementation of a shift in the dual-channel frequency (see Paragraph 6.2.2) for rejection of the cross-correlation components in the PARSAX radar becomes possible. Performance analysis for different values of frequency shifts.
9. The efficiency of the technique for decreasing the cross-correlation components (Chapter 7) as function of type and size of the weighting window. Recommendations for selected windows choice depending on the radar parameters (maximum roundtrip time delay, analyzed time interval etc) are still needed.
10. Combination of flexible de-ramping processing with filtering the cross-correlation components. For example, selection of a range interval sensed with high range resolution in a dual-channel polarimetric radar (Paragraph 6.2.3) and combined with signal suppression (Section 7.2) along a small part of the analyzed time interval for decreasing cross-correlation components is of interest. A performance analysis using real measured data from the PARSAX radar is realistic in our the near future research.
11. Development of adaptive techniques for the rejection of cross-correlated signal components in FM-CW polarimetric radar with simultaneous measurement of SM elements. These techniques should take into account the time-frequency representation of de-ramped signals (using the Wavelet Transform or Short Time Fourier Transform) and the estimations of the cross-correlation components obtained due to the tone signals from the cross-branches in the receiver channels.

Appendix A

PARSAX Radar System

PARSAX is a polarimetric agile radar in S-band, which will be refined also into a design for X-band. The goal of the PARSAX project is to design, develop and investigate the feasibility of an FM-CW type and PCM type of full-polarimetric radar, which uses sounding signals with dual-orthogonality (in polarimetric and in time-frequency space) for simultaneous measurement of all elements of radar target's polarization scattering matrix. The antenna system of PARSAX, is shown in Fig. A.1.

Fig. A.1 – PARSAX radar system.

Main characteristics of the sophisticated signals in PARSAX are summarized in Table A.1.

Table A.1

Main characteristics of the PARSAX radar signals

Central frequency (S-band)	3.315 GHz
Modulation bandwidth	2 – 50 MHz
Sweep time (for frequency modulated signals)	1 ms
Sampling of the digital vector waveform generator	up to 500 MHz, 14 bits
Intermediate frequency	125 MHz
Sampling in the receiver at intermediate frequency	400 MHz, 14 bits

List of Acronyms

BPF	Band-Pass Filter
BT	Bandwidth-Time
CW	Continuous Wave
FCM	Frequency Code Modulation
FFT	Fast Fourier Transform
FIR	Finite Impulse Response
FM-CW	Frequency Modulated Continuous Wave
FT	Fourier Transform
IRCTR	International Research Centre for Telecommunications and Radar
LFM	Linear Frequency Modulation
LFM-CW	Linear Frequency Modulated Continuous Wave
LPF	Low-Pass Filter
MF	Matched Filter
PARSAX	Polarimetric Agile Radar S- And X-band
PCM	Phase Code Modulation
PSL	Peak Side-lobe Level
SM	Scattering Matrix
SNR	Signal to Noise Ratio

Summary

Polarimetric radar enables the utilization of complete electromagnetic vector information about observed objects. It measures the four complex elements of the scattering matrix, which describe amplitude, phase and polarization transformation of an electromagnetic wave incident on the objects. All these four elements can be retrieved simultaneously using sounding signals that are orthogonal from two points of view (dual-orthogonality). The first point of view regarding orthogonality is by transmitting two signals in an orthogonal polarimetric basis. The second point of view concerns to the two waveforms (i.e. the sophisticated signals that are mutually orthogonal). They also allow such advantages as high resolution and high energy due to signal compression in the radar receiver. Continuous wave (CW) transmission and reception of the radar signals provides an additional way to decrease their peak power, whilst maintaining the detection capability: In comparison with the pulsed transmissions CW signals have low peak power for the same detection performance because a 100% duty cycle radar is used. However, dual-orthogonal CW polarimetric radar signals are not still widely used and call for investigation. So this PhD thesis is focused on processing of such signals.

The thesis consists of two parts. The first part is devoted to the theory of dual-orthogonal polarimetric radar signals with continuous waveforms. The first orthogonality, namely the polarimetric orthogonality, is a well-known property of polarimetric radar. It is observed that the choice of the second (extra) orthogonality is not evident for many radar designers. All types of signal orthogonality are considered. The concept of dual-orthogonal polarimetric radar signals and some signal types is presented.

Sophisticated signal processing means signal compression in one way or another. When dual-orthogonal sounding signals are used then the received signal compression is utilized in two polarimetric radar receiver channels (corresponding to the two orthogonal polarizations). Both radar receiver channels are split into two branches (corresponding to the two orthogonal waveforms). The thesis presents a comparison of the compression techniques, namely correlation and de-ramping methods, for the dual-orthogonal sophisticated signals. The novel time-frequency representation of beat signals in frequency modulated continuous wave (FM-CW) polarimetric radar with simultaneous measurement of scattering matrix elements is shown.

Polarimetric radar can observe fast-moving objects. Since the sounding sophisticated signals usually have large time-bandwidth product, the observed object motion can result in specific bandwidth effects in the scattered signals. A conventional Doppler approximation corresponding to the narrow-band signal model can impose constraints to the time-bandwidth product of sounding sophisticated signals and/or the velocity of the observed radar objects. A novel wide-band

correlation processing for overcoming the limitations is proposed for polarimetric radar signals. Also a novel wideband model of the de-ramped signals is described.

The second part of the thesis is devoted to advanced processing in polarimetric radar with continuous waveforms (and focus on polarimetric FM-CW radar).

Although sophisticated sounding signals are orthogonal in terms of their inner products, in practice their cross-correlation is not equal to zero because of their finite lengths (repetition periods). It limits the isolation between the branches in the radar receiver channels. So a novel technique for continuous “quasi-simultaneous” measurement of the elements of the scattering matrix, which can provide high isolation level, has been proposed in this PhD thesis.

The ambition to increase the radar performance, namely to improve the radar range resolution, has led to the development of a novel flexible de-ramping processing applicable in single-channel and in polarimetric FM-CW radar.

The problem of isolation in the polarimetric FM-CW radar receiver is especially acute. A novel method allowing to mitigate the problem is developed. It is based on a de-ramped signal representation in the time-frequency plane described in the first part of the thesis. The modeling results of the proposed method show its high efficiency.

A number of topics for future research have been proposed.

This PhD thesis was prepared at the International Research Centre for Telecommunications and Radar (IRCTR), Delft University of Technology. Demonstration of the proposed and described techniques takes place in the Delft Radar PARSAX: Polarimetric Agile Radar in S and X band.

Samenvatting

Polarimetrische radar maakt het mogelijk om de volledige elektromagnetische vectoriële beschrijving van waargenomen objecten te gebruiken. Hij meet de vier complexe elementen van de verstrooiïngsmatrix, die de transformatie van een elektromagnetisch veld dat reflecteert op een object beschrijft in amplitude en fase. Alle vier elementen kunnen gelijktijdig teruggevonden worden door het uitgezonden signaal samen te stellen uit twee signalen die vanuit twee gezichtspunten orthogonaal (dubbel-orthogonaal) zijn: Het eerste gezichtspunt is dat de twee samenstellende signalen in de twee orthogonale richtingen van een polarisatie basis liggen. Het tweede gezichtspunt is dat de beide samenstellende signalen onderling orthogonaal zijn. De golfvormen zijn ingewikkeld en bieden voordelen zoals een hoge resolutie en een hoog vermogen door compressie van het ontvangen signaal in de ontvanger. Continue golfvormen (CW – Continuous Wave) voorzien in een additionele manier om het piek vermogen te reduceren met behoud van de detectie prestatie: In vergelijking met pulsvormige uitzendingen hebben CW-signalen een laag piek vermogen, omdat zij met een 100% duty cycle werken. Echter dubbel-orthogonale polarimetrische CW-radar signalen zijn nog niet in algemeen gebruik en vergen nader onderzoek. Daarom is dit proefschrift gericht op de bewerking van dit soort signalen.

Het proefschrift bestaat uit twee delen. Het eerste deel is gewijd aan de theorie van dubbel-orthogonale polarimetrische CW-radarsignalen. De eerste orthogonaliteit, de polarimetrische, is een bekende eigenschap van polarimetrische radar. De keuze van de tweede orthogonaliteit, die van de samenstellende signalen, is niet vanzelfsprekend duidelijk voor veel radar ontwerpers. Alle soorten van orthogonaliteit tussen radarsignalen zijn beschreven. Het concept van dubbel-orthogonale polarimetrische radarsignalen en enkele soorten signalen zijn gepresenteerd.

De bewerking van de ingewikkelde signalen houdt in dat ze op de een of andere wijze gecomprimeerd worden. Indien dubbel-orthogonale signalen worden uitgezonden, dan vindt de compressie plaats in twee polarimetrische radar ontvanger kanalen (in overeenstemming met de orthogonale polarizaties). Beide ontvangerkanalen zijn bovendien gesplitst in twee takken (overeenkomend met de twee orthogonale signalen). Het proefschrift presenteert een vergelijking van de compressietechnieken voor de dubbel-orthogonale ingewikkelde signalen, namelijk correlatie en "de-ramping". De nieuwe tijd-frequentie representatie van het zwevingssignaal ("beat signal") in frequentiegemoduleerde CW (FMCW) polarimetrische radar met gelijktijdige meting van alle elementen van de verstrooiïngsmatrix is beschreven.

Met polarimetrische radar kunnen snel bewegende objecten waargenomen worden. Omdat de ingewikkelde signalen gebruikelijk een groot tijd-bandbreedte product kennen, kan de ondervonden beweging van het object tot specifieke effecten betreffende de bandbreedte van het verstrooide signaal leiden. De gebruikelijke benadering van het Doppler effect in smalbandige signaalmodellen

legt beperkingen op aan het tijd-bandbreedte product van het ingewikkelde signaal en/of de snelheid van de waargenomen objecten. Een nieuw breedband correlatie proces dat deze beperkingen overwint is voorgesteld voor polarimetrische radar signalen. Ook een nieuw breedband model van de “de-ramped” signalen is beschreven.

Het tweede deel van het proefschrift is gewijd aan geavanceerde signaalbewerking in polarimetrische radar met continue golfvorm (en een focussering op polarimetrische FMCW radar).

Hoewel de ingewikkelde uitgezonden signalen orthogonaal zijn in termen van hun inwendig product, is hun kruiscorrelatie in de praktijk niet nul, vanwege de effecten van hun eindige lengte in tijd (herhalingsinterval). Dit beperkt de isolatie tussen de signaalvertakkingen in de radar ontvanger. Daarom stelt het proefschrift een nieuwe techniek voor ten behoeve van “quasi-gelijktijdige” meting van de elementen van de verstrooiïngsmatrix, die een hoog niveau van isolatie kan bereiken.

De ambitie om de radarprestatie te verbeteren, namelijk de verbetering van het oplossend vermogen in afstand, heeft geleid tot de ontwikkeling van een nieuwe flexibele “de-ramping” bewerking, die toepasbaar is in zowel één-kanaals als in polarimetrische FMCW-radar.

Het isolatieprobleem in de polarimetrische FMCW radar in het bijzonder is accuut. Een nieuwe methode die het probleem verlicht is ontworpen. Hij is gebaseerd op een representatie van het “de-ramped” signaal in het tijd-frequentievlak dat in het eerste deel van het proefschrift werd beschreven. Modellering van de voorgestelde methode demonstreerde de hoge effectiviteit ervan.

Enkele onderwerpen voor toekomstig onderzoek zijn voorgesteld.

Dit proefschrift is geschreven bij het International Research Centre for Telecommunications and Radar (IRCTR) van de Technische Universiteit Delft. De demonstratie van de voorgestelde en beschreven technieken vindt plaats in de Delftse radar PARSAX: Polarimetric Agile Radar in S- and X-band.

Acknowledgments

First of all I would like to thank my promotor Prof.dr.ir. Leo Ligthart. His precious thoughts and valuable ideas have inspired me a lot. He carefully corrected my thesis and patiently discussed with me every step I made forward. What is more he had encouraged me to do my Ph.D. study in the Netherlands. He has also been a great support to move on when some unexpected things happened in my life. "We can not change the past, but we can change our future." – His words are deeply rooted in my mind. I am extremely appreciative of the assistance of Professor Ligthart.

I would also like to express my gratitude to Dr. Oleg Krasnov. He has helped me a lot throughout my Ph.D. study. I am very grateful for his help as well as the valuable experience of working together in the PARSAX project.

I would also like to thank all my colleagues in IRCTR and in the PARSAX project in which I have been involved. My special thanks go to Fred van der Zwan for his support and hospitality, to Zhijian Li and Pidio Lys for their sense of humor and creating a nice working environment.

Special thanks to my close friends Xiaohua Lian, Muge Tanyer, Berna Torun for their amity. They probably know me much better now than I do myself. It has been a pleasure to work with them and talk to them in the coffee room.

I am particularly indebted to my teacher and friend Prof. N.A. Karataeva for her wisdom and patience. This brilliant woman opened the world of the signal processing for me when I was a student.

I would also like to express gratitude to all my friends and ex-colleagues in Tomsk, Russia.

Many thanks to Laura Bauman, Mia van der Voort-Kester, Dominique Meijer and Rowena Sardjoe for their constant help with administrative matters.

Finally, I want to thank my family for their unwavering support and understanding of my decision to follow this Ph.D. study.

Galina Babur
Delft, May 2009

About the author

Galina Babur was born in Sobolivka, Ukraine March 3, 1980. She received her Engineering degree with honours in Tomsk State University of Control Systems and Radioelectronics, Russia, in 2003. In 2003-2008, she worked at the Department of Radioengeneering Systems, Tomsk State University of Control Systems and Radioelectronics (TUCSR) on a cooperative project between TUCSR and the International Research Centre fro Telecommunications and Radar (IRCTR) of the Technical University of Delft (TUD).

Since February 2008 Galina Babur worked at TUD to finalize her PhD thesis, to be defended at Delft. Her main research interests are in signal processing, in particular in processing of sophisticated signals for polarimetric radars with simultaneous measurement of scattering matrix elements.

Currently Galina Babur continues her research in IRCTR, TUDelft. She is engaged in the project PARSAX where she works at sophisticated signal processing in polarimetric radars.

Award

EuMA Young Scientist 2nd Prize, MIKON-2008, Wroclaw, Poland, May 2008.
Awarded for the titled: "*Wideband Correlation Processing in Polarimetric Radar with Compound Signals and Simultaneous Measurement of Scattering Matrix Elements*".

Author's Publications

Patent

1. G.P. Babur "Polarimetric Radar Filter for reception of Phase Code Modulated Signals" Russian Federation Patent № 2333511, September 2008.

Journals

1. G. Babur, O. Krasnov, L.P. Ligthart, "High Range Resolution FM-CW Radar Utilizing Flexible De-Ramping Processing", IEEE Transactions on Aerospace and Electronic Systems, submitted.
2. G.P. Babur, "Adaptive Algorithm for Reduction of Side-Lobes in the Response at a Matched filter Output in the context of Radar Target Identification", Scientific Newsletter of NSTU № 1(26), pp. 15-22 2007 (in Russian).

Conferences

1. G.P. Babur, L.P. Ligthart, "Wideband correlation processing in polarimetric radar with compound signals and simultaneous measurement of scattering matrix elements" Microwaves, Radar and Wireless Communications, 2008. MIKON 2008,19-21 May 2008.
2. G.P. Babur, L.P. Ligthart, "Wideband Ambiguity Matrix of LFM-signals Used in Polarimetric Radar Allowing Simultaneous Measurement of Scattering Matrix Elements", 5th European Radar Conference, 2008. EuRAD, 30-31 October 2008.
3. G.P. Babur, "Adaptive Pulse Compression with the Use of Sounding PSK Sequences", First Interregional Scientific Conference "Modern Problems of Electronic Engineering", March 30-31, 2006, Rostov-on-Don, Russia. Proceedings, Iss. 1. RGPU, pp. 88-90 (ISBN 5-8480-0523-0), (in Russian).
4. G.P. Babur, "Identification of a Scalar Channel by Using Noise-Like Signals", Proc. All-Russian Scientific and Engineering Conference of Students, Post-graduates and Young Scientists, TUCSR Scientific Session-2006. Tomsk, Publ. "B-Spectrum", Part 1. pp. 21-23, (in Russian).
5. G.P. Babur, "Adaptive Suppression in the Side Lobes of Response of a Matched Filter when using Sounding PSK Signals", Proc. All-Russian Scientific and Engineering Conference of Students, Post-graduates and Young Scientists, TUCSR Scientific Session-2006, Tomsk, Publ. B-Spectrum, Part 1, pp. 24-26, (in Russian).
6. G.P. Babur, "Adaptive Filter of Polarimetric Radar with Compound Signals", Transactions of Tomsk Polytechnic University, Vol. 309, №8, 2006. PP. 89-93, (in Russian).
7. G.P. Babur, A.S. Berngardt, "Application of Algorithm of Adaptive Pulse Compression to Identification Problem of Radio Channel", Proc. All-Russian Scientific and Engineering Conference of Students, Post-graduates and Young Scientists "TUCSR Scientific Session-2006". Tomsk, Publ. "B-Spectrum", Part 1. pp. 18-20, (in Russian).
8. G.P.Babur, "Dynamic Range Increase of Polarimetric Radar using Compound Signals without Increase of Their BT-Product", Transactions of TUCSR Postgraduates. Publ. TUSUR, 2005, pp. 26-34 (ISBN 5-86889-256-9), (in Russian).
9. G.P.Babur, "Procedure of Removal of Side Lobes of Response of Matched Filter with the Use of Sounding PSK Sequences", Third International Scientific and Practical Conference Electronic Tools and Control Systems, October 12-14, 2005. Tomsk, Russia. Publ. IOA SB RAS, Part 1 (ISBN 5-94458-060-7), (in Russian).
10. G.P.Babur, "Dynamic Range Expansion of Polarimetric Radar by Methods of Secondary Signal Processing", First Interregional Scientific Conference "Modern Problems of Electronic

Engineering, March 30-31, 2006, Rostov-on-Don, Russia. Proceedings, Iss. 1. Rostov-on- Don: RGPU, pp. 93-96 (ISBN 5-8480-0523-0), (in Russian).

Report

1. G.P.Babur, “Using Sophisticated Signals for Correct Estimation of the Scattering Matrix of a Radar Object", within Project RI-111/004/006 of Federal Principal Scientific and Engineering Project "Investigations and Developments on Priority Directions of Science and Technology Development" for 2002-2006 (State Registration Numbers: Registration № 01200611495, Inventory № 02200606700), (in Russian).